Electronic Supporting Information for

NHC-ligated Nickel(II) Cyanoborate Complexes and Salts

Martin S. Luff[a], Luis Walther[a], Maik Finze*[a,b], Udo Radius*[a]

[a] Institute for Inorganic Chemistry, Julius-Maximilians-Universität Würzburg, Am Hubland, 97074 Würzburg, Germany.

[b] Institute for Sustainable Chemistry & Catalysis with Boron, Julius-Maximilians-Universität Würzburg, Am Hubland, 97074 Würzburg, Germany.

*Corresponding author Email address: u.radius@uni-wuerzburg.de, maik.finze@uni-wuerzburg.de

Table of Content

1 Additional Figures

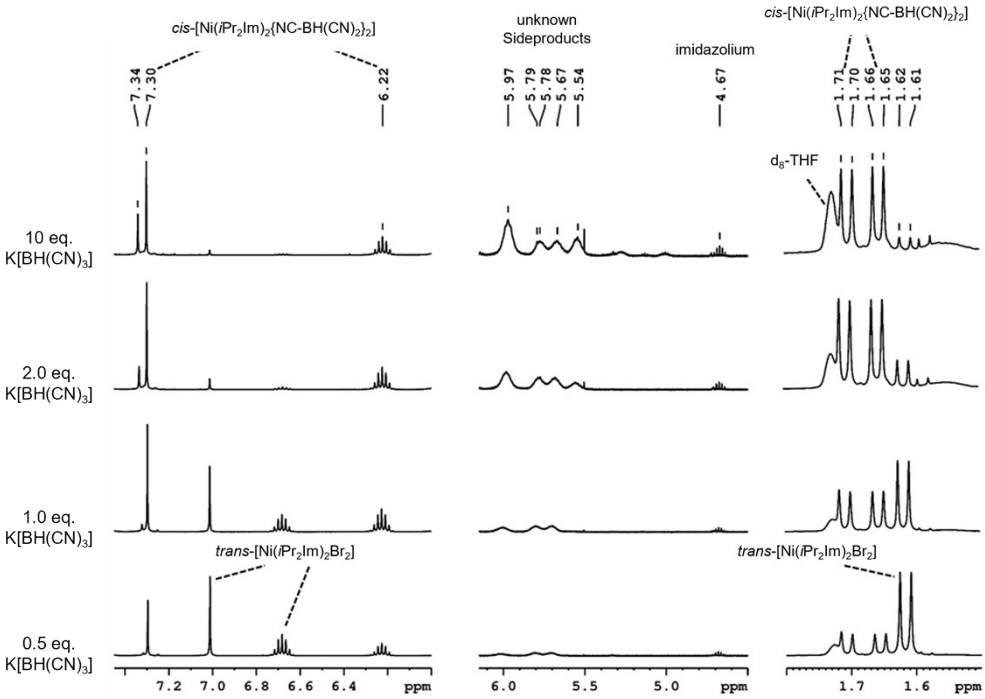

Figure S1. ^{1}H NMR spectra of the reaction of *trans*-[Ni(*i*Pr$_2$Im)$_2$Br$_2$] with different equivalents of K[BH(CN)$_3$] in d$_8$-THF after 1 h at room temperature. Only the relevant regions from 7.4 – 4.5 ppm and 1.8 – 1.5 ppm are shown in which the C*H*$_{backbone}$ (s), the C*H*$_{methine}$ (sept, br. sept) and C*H*$_3$ (d) resonances were detected. Upon addition of K[BH(CN)$_3$]$^-$ the starting material *trans*-[Ni(*i*Pr$_2$Im)$_2$Br$_2$] reacts to *cis*-Ni(*i*Pr$_2$Im)$_2${NC-BH(CN)$_2$}$_2$] (*cis*-**14c**) and other unknown sideproducts. Sideproduct formation is indicated by the presence of five additional characteristic septet resonances of the C*H*$_{methine}$ groups of the NHC between 4.5 ppm and 6.1 ppm besides the septet signals of the main product at 6.22 ppm. The stoichiometry studies suggest this product to be the disubstituted *cis*-[Ni(*i*Pr$_2$Im){NC-BH(CN)$_2$}$_2$] (*cis*-**14c**). The *cis*-conformation is indicated by the splitting of the doublets of the *iso*-propyl groups at 1.70 ppm and 1.65 ppm. The detected characteristic septet at 4.67 ppm suggests imidazolium salt formation.

2 Experimental Section

2.1 General Information

All reactions and subsequent manipulations involving organometallic reagents were performed under argon atmosphere by using standard Schlenk techniques or in a Glovebox (Innovative Technology Inc. and MBraun Uni Lab) as reported previously.[1] All reactions were carried out in oven-dried glassware. Dichloromethane, chloroform, toluene, *n*-hexane and THF were obtained from a solvent purification station (Innovative Technology) by previous purification through alumina columns. Benzene and diglyme were purchased from Sigma-Aldrich, dried over sodium and freshly distilled onto activated molecular sieves. The deuterated solvents were purchased from Sigma-Aldrich and dried thoroughly over molecular sieves. All solvents were degassed *via* three *freeze-pump-thaw* cycles prior to use. The carbene ligands Mes_2Im,[2] $Dipp_2Im$,[2] iPr_2Im,[3] iPr_2Im^{Me3} and Me_2Im^{Me},[4] the cyanoborate salts $Ni[BH_2(CN)_2]_2 \cdot H_2O$ (**Ib**$\cdot H_2O$),[5] $Ni[BH(CN)_3]_2 \cdot 0.5H_2O$ (**Ic**$\cdot 0.5H_2O$),[5] $Ni[B(CN)_4]_2 \cdot H_2O$ (**Id**$\cdot H_2O$),[5] $Ag[BH_2(CN)_2]$,[6] $Ag[BH(CN)_3]$,[6] $Ag[B(CN)_4]$,[7] $K[BH_2(CN)_2]$,[8] $K[BH(CN)_3]$,[8] $Na[B(CN)_4]$,[8,9] and the nickel complexes *trans*-$[Ni(Me_2Im^{Me})_2Br_2]$,[10] *trans*-$[Ni(iPr_2Im)_2Br_2]$,[11] *trans*-$[Ni(iPr_2Im^{Me})_2Br_2]$,[10] *trans*-$[Ni(Mes_2Im)_2Br_2]$[11] were prepared using published procedures. Elemental analyses were performed in the microanalytical laboratory of the University of Würzburg with an Elementar Vario Micro Cube. Infrared spectra were recorded on a Bruker Alpha II spectrometer as solids by using an ATR unit.

2.2 Experimental Details

Synthesis of $[Ni(Me_2Im^{Me})_4][BH(CN)_3]_2$ (1c)

$Ni[BH(CN)_3]_2 \cdot 0.5H_2O$ (**Ic**·$0.5H_2O$) (50.0 mg, 202 *µ*mol, 1.0 eq.) and Me_2Im^{Me} (112.9 mg, 909 *µ*mol, 4.5 eq.) were dissolved in THF (10 mL) and stirred at room temperature for 15 hours. The solvent was removed *in vacuo* and the residue was suspended and washed with *n*-hexane (8 x 10 mL) to give $[Ni(Me_2Im^{Me})_4][BH(CN)_3]_2$ (**1c**) (40.1 mg, 72.2 *µ*mol) as a yellow solid. **Yield**: 27% (40.1 mg, 54.5 *µ*mol). **Elemental Analysis**: $C_{34}H_{50}B_2N_{14}Ni$ [735.19 g/mol] found (calc.): C 54.76 (55.55), H 7.06 (6.86), N 26.62 (26.67)%. **^{1}H{^{11}B} NMR** (400.1 MHz, d_8-THF, 298 K): δ = 3.57 (s, 24H, N-CH_3), 2.09 (s, 24H, $C_{backbone}$-CH_3), 1.74 (s, 2H, [BH(CN)$_3$]$^-$) ppm. **^{11}B NMR** (128.5 MHz, d_8-THF, 298 K): δ = –40.0 (d, $^1J_{B\text{-}H}$ = 97.7 Hz, [BH(CN)$_3$]$^-$) ppm. **^{13}C{^{1}H} NMR** (100.6 MHz, d_8-THF, 298 K): δ = 168.9 (NCN), 127.5 ($C_{backbone}$), 35.1 (N-CH$_3$), 8.6 ($C_{backbone}$-CH$_3$) ppm. **IR** (ATR [cm^{-1}]): ν = 2955 (w), 2928 (m), 2867 (vw), 2401 (m, BH), 2242 (vw, CN), 2210 (vw, CN), 1659 (m), 1454 (s), 1434 (s), 1380 (vs), 1222 (w), 1052 (vs), 849 (s), 740 (m).

Synthesis of $[Ni(Me_2Im^{Me})_4][B(CN)_4]_2$ (1d)

$Ni[B(CN)_4]_2 \cdot H_2O$ (**Id**·H_2O) (50.0 mg, 163 *µ*mol, 1.0 eq.) and Me_2Im^{Me} (101.3 mg, 816 *µ*mol, 5.0 eq.) were dissolved in THF (10 mL) and ultrasonicated for 20 min. The solvent was removed *in vacuo* and the residue was washed with *n*-hexane (3 x 2 mL) to give $[Ni(Me_2Im^{Me})_4][(B(CN)_4]_2$ (**6d**) as a yellow solid. Single crystals suitable for X-ray diffraction of **1d** were obtained out of the reaction mixture. **Yield**: 35% (45.0 mg, 57.3 *µ*mol). Due to decomposition no conclusive elemental analytical data was obtained. **^{1}H NMR** (400.1 MHz, d_8-THF, 298 K): δ = 3.53 (s, 24H, N-CH_3), 2.09 (s, 24H, $C_{methine}$-CH_3) ppm. **^{11}B NMR** (128.5 MHz, d_8-THF, 298 K): δ = –38.6 (s, [B(CN)$_4$]$^-$) ppm. **^{13}C{^{1}H} NMR** (100.6 MHz, d_8-THF, 298 K): δ = 168.7 (NCN), 127.6 ($C_{backbone}$), 123.0 (q, $^2J_{B\text{-}C}$ = 70.5 Hz, BCN) 34.9 (N-CH$_3$), 8.7 ($C_{backbone}$-CH$_3$) ppm.

Synthesis of $[Ni(i Pr_2Im)_4][BH(CN)_3]_2$ (2c)

$Ni[BH(CN)_3]_2 \cdot 0.5H_2O$ (**Ic**·$0.5H_2O$) (20.0 mg, 80.8 *µ*mol, 1.0 eq.) was suspended in THF (5 mL). Subsequently $i Pr_2Im$ (123.0 mg, 808 *µ*mol, 10.0 eq) was added and the reaction mixture was stirred at room temperature for 64 h. After addition of *n*-hexane (10 mL) a solid precipitated, which was dried *in vacuo* and then washed with benzene (2 x 10 mL) and *n*-hexane (3 x 3 mL). The resulting crude solid was dried *in vacuo*. Single crystals of **2c** suitable for X-ray diffraction were obtained by diffusion of *n*-hexane into a saturated solution of the crude product in

acetonitrile. **Yield**: Compound 2c was not isolated in pure form. All NMR spectra presented were taken from a mixture containing $[Ni(i\mathrm{Pr_2Im})_4][BH(CN)_3]_2$ (**2c**), and contamination of the crude material also did not lead to correct elemental analytical data. **^{1}H{^{11}B} NMR** (400.1 MHz, CD_3CN, 298 K): δ = 7.35 (s, 8H, C$H_{backbone}$), 4.83 (sept, $^3J_{H\text{-}H}$ = 6.5 Hz, 8H, C$H_{methine}$),), 1.76 (s, 2H, [BH(CN)$_3$]$^-$), 1.55 (d, $^3J_{H\text{-}H}$ = 6.5 Hz, 24H, $C_{methine}$-CH_3), 0.41 (d, $^3J_{H\text{-}H}$ = 6.5 Hz, 24H, $C_{methine}$-CH_3) ppm. **^{11}B NMR** (128.5 MHz, CD_3CN, 298 K): δ = −40.2 (d, $^1J_{B\text{-}H}$ = 97.6 Hz, [BH(CN)$_3$]$^-$) ppm.

Synthesis of $[Ni(i\mathrm{Pr_2Im})_4][B(CN)_4]_2$ (2d), $[Ni(i\mathrm{Pr_2Im})_3OH][B(CN)_4]$ (7d), $[\{Ni(i\mathrm{Pr_2Im})(\mu^2\text{-}OH)\}_2][B(CN)_4]_2$ (8d) and $[Hi\mathrm{Pr_2Im}][B(CN)_4]$

$Ni[B(CN)_4]_2{\cdot}H_2O$ (**Id**·H_2O) (50.0 mg, 163 μmol, 1.0 eq.) was suspended in THF (10 mL), $i\mathrm{Pr_2Im}$ (248.4 mg, 1.63 mmol, 10.0 eq.) added and the reaction mixture was stirred at room temperature for 48 h. After addition of *n*-hexane (10 mL) a yellow oil precipitated which was washed with benzene (3 x 5 mL) and dried *in vacuo*. The leftover oily solid was then filtered and washed with diglyme (3 x 5 mL), which yields $[Ni(i\mathrm{Pr_2Im})_4][B(CN)_4]_2$ (**2d**) as a colorless solid. The filtrate still contains **2d** and the side products $[Ni(i\mathrm{Pr_2Im})_3OH][B(CN)_4]$ (**7d**) and $[Hi\mathrm{Pr_2Im}][B(CN)_4]$ (confirmed by NMR). By diffusion of *n*-hexane into this mixture single crystals suitable for XRD of **2d**, **7d** and $[\{Ni(i\mathrm{Pr_2Im})(\mu^2\text{-}OH)\}_2][B(CN)_4]_2$ (**8d**) were obtained. $[Ni(i\mathrm{Pr_2Im})_4][B(CN)_4]_2$ (**2d**): **Yield**: 25% (37.0 mg, 41.2 μmol). **Elemental Analysis**: $C_{44}H_{64}B_2N_{16}Ni$ [855.34 g/mol] found (calc.): C 58.04 (58.89), H 7.48 (7.19), N 23.49 (24.37)%. **^{1}H NMR** (400.1 MHz, CD_3CN, 298 K): δ = 7.35 (s, 8H, C$H_{backbone}$), 4.82 (sept, $^3J_{H\text{-}H}$ = 6.5 Hz, 8H, C$H_{methine}$), 1.55 (d, $^3J_{H\text{-}H}$ = 6.5 Hz, 24H, $C_{methine}$-CH_3), 0.40 (d, $^3J_{H\text{-}H}$ = 6.5 Hz, 24H, $C_{methine}$-CH_3) ppm. **^{11}B NMR** (128.5 MHz, CD_3CN, 298 K): δ = −38.6 (s, [B(CN)$_4$]$^-$) ppm. **IR** (ATR [cm^{-1}]): ν = 3127 (w), 2985 (m), 2941 (w), 2879 (w), 2222 (vw, CN), 1549 (w), 1464 (m), 1424 (m), 1398 (s), 1368 (s), 1291 (m), 1267 (m), 1211 (vs), 1126 (m), 1026 (w), 931 (vs), 879 (w), 850 (w), 731 (m), 701 (s), 676 (m), 578 (w), 555 (w), 495 (w), 440 (w). $[Ni(i\mathrm{Pr_2Im})_3(OH)][B(CN)_4]$ (**7d**): No yield was determined, the compound was only analysed in solution *via* NMR spectroscopy and by XRD of a few single crystals. **^{1}H NMR** (400.1 MHz, CD_3CN, 298 K): δ = 7.16 (s, 4H, C$H_{backbone}$), 7.15 (s, 2H, C$H_{backbone}$), 5.62 (br., 4H, C$H_{methine}$), 5.30 (m, 2H, C$H_{methine}$), 1.52 (d, 12H, $C_{methine}$-CH_3), 1.17 (br., 12H, $C_{methine}$-CH_3), 0.99 (br., 12H, $C_{methine}$-CH_3) ppm. **^{11}B NMR** (128.5 MHz, CD_3CN, 298 K): δ = −38.6 (s, [B(CN)$_4$]$^-$) ppm. $[\{Ni(i\mathrm{Pr_2Im})(\mu^2\text{-}OH)\}_2][B(CN)_4]_2$ (**8d**): No yield was determined, only a few single crystals suitable for X-ray diffraction were analysed. $[Hi\mathrm{Pr_2Im}][B(CN)_4]$: No yield was determined, the compound was only analysed in solution *via* NMR spectroscopy. **^{1}H NMR** (400.1 MHz, CD_3CN, 298 K): δ = 7.45 (s, 1H, NCHN), 7.34 (s, 2H, C$H_{backbone}$), 4.46 (sept, $^3J_{H\text{-}H}$ = 6.7 Hz,

2H, C$H_{methine}$), 1.55 (d, $^3J_{H\text{-}H}$ = 6.7 Hz, 6H, $C_{methine}$-CH_3), 0.41 (d, $^3J_{H\text{-}H}$ = 6.7 Hz, 6H, $C_{methine}$-CH_3) ppm. **^{11}B NMR** (128.5 MHz, CD_3CN, 298 K): δ = −38.6 (s, [B(CN)$_4$]$^-$) ppm.

Synthesis of [Ni(*i*Pr$_2$Im^{Me})$_3$(NC-BH$_2$CN)][BH$_2$(CN)$_2$] (3b)

Ni[BH$_2$(CN)$_2$]$_2$·H$_2$O (**Ib**·H$_2$O) (50.0 mg, 242 μmol, 1.0 eq.) and *i*Pr$_2$Im^{Me} (218.4 mg, 1.21 mmol, 5.0 eq.) were suspended in THF (15 mL). After stirring the reaction mixture for 48 h, *n*-hexane (30 mL) was added, and the resulting yellow solution was separated from the precipitated orange oil. The yellow oil was then washed with Et_2O (3 x 5 mL), solvated in $CHCl_3$ (3 mL) and precipitated with benzene (20 mL). Drying *in vacuo* afforded **3b** as an orange oily solid. Single crystals suitable for X-ray diffraction were obtained by diffusion of *n*-hexane into a saturated solution of **3b** in THF. **Yield**: 41% (72.1 mg, 98.9 μmol). **^{1}H{^{11}B} NMR** (400.1 MHz, $CDCl_3$, 298 K): δ = 5.80 (br. sept, $^3J_{H\text{-}H}$ = 6.1 Hz, 2H, *cis*-NHC: C$H_{methine}$), 5.40 (br. sept, $^3J_{H\text{-}H}$ = 6.1 Hz, 2H, *cis*-NHC: C$H_{methine}$), 5.26 (sept, $^3J_{H\text{-}H}$ = 6.1 Hz, 2H, *trans*-NHC: C$H_{methine}$), 2.28 (s, 6H, *cis*-NHC: $C_{backbone}$-CH_3), 2.24 (s, 6H, *trans*-NHC: $C_{backbone}$-CH_3), 2.20 (s, 6H, *cis*-NHC: $C_{backbone}$-CH_3), 1.78 (d, $^3J_{H\text{-}H}$ = 6.1 Hz, 6H, *cis*-NHC: $C_{methine}$-CH_3), 1.70 (d, $^3J_{H\text{-}H}$ = 6.1 Hz, 6H, *cis*-NHC: $C_{methine}$-CH_3), 1.66 (d, $^3J_{H\text{-}H}$ = 6.1 Hz, 12H, *trans*-NHC: $C_{methine}$-CH_3), 1.14 (s, 2H, Ni-NC-BH_2CN), 1.10 (s, 2H, BH_2(CN)$_2$), 1.00 (d, $^3J_{H\text{-}H}$ = 6.1 Hz, 6H, *cis*-NHC: $C_{methine}$-CH_3), 0.58 (d, $^3J_{H\text{-}H}$ = 6.1 Hz, 6H, *cis*-NHC: $C_{methine}$-CH_3) ppm. **^{1}H{^{11}B} NMR** (400.1 MHz, CD_3CN, 298 K): 6.21 (br. sept, 2H, *cis*-NHC: C$H_{methine}$), 5.91 (br. sept, 2H, *cis*-NHC: C$H_{methine}$), 5.46 (sept, $^3J_{H\text{-}H}$ = 7.1 Hz, 2H, *trans*-NHC: C$H_{methine}$), 2.23 (br. s, 6H, *cis*-NHC: $C_{backbone}$-CH_3), 2.18 (s, 6H, *trans*-NHC: $C_{backbone}$-CH_3), 2.15 (br. s, 6H, *cis*-NHC: $C_{backbone}$-CH_3), 1.68 (m, 18H, *cis*/*trans*-NHC: $C_{methine}$-CH_3), 1.56 (br. d, 6H, *cis*-NHC: $C_{methine}$-CH_3), 0.98 (br. d, 6H, *cis*-NHC: $C_{methine}$-CH_3), 0.97 (br. s, 4H, BH_2), 0.56 (br. d, 6H, *cis*-NHC: $C_{methine}$-CH_3) ppm. **^{11}B NMR** (128.5 MHz, CD_3CN, 298 K): δ = −40.6 (br. t, $^1J_{B\text{-}H}$ = 96.3 Hz, Ni-NC-BH$_2$CN), –41.8 (t, $^1J_{B\text{-}H}$ = 94.5 Hz, [BH$_2$(CN)$_2$]$^-$) ppm. **^{13}C{^{1}H} NMR** (100.6 MHz, CD_3CN, 298 K): δ = 167.3 (*cis*-NHC: NCN), 157.8 (*trans*-NHC: NCN), 129.2 (*cis*-NHC: $C_{backbone}$), 126.3 (*trans*-NHC: $C_{backbone}$), 54.8 (*cis*-NHC: $C_{methine}$), 54.7 (*cis*-NHC: $C_{methine}$), 54.4 (*trans*-NHC: $C_{methine}$), 24.5 (*cis*-NHC: $C_{methine}$-CH$_3$), 22.0 (*cis*-NHC: $C_{methine}$-CH$_3$), 21.1 (*trans*-NHC: $C_{methine}$-CH$_3$), 11.1 (*cis*-NHC: $C_{backbone}$-CH$_3$), 10.6 (*trans*-NHC: $C_{backbone}$-CH$_3$) ppm. **IR** (ATR [cm^{-1}]): ν = 2924 (m), 2853 (m), 2370 (m, BH), 2227 (vw, CN_{coord}), 2191 (vw, $CN_{non\text{-}coord}$), 1636 (w), 1560 (w), 1463 (m), 1369 (s), 1293 (m), 1260 (m), 1211 (m), 1105 (m), 1084 (vs), 1020 (m), 904 (vw), 797 (m), 754 (m), 712 w), 548 (w), 468 (w).

Synthesis of *trans*-[Ni(Dipp$_2$Im)$_2$(NC-BH$_2$CN)$_2$] (*trans*-4b) and [{Ni(Dipp$_2$Im)(NC-BH$_2$CN)(μ^2-OH)}$_2$] (9b)

$Ni[BH_2(CN)_2]_2 \cdot H_2O$ (**Ib**·H_2O) (50.0 mg, 242 *µ*mol, 1.0 eq.) and $Dipp_2Im$ (470.6 mg, 1.21 mmol, 5.0 eq.) were suspended in THF (15 mL). After stirring the reaction mixture for 48 h at room temperature, the formed yellow solid was collected by filtration and washed with *n*-hexane (3 x 5 mL). Drying *in vacuo* affords the product *trans*-$[Ni(Dipp_2Im)_2(NC\text{-}BH_2CN)_2]$ (*trans*-**4b**) as a yellow solid. Single crystals of *trans*-**4b** that were suitable for XRD were grown by diffusion of *n*-hexane into a saturated solution of the product in THF. Further, by storing the mother liquor at –30°C for 3 days a few single crystals of $[\{Ni(Dipp_2Im)(NC\text{-}BH_2CN)(\mu^2\text{-}OH)\}_2]$ (**9b**) were obtained, which were suitable for XRD. *trans*-$[Ni(Dipp_2Im)_2(NC\text{-}BH_2CN)_2]$ (***trans*-4b**): **Yield**: 68% (160.0 mg, 166 *µ*mol). **Elemental analysis**: $C_{58}H_{76}B_2N_8Ni$ [965.62 g/mol] found (calc.): C 71.63 (72.14), H 8.34 (7.93), N 10.76 (11.60)%. **^{1}H{^{11}B} NMR** (400.1 MHz, $CDCl_3$, 298 K): δ = 7.57 (t, $^3J_{H\text{-}H}$ = 7.1 Hz, 4H, aryl-CH_{para}), 7.28 (d, $^3J_{H\text{-}H}$ = 7.1 Hz, 8H, aryl-CH_{meta}), 6.98 (s, 4H, C$H_{backbone}$), 2.36 (sept, $^3J_{H\text{-}H}$ = 6.8 Hz, 8H, C$H_{methine}$), 1.21 (d, $^3J_{H\text{-}H}$ = 6.8 Hz, 24H, $C_{methine}$-CH_3), 0.99 (d, $^3J_{H\text{-}H}$ = 6.8 Hz, 24H, $C_{methine}$-CH_3) ppm. **^{11}B NMR** (128.5 MHz, $CDCl_3$, 298 K): δ = −40.3 (br. s, Ni-NC-*B*H_2CN) ppm. **^{13}C{^{1}H} NMR** (100.6 MHz, $CDCl_3$, 298 K): δ = 158.3 (Ni-$C_{carbene}$), 146.2 (aryl-C_{ipso}), 134.2 (aryl-C_{ortho}), 131.0 (aryl-C_{para}), 127.6 ($C_{backbone}$), 124.9 (aryl-C_{meta}), 28.8 ($C_{methine}$), 27.2 ($C_{methine}$-CH$_3$), 22.9 ($C_{methine}$-CH$_3$) ppm. **IR** (ATR [cm^{-1}]): ν = 3172 (w), 3125 (w), 3093 (w), 2963 (m), 2868 (m), 2422 (m, BH), 2402 (m, BH), 2227 (w, CN_{coord}), 2198 (w, $CN_{non\text{-}coord}$), 1592 (w), 1565 (w), 1458 (s), 1403 (m), 1387 (m), 1365 (m), 1349 (w), 1327 (m), 1306 (w), 1277 (m), 1207 (m), 1183 (w), 1139 (w), 1076 (s), 966 (w), 936 (m), 912 (m), 801 (s), 755 (s), 731 (s), 718 (m), 667 (m), 634 (m), 547 (w), 450 (m), 433 (m). $[\{Ni(Dipp_2Im)(NC\text{-}BH_2CN)(\mu^2\text{-}OH)\}_2]$ (**9b**): No yield was determined and the compound was not further characterized as only a few single crystals were isolated.

Synthesis of a mixture of *trans*-$[Ni(Mes_2Im)_2\{NC\text{-}BH(CN)_2\}_2]$ (*trans*-5c) and *trans*-$[Ni(Mes_2Im)_2\{NC\text{-}BH(CN)_2\}Cl]$ (*trans*-6c)

$Ni[BH(CN)_3]_2 \cdot 0.5H_2O$ (**Ic**·$0.5H_2O$) (50.0 mg, 202 *µ*mol, 1.0 eq.) and Mes_2Im (153.8 mg, 505 *µ*mol, 2.5 eq.) were suspended in toluene (15 mL) and the reaction mixture was stirred for 18 h at 110 °C. After filtration, the solids were washed with benzene (3 x 10 mL), then extracted with CH_2Cl_2 (10 mL). Removal of the solvent *in vacuo* gives crude material containing *trans*-$[Ni(Mes_2Im)_2\{NC\text{-}BH(CN)_2\}_2]$ (*trans*-**5c**) and *trans*-$[Ni(Mes_2Im)_2\{NC\text{-}BH(CN)_2\}Cl]$ (*trans*-**6c**) as a decomposition product of *trans*-**5c** in chlorinated solvents. Single crystals suitable for X-ray diffraction of *trans*-**5c** and *trans*-**6c** could be obtained by diffusion of *n*-hexane to a saturated solution of the crude material in CH_2Cl_2. **Yield**: 73.0 mg of a 50:50 mixture of *trans*-**5c** and *trans*-**6c**. *trans*-$[Ni(Mes_2Im)_2\{NC\text{-}BH(CN)_2\}_2]$ (*trans*-**5c**): **Yield**: 22% (37.7 mg, 44.5 *µ*mol). **^{1}H{^{11}B} NMR** (400.1 MHz, $CDCl_3$, 298 K): δ = 6.72 (s, 8H, aryl-CH_{meta}), 6.69 (s, 4H, aryl-C$H_{backbone}$), 1.67 (s, 12H, aryl-C_{para}CH_3), 1.39 (s, 24H, aryl-C_{ortho}CH_3), 1.35 (s, 2H, Ni-NC-

B*H*$(CN)_2$) ppm. **^{11}B NMR** (128.5 MHz, $CDCl_3$, 298 K): δ = –33.6 (d, $^1J_{B-H}$ = 94.7 Hz, Ni-NC-*B*H$(CN)_2$) ppm. *trans*-[Ni$(Mes_2Im)_2${NC-BH$(CN)_2$}Cl] (*trans*-**6c**): **Yield**: 22% (35.3 mg, 44.5 μmol). **^{1}H{^{11}B} NMR** (400.1 MHz, $CDCl_3$, 298 K): δ = 6.81 (s, 4H, aryl-CH_{meta}), 6.77 (s, 4H, aryl-CH_{meta}), 6.75 (s, 4H, aryl-C$H_{backbone}$), 2.15 (s, 12H, aryl-CCH_3), 1.93 (s, 12H, aryl-CCH_3), 1.35 (s, 1H, Ni-NC-B*H*$(CN)_2$), 1.30 (s, 12H, aryl-CCH_3) ppm. **^{11}B NMR** (128.5 MHz, $CDCl_3$, 298 K): δ = –34.8 (d, $^1J_{B-H}$ = 99.3 Hz, Ni-NC-*B*H$(CN)_2$) ppm.

Synthesis of *cis*-[Ni$(Me_2Im^{Me})_2${NC-BH$(CN)_2$}Br] (*cis*-10c)

trans-[Ni$(Me_2Im^{Me})_2Br_2$] (150 mg, 321 μmol, 1.0 eq.) and Ag[BH$(CN)_3$] (63.5 mg, 321 μmol, 1.0 eq.) were suspended in THF (10 mL) and stirred at room temperature for 2 h. The suspension was filtered through a pad of Celite and the solvent of the clear yellow filtrate was removed *in vacuo*. After washing with Et_2O (2 x 10 mL) and suspending the oily residue with Et_2O (10 mL) and ultrasonification for 15 min and subsequent removal of the solvent for three times *in vacuo cis*-[Ni$(Me_2Im^{Me})_2${NC-BH$(CN)_2$}Br] (*cis*-**15c**) was obtained as a yellow solid. Single crystals suitable for X-ray diffraction may be obtained by diffusion of benzene into a saturated solution of the compound in CH_2Cl_2. **Yield**: 56% (86.4 mg, 181 μmol). **Elemental Analysis**: $C_{17}H_{25}BBrN_7Ni$ [476.84 g/mol] found (calc.): C 43.59 (42.82), H 5.27 (5.28), N 21.17 (20.56)%. **^{1}H{^{11}B} NMR** (400.1 MHz, CD_3CN, 298 K): δ = 3.96 (s, 12H, N-CH_3), 2.03 (s, 12H, C-CH_3), 1.74 (s, 1H, Ni-NC-B*H*$(CN)_2$) ppm. **^{11}B NMR** (128.5 MHz, CD_3CN, 298 K): δ = –40.2 (d, $^1J_{B-H}$ = 94.1 Hz, Ni-NC-*B*H$(CN)_2$) ppm. **^{13}C{^{1}H} NMR** (100.6 MHz, $CDCl_3$, 298 K): δ = 166.5 (N*C*N), 127.7 ($C_{backbone}$), 35.3 (N-*C*H_3), 9.3 ($C_{backbone}$-*C*H_3) ppm. **IR** (ATR [cm^{-1}]): ν = 2962 (vw), 2950 (w), 2928 (m), 2863 (vw), 2408 (m, BH), 1657 (m), 1575 (w), 1436 (s), 1387 (s), 1366 (s), 1051 (vs), 847 (s), 694 (m), 574 (w).

Synthesis of a mixture of *trans*-[Ni$(Mes_2Im)_2$(NC-BH_2CN)$_2$] (*trans*-5b) and *trans*-[Ni$(Mes_2Im)_2$(NC-BH_2CN)Br] (*trans*-12b)

trans-[Ni$(Mes_2Im)_2Br_2$] (100 mg, 121 μmol, 1.0 eq.) and Ag[$BH_2(CN)_2$] (43.8 mg, 254 μmol, 2.1 eq.) were suspended in THF (5 mL) and ultrasonicated for 15 minutes. The solvent was removed *in vacuo* and the residue extracted, filtered, and washed with CH_2Cl_2 (3 x 10mL) over a pad of Celite. The solvent was removed *in vacuo* and the residue suspended and washed with *n*-hexane (3 x 10 mL) to give 40.0 mg of a yellow solid containing both *trans*-[Ni$(Mes_2Im)_2$(NC-BH_2CN)$_2$] (*trans*-**5b**) and [Ni$(Mes_2Im)_2$(NC-BH_2CN)Br] (*trans*-**12b**) in a ratio of 70:30. Single crystals suitable for X-ray diffraction were obtained by diffusion of *n*-hexane into a saturated solution of the crude product in CH_2Cl_2. **Yield**: 40.0 mg of a yellow solid containing *trans*-**5b** and *trans*-**12b** (70:30). *trans*-[Ni$(Mes_2Im)_2$(NC-BH_2CN)$_2$] (*trans*-**5b**):

Yield: 29% (27.9 mg, 35.0 *µ*mol). **^{1}H{^{11}B} NMR** (400.1 MHz, $CDCl_3$, 298 K): *δ* = 7.19 (s, 4H, aryl-C$H_{backbone}$), 7.00 (s, 8H, aryl-CH_{meta}), 2.40 (s, 12H, aryl-C$_{para}$CH_3), 2.07 (s, 24H, aryl-C$_{ortho}$CH_3), 1.18 (s, 4H, Ni-NC-BH_2CN) ppm. **^{11}B NMR** (128.5 MHz, $CDCl_3$, 298 K): *δ* = –40.9 (m, Ni-NC-*B*H_2CN) ppm. *trans*-[Ni(Mes_2Im)$_2$(NC-BH_2CN)Br] (*trans*-**12b**): **Yield**: 12% (12.1 mg, 14.5 *µ*mol). **^{1}H{^{11}B} NMR** (400.1 MHz, $CDCl_3$, 298 K): *δ* = 7.07 (s, 4H, aryl-CH$_{meta}$), 7.00 (s, 4H, aryl-CH$_{meta}$), 6.77 (s, 4H, C$H_{backbone}$), 2.56 (s, 12H, aryl-C$_{para}$CH_3), 1.95 (s, 12H, aryl-C$_{ortho}$CH_3), 1.83 (s, 12H, aryl-C$_{ortho}$CH_3), 1.05 (s, 2H, Ni-NC-BH_2CN) ppm. **^{11}B NMR** (128.5 MHz, $CDCl_3$, 298 K): *δ* = –42.0 ppm.

Synthesis of *cis*-[Ni(Me_2Im^{Me})$_2$(NC-BH_2CN)$_2$] (*cis*-13b)

trans-[Ni(Me_2Im^{Me})$_2$$Br_2$] (80.0 mg, 171 *µ*mol, 1.0 eq.) and Ag[$BH_2(CN)_2$] (59.2 mg, 342 *µ*mol, 2.0 eq.) were suspended in THF (5 mL) and ultrasonicated for 5 minutes. The precipitate was removed by filtration and extracted with THF (3 x 5 mL). The solvent of the filtrate was then removed *in vacuo* and the resulting residue was extracted with CH_2Cl_2 (3 x 10 mL) and filtered through a pad of Celite. The clear yellow filtrate was evaporated *in vacuo* to give crystalline *cis*-[Ni(Me_2Im^{Me})$_2$(NC-BH_2CN)$_2$] (*cis*-**13b**). The single crystals obtained this way were suitable for X-ray diffraction. **Yield**: 32% (30.0 mg, 214 *µ*mol). **Elemental Analysis**: $C_{18}H_{28}B_2N_8Ni$ [436.79 g/mol] found (calc.): C 49.88 (49.50), H 6.59 (6.46), N 25.23 (25.65)%. **^{1}H{^{11}B} NMR** (400.1 MHz, CD_3CN, 298 K): *δ* = 3.86 (s, 12H, N-CH_3), 2.04 (s, 12H, C$_{backbone}$-CH_3), 1.03 (q, $^{1}J_{B\text{-}H}$ = 82.6 Hz, 4H, Ni-NC-BH_2CN) ppm. **^{11}B NMR** (128.5 MHz, CD_3CN, 298 K): *δ* = –41.8 (t, $^{1}J_{B\text{-}H}$ = 82.6 Hz, *B*$H_2(CN)_2$) ppm. **^{13}C{^{1}H} NMR** (100.6 MHz, CD_3CN, 298 K): *δ* = 146.6 (N*C*N), 129.2 (*C*$_{backbone}$), 35.7 (N-*C*H_3), 9.0 (C$_{backbone}$-*C*H_3) ppm. **IR** (ATR [cm^{-1}]): *ν* = 2930 (w), 2392 (m, BH), 2239, (m, CN_{coord}), 2200 (w, $CN_{non\text{-}coord}$), 2193 (vw), 2190 (vw), 1769 (m), 1654 (m), 1580 (m), 1389 (s), 1083 (vs), 847 (m), 731 (s).

Synthesis of *trans*-[Ni(*i*Pr_2Im)$_2$(NC-BH_3)$_2$] (*trans*-14a)

A solution of *trans*-[Ni(*i*Pr_2Im)$_2$$Br_2$] (250.0 mg, 477 *µ*mol, 1.0 eq.) in THF (5 mL) was slowly added with a solution of Na[$BH_3(CN)$] (300.0 mg, 4.77 mmol, 10 eq.) in THF (10 mL) while stirring at –78 °C. After 3 hours the solvent was removed *in vacuo*. The residue was extracted and filtered over a pad of Celite with $CHCl_3$ (5 x 5 mL). The solvent of the filtrate was removed *in vacuo*. The resulting residue was suspended and washed with *n*-hexane (3 x 5 mL) and dried *in vacuo* to give *trans*-[Ni(*i*Pr_2Im)$_2$(NC-BH_3)$_2$] (*trans*-**14a**) as a yellow solid. The *cis*-isomer may be detected *via* NMR-spectroscopy in solution of the reaction mixture. **Yield**: 27% (56.8 mg, 128.3 *µ*mol). **Elemental Analysis**: $C_{20}H_{40}B_2N_6Ni$ [440.90 g/mol] found (calc.): C 54.20 (53.99), H 8.57 (9.06), N 19.14 (18.89)%. **^{1}H{^{11}B} NMR** (400.1 MHz, d_8-THF, 298 K):

δ = 6.85 (s, 4H, aryl-C*H*), 5.73 (sept, $^{3}J_{H\text{-}H}$ = 6.9 Hz, 4H, C$H_{methine}$), 1.55 (d, $^{3}J_{H\text{-}H}$ = 6.9 Hz, 24H, $C_{methine}$-CH_3), 0.17 (br. s, 6H, Ni-NC-BH_3) ppm. **^{11}B NMR** (128.5 MHz, d_8-THF, 298 K): δ = –43.4 (br. q, $^{1}J_{B\text{-}H}$ = 97.2 Hz, Ni-NC-*B*H_3) ppm. **^{13}C{^{1}H} NMR** (100.6 MHz, $CDCl_3$, 298 K): δ = 159.3 (Ni-$C_{carbene}$), 118.5 (aryl-*C*), 53.3 ($C_{methine}$), 23.8 ($C_{methine}$-*C*H_3) ppm. **IR** (ATR[cm^{-1}]): ν = 3158 (vw), 3128 (vw), 3105 (vw), 2982 (w), 2926 (w), 2854 (vw), 2357 (m, BH), 2213 (m, CN_{coord}), 1590 (m), 1464 (w), 1433 (m), 1421 (m), 1407 (m), 1394 (m), 1394 (m), 1300 (w), 1260 (w), 1212 (vs), 1180 (w), 1136 (w), 1119 (w), 1109 (vs), 1064 (m), 1033 (m), 1006 (m), 879 (w), 847 (w), 800 (m), 745 (s), 711 (s), 667 (m), 628 (m), 468 (m), 454 (m). *cis*-[Ni(*i*Pr_2Im)$_2$(NC-BH_3)$_2$] (*cis*-**14a**): **^{1}H{^{11}B} NMR** (400.1 MHz, CD_2Cl_2, 298 K): δ = 7.06 (s, 4H, aryl-C*H*), 5.56 (sept, $^{3}J_{H\text{-}H}$ = 6.8 Hz, 4H, C$H_{methine}$), 1.57 (d, $^{3}J_{H\text{-}H}$ = 6.8 Hz, 12H, $C_{methine}$-CH_3), 1.22 (d, $^{3}J_{H\text{-}H}$ = 6.8 Hz, 12H, $C_{methine}$-CH_3), 0.35 (br. s, 6H, Ni-NCBH_3) ppm. **^{11}B NMR** (128.5 MHz, CD_2Cl_2, 298 K): δ = –42.7 (br. q, $^{1}J_{B\text{-}H}$ = 91.2 Hz, Ni-NC-*B*H_3) ppm.

Synthesis of *cis*-/*trans*-[Ni(*i*Pr_2Im)$_2$(NC-BH_2CN)$_2$] (*cis*-/*trans*-14b)

A solution of *trans*-[Ni(*i*Pr_2Im)$_2$$Br_2$] (201.1 mg, 385 μmol, 1.0 eq.) in THF (5 mL) was added dropwise with a solution of K[BH_2(CN)$_2$] (80.0 mg, 770 μmol, 2.0 eq.) in THF (5 mL) while stirring at room temperature. After 12 hours the suspension was filtered and washed with THF (2 x 5 mL) through a pad of Celite. The solvent of the filtrate was removed *in vacuo* and the resulting residue was suspended and washed with *n*-hexane (3 x 10 mL). After drying *in vacuo* a mixture (61:39) of *cis*-**14b** and *trans*-**14b** is obtained as a yellow solid. Single crystals suitable for X-ray diffraction of *cis*-**14b** were obtained *via* diffusion of *n*-hexane to a saturated solution of the product in THF. **Yield**: 64% (121 mg, 245 μmol) of a *cis*-/*trans*-mixture of **14b** (61:39). **Elemental Analysis**: $C_{22}H_{38}B_2N_{80}Ni$ [494.92 g/mol] found (calc.): C 53.65 (53.39), H 6.86 (7.74), N 22.16 (22.64)%. **IR** (ATR [cm^{-1}]): ν = 3165 (vw), 3129 (vw), 3100 (vw), 2990 (m), 2936 (w), 2876 (w), 2379 (m, BH), 2238 (m, CN_{coord}), 2200 (w, $CN_{non\text{-}coord}$), 1567 (vw), 1429 (m), 1415 (m), 1398, (m), 1375 (m), 1210 (vs), 1081 (vs), 743 (m), 708 (s), 693 (s), 670 (m), 575 (w), 455 (w). *cis*-[Ni(*i*Pr_2Im)$_2$(NC-BH_2CN)$_2$] (*cis*-**14b**): **Yield**: 39% (73.8 mg, 149 μmol). **^{1}H{^{11}B} NMR** (400.1 MHz, CD_2Cl_2, 298 K): δ = 7.14 (br. s, 4H, aryl-C*H*), 5.48 (br. sept, $^{3}J_{H\text{-}H}$ = 6.5 Hz, 4H, -C*H*$(CH_3)_2$), 1.57 ppm (d, $^{3}J_{H\text{-}H}$ = 5.9 Hz, 12H, -CH(CH_3)$_2$), 1.24 (d, $^{3}J_{H\text{-}H}$ = 6.5 Hz, 12H, -CH(CH_3)$_2$), 1.01 (br. s, 4H, Ni-NC-BH_2CN) ppm. **^{11}B NMR** (128.5 MHz, CD_2Cl_2, 298 K): δ = –41.6 (br. t, $^{1}J_{B\text{-}H}$ = 89.9 Hz, Ni-NC-*B*H_2(CN)) ppm. **^{13}C{^{1}H} NMR** (100.6 MHz, CD_2Cl_2, 298 K): δ = 156.3 (Ni-$C_{carbene}$), 119.6 ($C_{backbone}$), 53.9 ($C_{methine}$), 23.8 $C_{methine}$-*C*H_3), 22.6 ($C_{methine}$-*C*H_3) ppm. *trans*-[Ni(*i*Pr_2Im)$_2$(NC-BH_2(CN))$_2$] (*trans*-**14b**): **Yield**: 25% (47.2 mg, 96 μmol). **^{1}H{^{11}B} NMR** (400.1 MHz, CD_2Cl_2, 298 K): δ = 7.14 (br. s, 4H, aryl-C*H*), 5.84 (sept, $^{3}J_{H\text{-}H}$ = 6.6 Hz, 4H, C$H_{methine}$), 1.73 (d, $^{3}J_{H\text{-}H}$ = 6.6 Hz, 24H, $C_{methine}$-CH_3), 1.02 (br. s, 4H, Ni-NC-BH_2CN) ppm. **^{11}B NMR** (128.5 MHz, CD_2Cl_2, 298 K): δ =

–41.6 (br. t, $^{1}J_{B\text{-}H}$ = 89.9 Hz, Ni-NC-*B*H_2(CN)) ppm. **^{13}C{^{1}H} NMR** (100.6 MHz, CD_2Cl_2, 298 K): δ = 147.6 (Ni-$C_{carbene}$), 120.7 (aryl-*C*), 53.9 ($C_{methine}$), 24.4 ($C_{methine}$-CH_3) ppm.

Synthesis of a mixture of *cis*-[Ni(*i*Pr$_2$Im)$_2${NC-BH(CN)$_2$}$_2$] (*cis*-14c), *cis*-[Ni(*i*Pr$_2$Im)$_2${NC-BH(CN)$_2$}Br] (*cis*-11c) and [Ni(*i*Pr$_2$Im)$_3${NC-BH(CN)$_2$}][BH(CN)$_3$] (16c)

A solution of *trans*-[Ni(*i*Pr$_2$Im)$_2$Br$_2$] (539 mg, 1.03 mmol, 1.0 eq.) in THF (5 mL) was slowly added to a solution of K[BH(CN)$_3$] (267 mg, 2.07 mmol, 2.0 eq.) in THF (5 mL) while stirring and room temperature. The resulting precipitate was removed *via* filtration through a pad of Celite and washed with THF (2 x 5 mL). The solvent was removed *in vacuo* and the residue was suspended and washed with *n*-hexane (2 x 10 mL). After drying *in vacuo* a yellow solid containing a mixture of *cis*-**11c**, *cis*-**14c**, **16c** and further unidentified side-products was obtained. Single crystals suitable for X-ray diffraction of *cis*-**11c** and **16c** were obtained by diffusion of *n*-hexane to a saturated solution of the product in THF. **Yield**: 311 mg of a crude yellow solid containing *cis*-**11c**, *cis*-**14c**, **16c** and unknown side-products. **IR** (ATR [cm^{-1}]): ν = 3170 (vw), 3137 (vw), 3108 (vw), 2977 (m), 2937 (w), 2879 (vw), 2399 (m, BH), 1605 (w), 1567 (w), 1429(m), 1398 (m), 1376 (m), 1212 (vs), 1050 (s), 737 (m), 700 (s), 686 (s), 672 (m), 575 (m), 442 (m). *cis*-[Ni(*i*Pr$_2$Im)$_2${NC-BH(CN)$_2$}$_2$] (*cis*-**14c**): **^{1}H{^{11}B} NMR** (400.1 MHz, d_8-THF, 298 K): δ = 7.29 (s, 4H, aryl-C*H*), 6.23 (br. sept, $^{3}J_{H\text{-}H}$ = 6.8 Hz, 4H, C$H_{methine}$), 1.73 (br. s, 2H, Ni-NC-B*H*(CN)$_2$), 1.71 (d, $^{3}J_{H\text{-}H}$ = 6.8 Hz, 12H, $C_{methine}$-CH_3), 1.66 (d, $^{3}J_{H\text{-}H}$ = 6.8 Hz, 12H, $C_{methine}$-CH_3) ppm. **^{11}B NMR** (128.5 MHz, d_8-THF, 298 K): δ = –39.6 (d, $^{1}J_{B\text{-}H}$ = 90.3 Hz, Ni-NC-*B*H(CN)$_2$) ppm.**^{13}C{^{1}H} NMR** (100.6 MHz, d_8-THF, 298K): δ = 162.7 (Ni-$C_{carbene}$), 119.2 (aryl-*C*), 53.5 ($C_{methine}$), 23.5 ($C_{methine}$-CH_3), 22.7 ($C_{methine}$-CH_3) ppm. [Ni(*i*Pr$_2$Im)$_3${NC-BH(CN)$_2$}][BH(CN)$_3$] (**16c**): **^{1}H{^{11}B} NMR** (400.1 MHz, $(CD_3)_2CO$, 298 K): δ = 7.79 (s, 2H, aryl-C*H*), 7.74 (s, 4H, aryl-C*H*), 5.45 (br. m, 4H, C$H_{methine}$), 5.20 (sept, $^{3}J_{H\text{-}H}$ = 6.6 Hz, 2H, C$H_{methine}$), 2.65 (d, $^{3}J_{H\text{-}H}$ = 6.6 Hz, 12H, $C_{methine}$-CH_3), 1.35 (br. m, 12H, $C_{methine}$-CH_3), 1.19 (br. m, 12H, $C_{methine}$-CH_3) ppm. **^{11}B NMR** (128.5 MHz, $(CD_3)_2CO$, 298 K): δ = –38.9 (d, $^{1}J_{B\text{-}H}$ = 95.8 Hz, Ni-NC-*B*H(CN)$_2$), –40.0 (d, $^{1}J_{B\text{-}H}$ = 96.7 Hz, [*B*H(CN)$_3$]$^-$) ppm.

Synthesis of *trans*-[Ni(*i*Pr$_2$Im^{Me})$_2$(NC-BH$_2$CN)$_2$] (*trans*-15b)

A solution of *trans*-[Ni(*i*Pr$_2$Im^{Me})$_2$Br$_2$] (100.0 mg, 173 μmol, 1.0 eq.) in CH_2Cl_2 (15 mL) was slowly added to Ag[BH$_2$(CN)$_2$] (59.7 mg, 345 μmol, 2.0 eq.) and stirred for 30 minutes. The reaction was filtered through a pad of Celite and washed with CH_2Cl_2 (5 mL). The solvent of the filtrate was removed *in vacuo* and the residue was suspended and washed with *n*-hexane (5 x 3 mL). After drying *in vacuo* a yellow solid is obtained containing *trans*-[Ni(*i*Pr$_2$Im^{Me})$_2$(NC-BH$_2$CN)$_2$] (*trans*-**15b**) and [H*i*Pr$_2$Im^{Me}][BH$_2$(CN)$_2$] (50:50). Single crystals suitable for X-ray

diffraction were obtained by diffusion of *n*-hexane into a saturated solution of the product in CH_2Cl_2. **Yield**: 42.0 mg of a yellow solid containing *trans*-**15b** and [H*i*Pr$_2$Im^{Me}][$BH_2(CN)_2$] (50:50). **IR** (ATR [cm^{-1}]): ν = 2984 (m), 2937 (m), 2410 (s, BH), 2379 (s, BH), 2233 (m, CN_{coord}), 2196 (w, $CN_{non\text{-}coord}$), 1634 (w), 1556 (w), 1373 (s), 1297 (s), 1138 (m), 1104 (m), 1078 (vs), 909 (w), 754 (m), 716 (w), 647 (w), 545 (w), 465 (w). *trans*-[Ni(*i*Pr$_2$Im^{Me})$_2$(NC-$BH_2CN)_2$] (*trans*-**15b**): **Yield**: 31% (29.0 mg, 52.8 μmol). **^{1}H{^{11}B} NMR** (400.1 MHz, $CDCl_3$, 298 K): δ = 6.21 (sept, 4H, $^3J_{C\text{-}H}$ = 7.1 Hz, C$H_{methine}$), 2.22 (s, 12H, $C_{backbone}$-CH_3), 1.84 (d, 24H, $^3J_{C\text{-}H}$ = 7.1 Hz, $C_{methine}$-CH_3), 1.08 (s, 4H, Ni-NC-BH_2CN) ppm. **^{11}B NMR** (128.5 MHz, $CDCl_3$, 298 K): δ = –41.6 (t, $^1J_{B\text{-}H}$ = 92.9 Hz, Ni-NC-*B*H_2CN) ppm. **^{13}C{^{1}H} NMR** (100.6 MHz, $CDCl_3$, 298K): δ = 154.3 (N*C*N), 127.7 ($C_{backbone}$), 53.8 (N-*C*H_3), 22.5 ($C_{backbone}$-*C*H_3), 10.4 ($C_{methine}$-*C*H_3) ppm. [H*i*Pr$_2$Im^{Me}][$BH_2(CN)_2$]: **Yield**: 31% (13.0 mg, 52.8 μmol). **^{1}H{^{11}B} NMR** (400.1 MHz, $CDCl_3$, 298 K): δ = 8.63 (s, 1H, NC*H*N), 4.49 (sept, $^3J_{C\text{-}H}$ = 6.5 Hz, 2H, C$H_{methine}$), 2.19 (s, 6H, $C_{backbone}$-CH_3), 1.57 (d, $^3J_{C\text{-}H}$ = 6.5 Hz, 12H, $C_{methine}$-CH_3), 1.24 (s, 2H, [B$H_2(CN)_2]^-$) ppm. **^{11}B NMR** (128.5 MHz, $CDCl_3$, 298 K): δ = –41.8 (t, $^1J_{B\text{-}H}$ = 90.9 Hz, [*B*$H_2(CN)_2]^-$) ppm.

3 NMR Section

3.1 General Information

NMR spectra were recorded at 298 K using Bruker Avance 400 (^{1}H, 400.1 MHz; ^{13}C, 100.6 MHz; ^{11}B, 128.5 MHz). Chemical shifts are listed in parts per million (ppm) and reported relative to TMS. ^{1}H NMR spectra were referenced via residual proton resonances of the deuterated solvents (C_6D_5H: 7.16 ppm, C_4D_7HO: 3.58 ppm, 1.72 ppm, CD_2HCN: 1.94 ppm, $CDHCl_2$: 5.32 ppm, $CHCl_3$: 7.26 ppm, $(CD_3)(CD_2H)SO$: 2.50 ppm ppm, $(CD_3)(CD_2H)CO$: 2.05); whereas $^{13}C\{^{1}H\}$ NMR spectra are reported relative to TMS using the natural abundance carbon resonances (C_6D_6: 128.06 ppm; d_8-THF: 67.21 ppm, 25.31 ppm; CD_3CN: 1.32 ppm, 118.26 ppm; CD_2Cl_2: 53.84 ppm, $CDCl_3$: 77.16 ppm, d_6-DMSO: 39.52 ppm, $(CD_3)_2CO$: 29.84 ppm, 206.26 ppm). ^{11}B NMR spectra were referenced relative to external $BF_3{\cdot}OEt_2$.

3.2 NMR Spectra

$[Ni(Me_2Im^{Me})_4][BH(CN)_3]_2$ (1c)

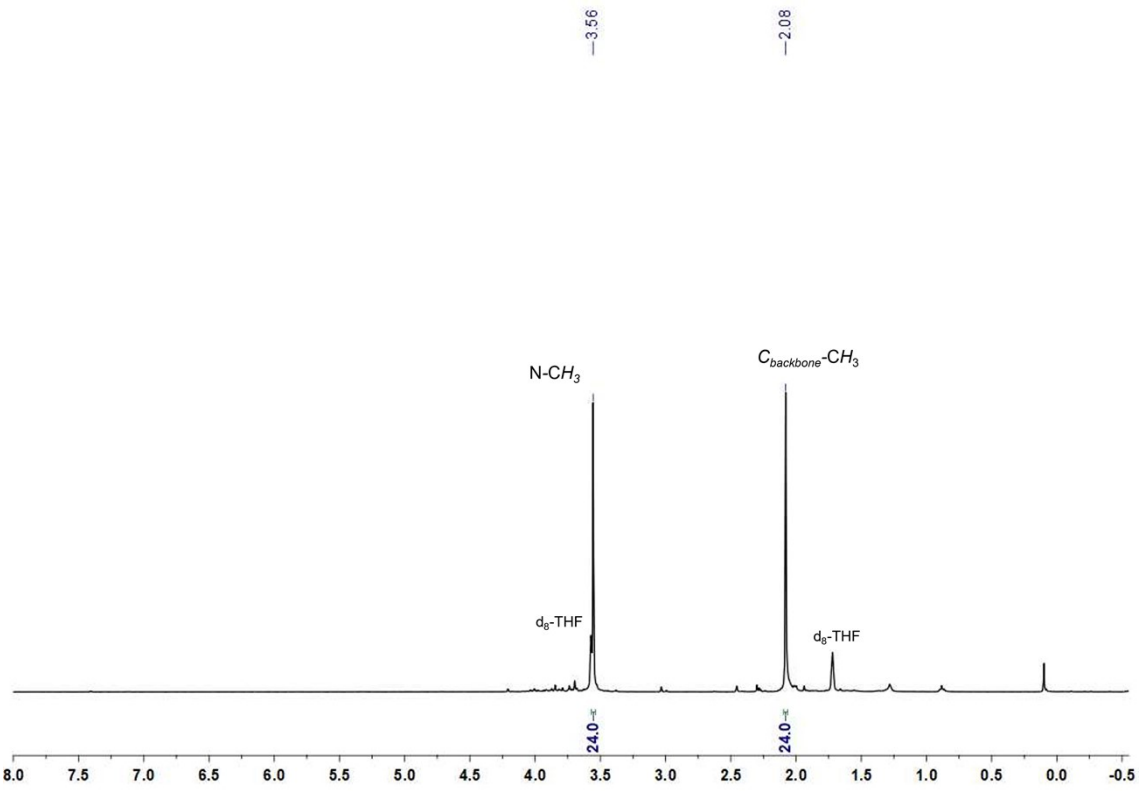

Figure S2. ^{1}H NMR spectrum of $[Ni(Me_2Im^{Me})_4][BH(CN)_3]_2$ (**1c**) in d_8-THF.

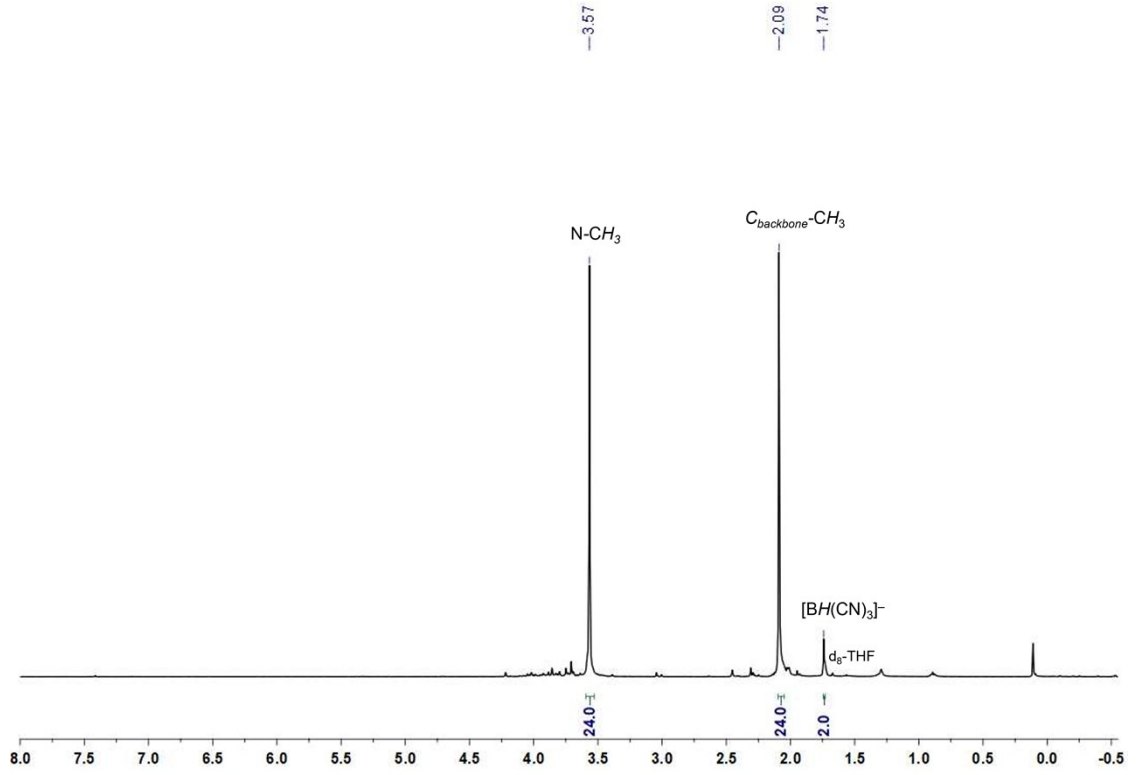

Figure S3. ^{1}H{^{11}B} NMR spectrum of $[Ni(Me_2Im^{Me})_4][BH(CN)_3]_2$ (**1c**) in d_8-THF.

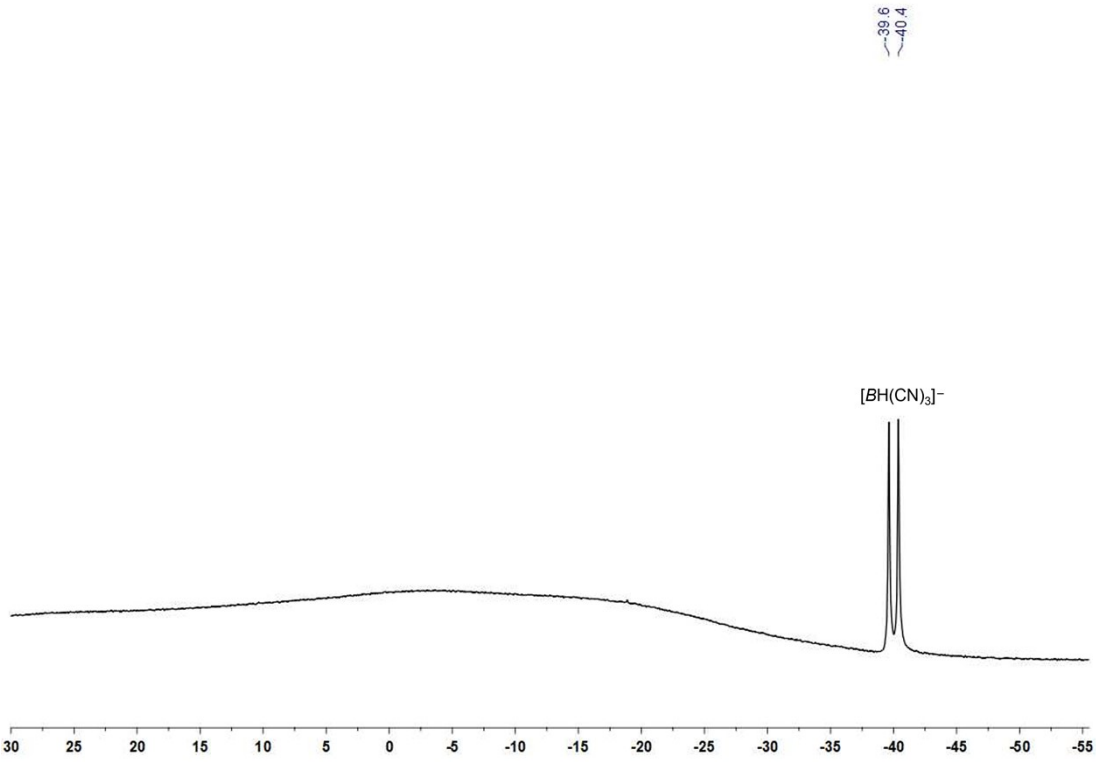

Figure S4. ^{11}B NMR spectrum of $[Ni(Me_2Im^{Me})_4][BH(CN)_3]_2$ (**1c**) in d_8-THF.

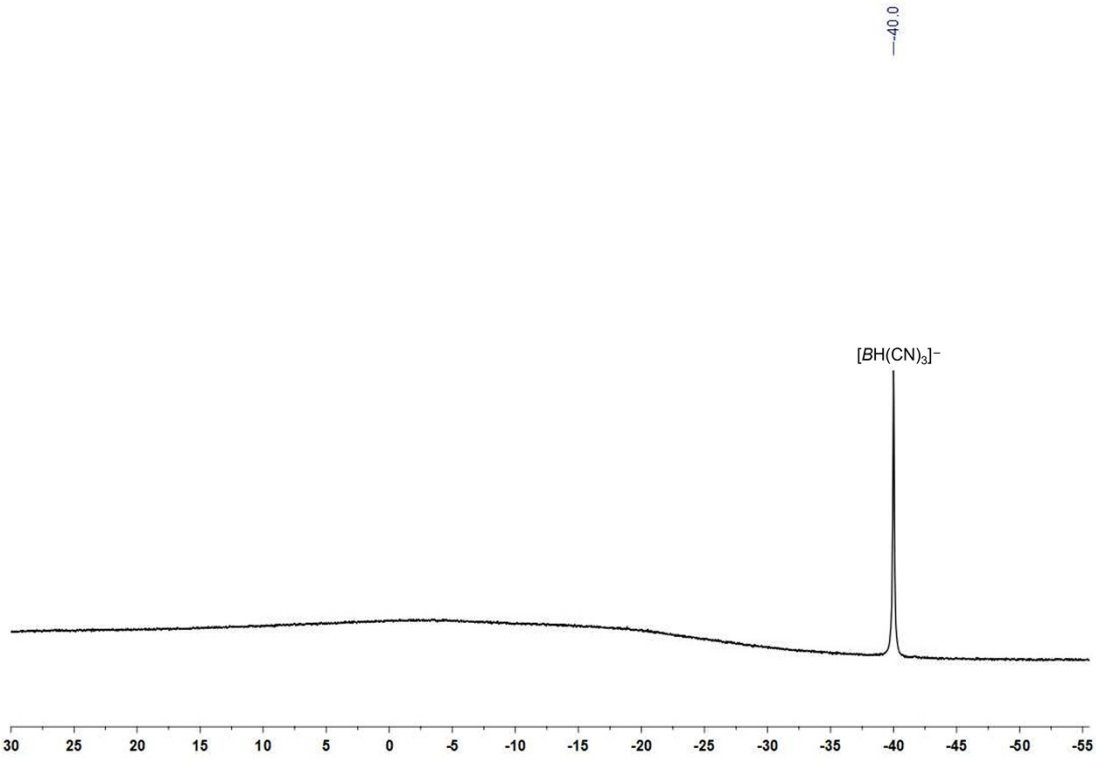

Figure S5. $^{11}B\{^1H\}$ NMR spectrum of $[Ni(Me_2Im^{Me})_4][BH(CN)_3]_2$ (**1c**) in d_8-THF.

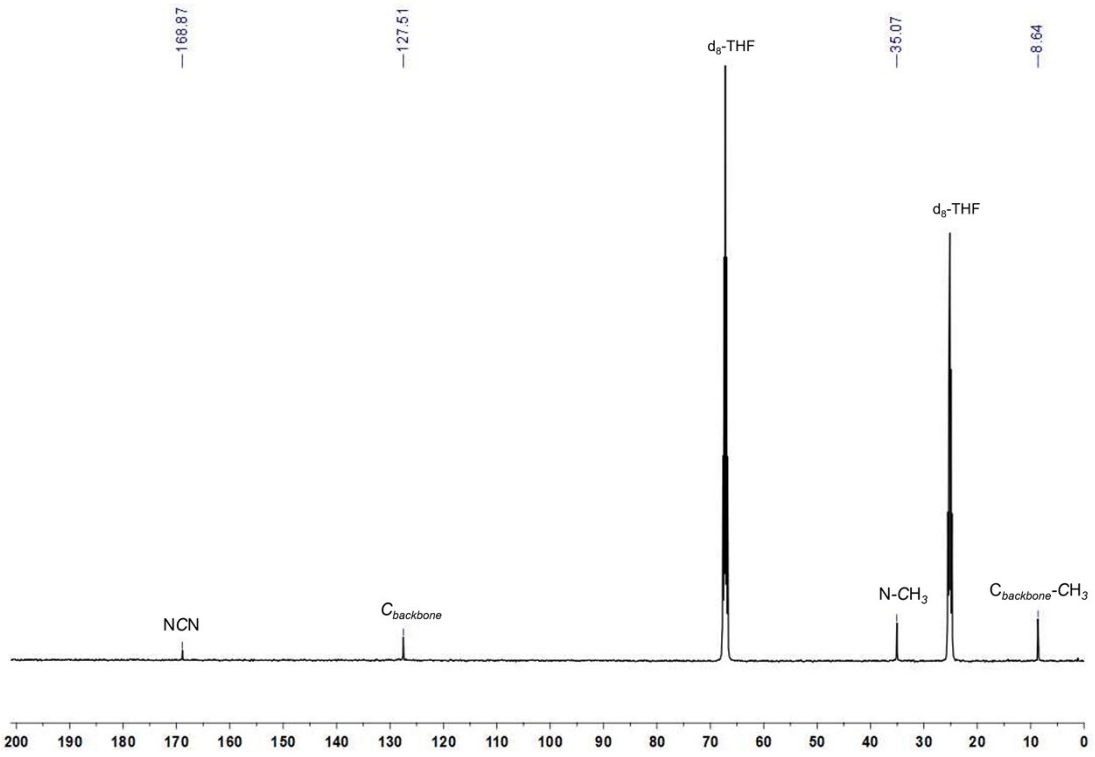

Figure S6. $^{13}C\{^{1}H\}$ NMR spectrum of $[Ni(Me_2Im^{Me})_4][BH(CN)_3]_2$ (**1c**) in d_8-THF. B-CN groups were not detected.

$[Ni(Me_2Im^{Me})_4][B(CN)_4]_2$ (1d)

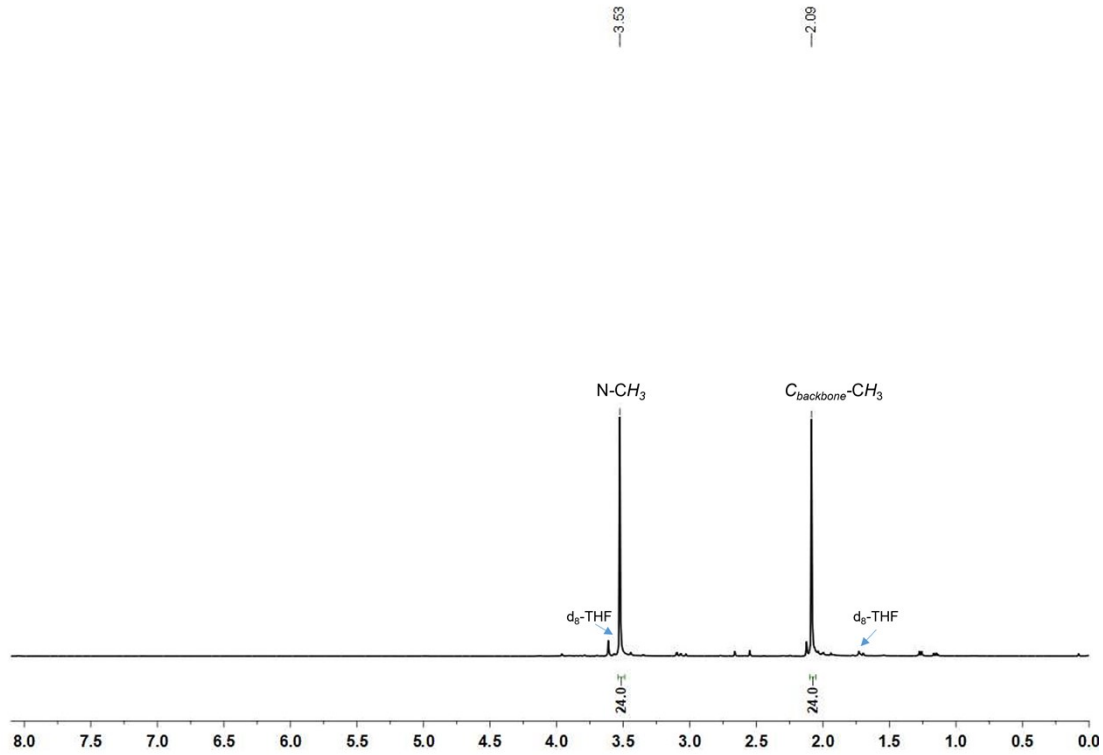

Figure S7. ^{1}H NMR spectrum of $[Ni(Me_2Im^{Me})_4][B(CN)_4]_2$ (**1d**) in d_8-THF.

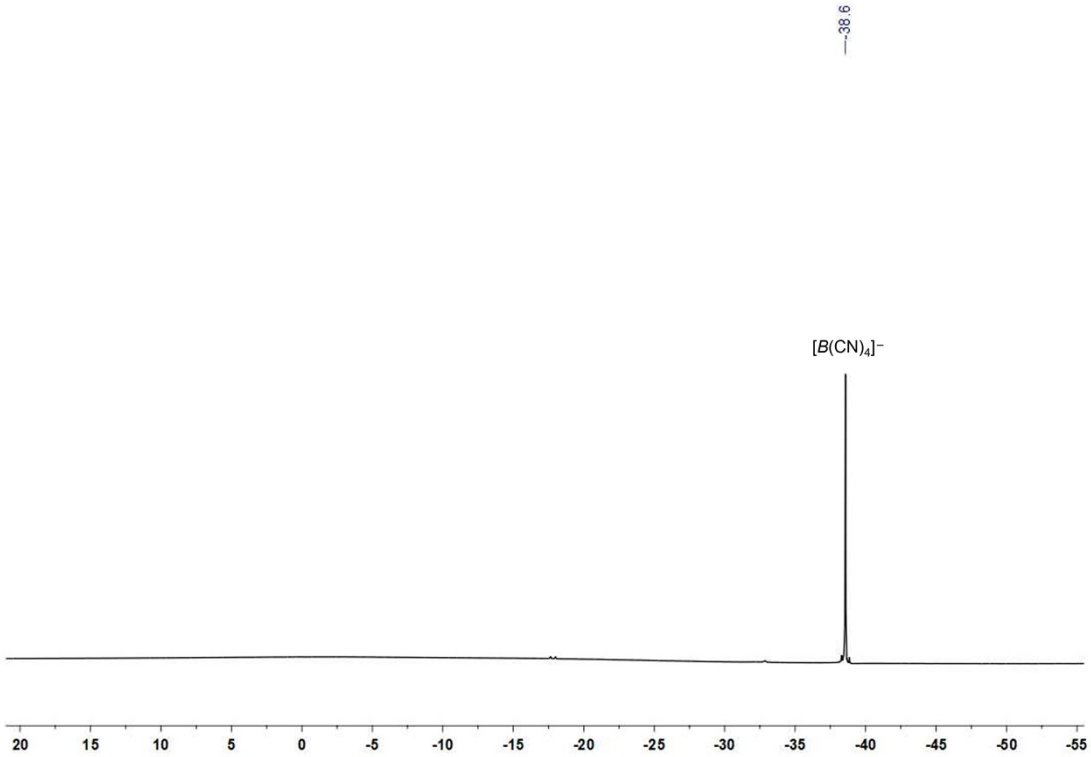

Figure S8. ^{11}B NMR spectrum of $[Ni(Me_2Im^{Me})_4][B(CN)_4]_2$ (**1d**) in d_8-THF.

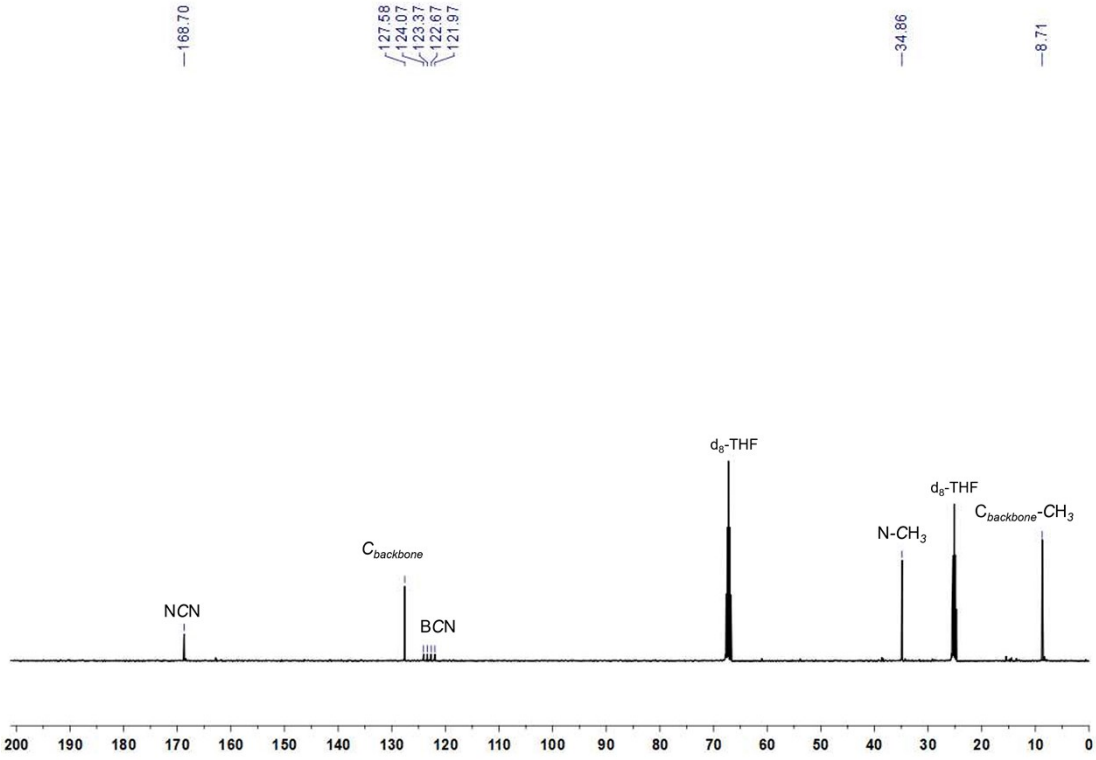

Figure S9. $^{13}C\{^1H\}$ NMR spectrum of $[Ni(Me_2Im^{Me})_4][B(CN)_4]_2$ (**1d**) in d_8-THF.

[Ni(*i*Pr$_2$Im)$_4$][BH(CN)$_3$]$_2$ (2c)

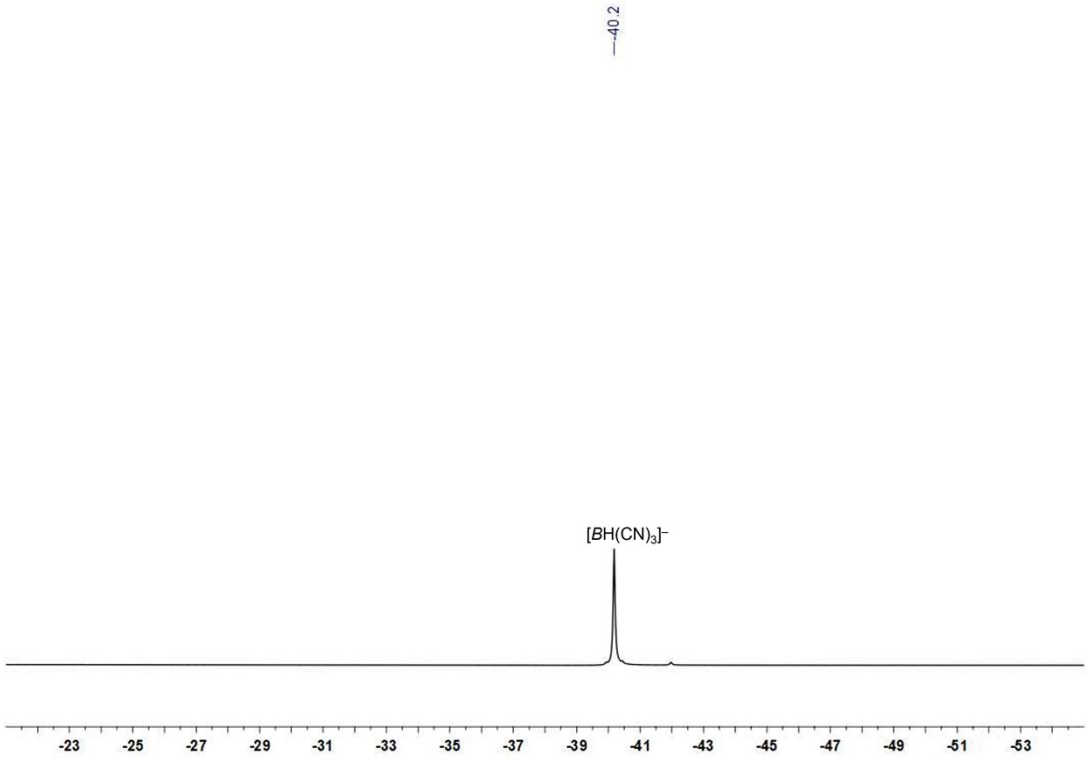

Figure S10. $^{11}B\{^1H\}$ NMR spectrum of a mixture of [Ni(*i*Pr$_2$Im)$_4$][BH(CN)$_3$]$_2$ (**2c**) with unknown side-products in CD_3CN.

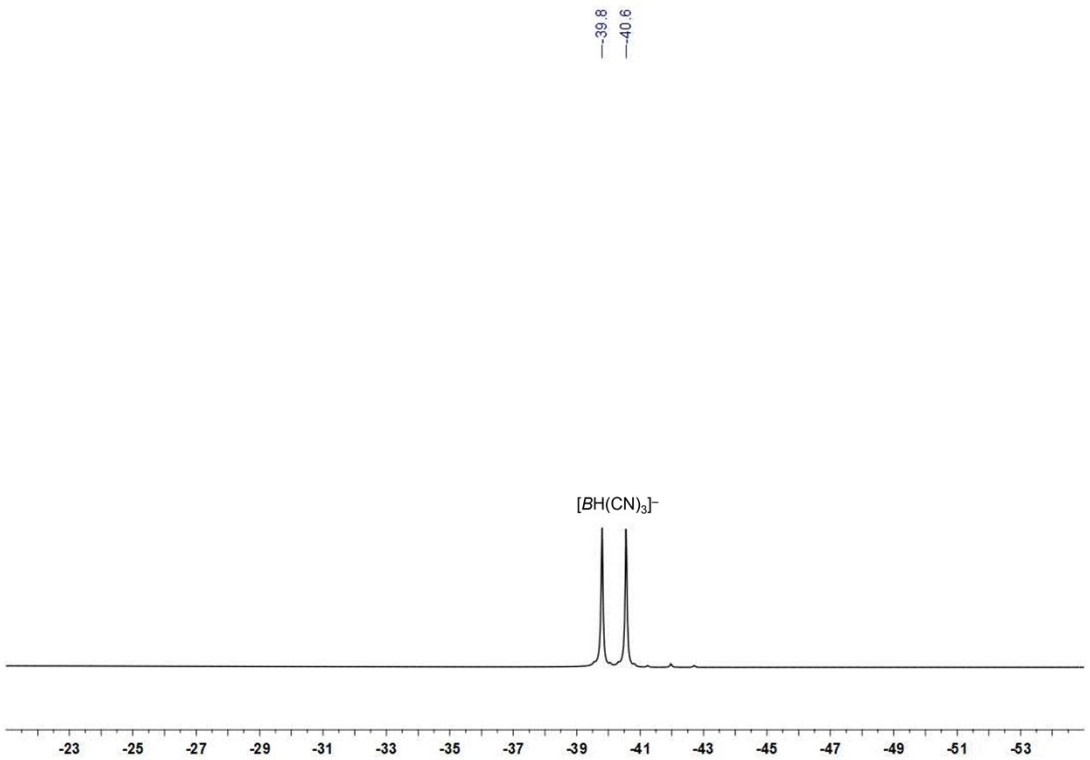

Figure S11. ^{11}B NMR spectrum of a mixture of [Ni(*i*Pr$_2$Im)$_4$][BH(CN)$_3$]$_2$ (**2c**) with unknown side-products in CD_3CN.

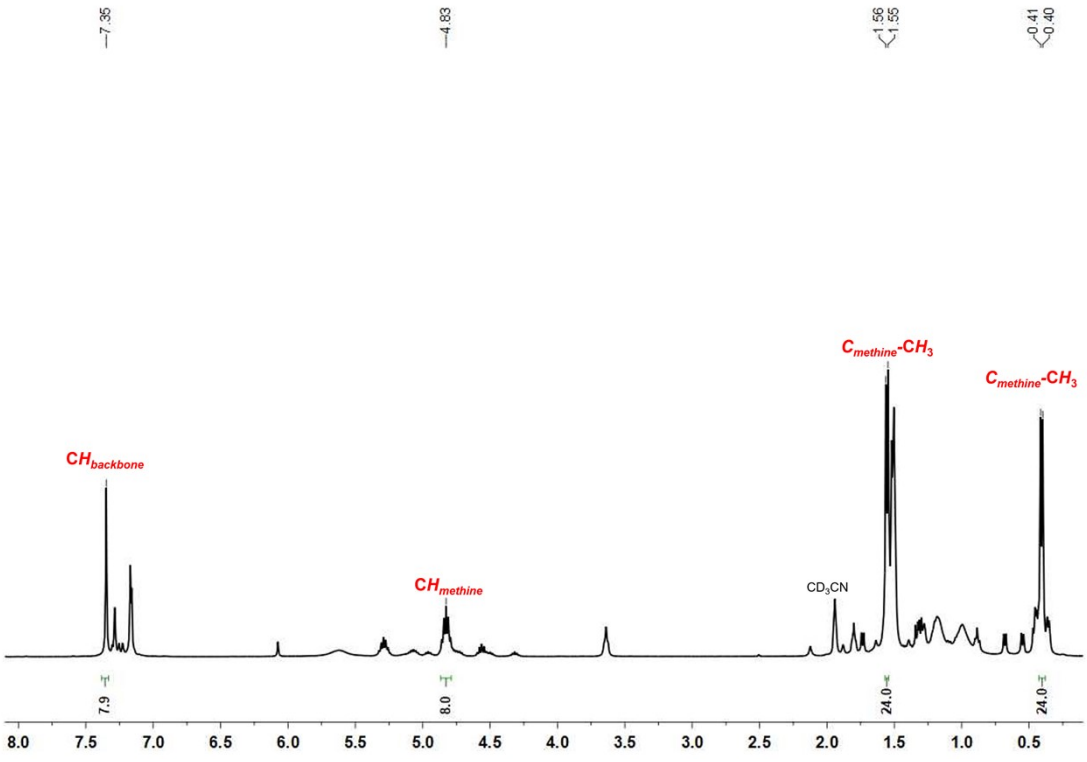

Figure S12. ^{1}H NMR spectrum of a mixture containing [Ni(*i*Pr$_2$Im)$_4$][BH(CN)$_3$]$_2$ (**2c**) in CD_3CN.

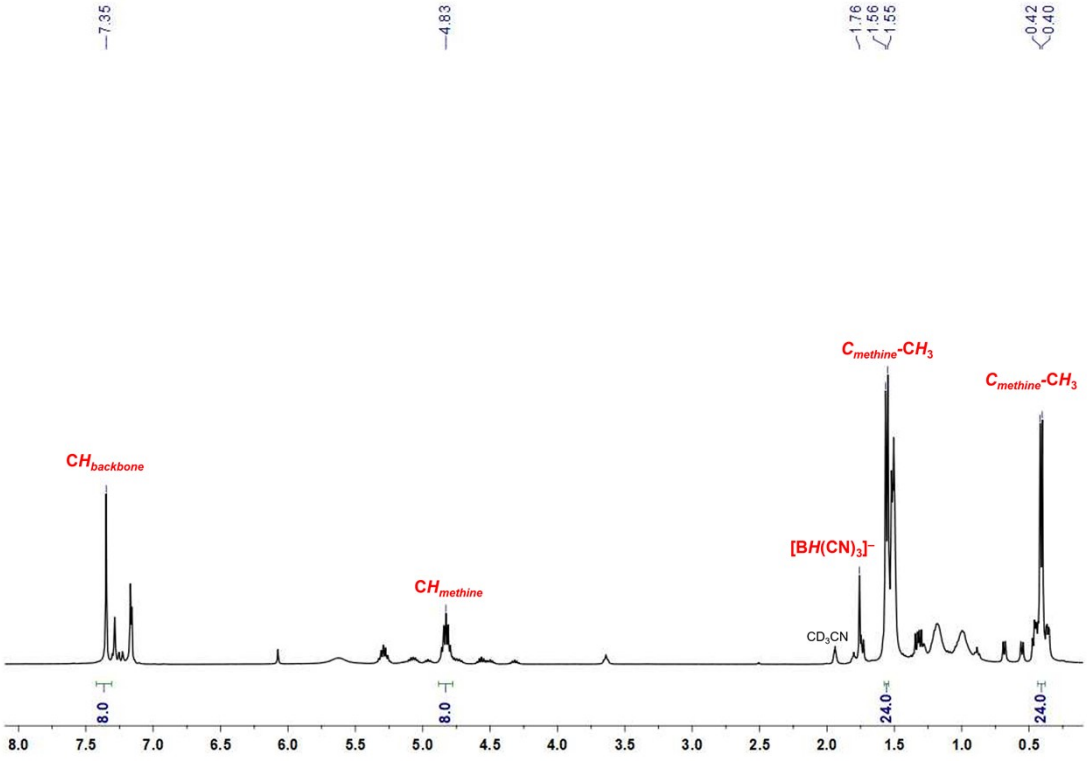

Figure S13. ^{1}H{^{11}B} NMR spectrum of a mixture containing [Ni(*i*Pr$_2$Im)$_4$][BH(CN)$_3$]$_2$ (**2c**) in CD_3CN.

[Ni(*i*Pr$_2$Im)$_4$][B(CN)$_4$]$_2$ (2d)

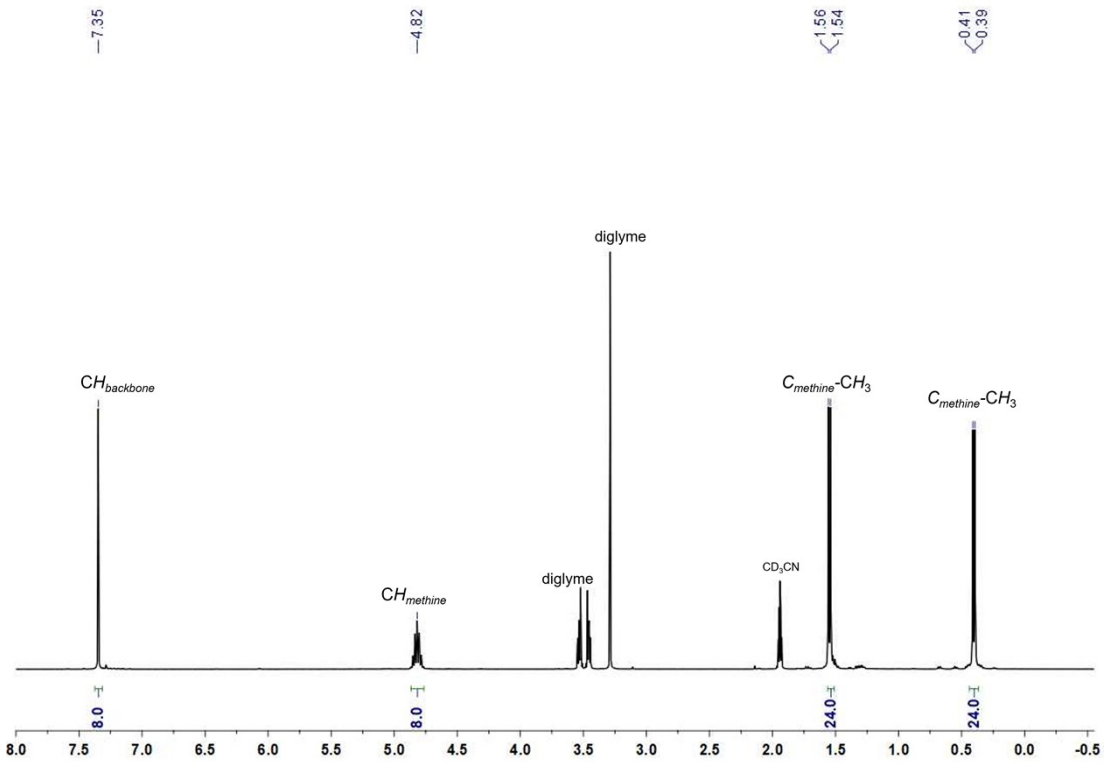

Figure S14. ^{1}H NMR spectrum of [Ni(*i*Pr$_2$Im)$_4$][B(CN)$_4$]$_2$ (**2d**) in CD_3CN.

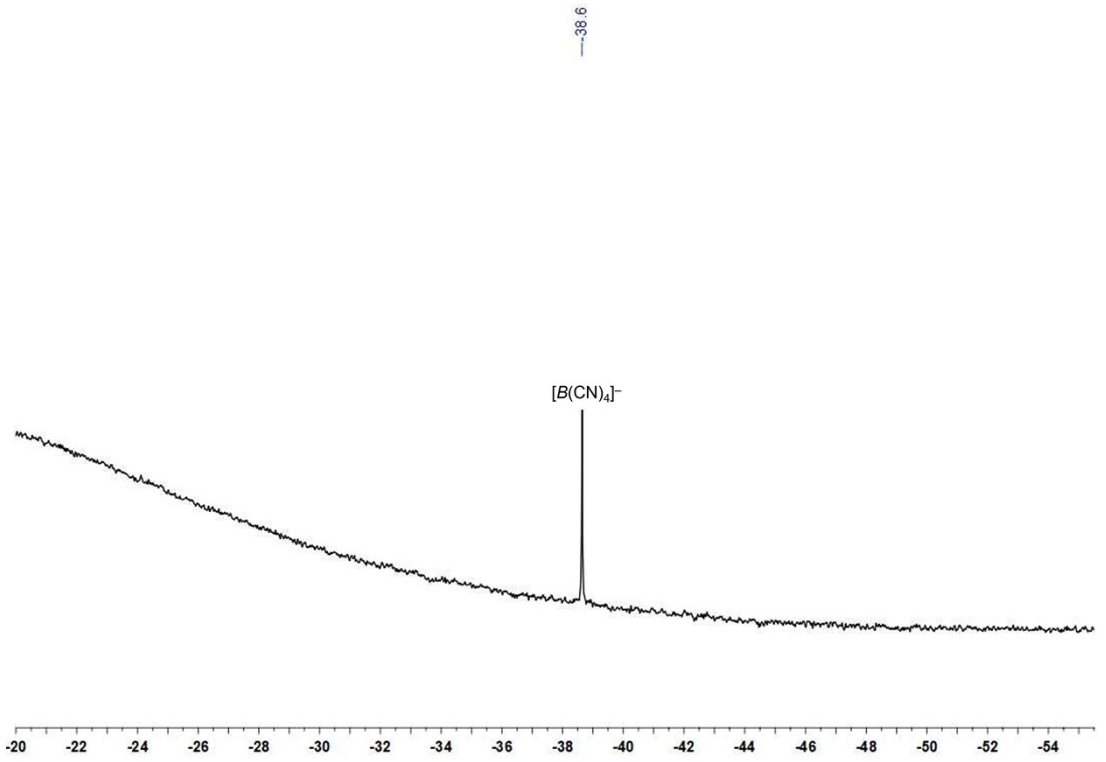

Figure S15. ^{11}B NMR spectrum of [Ni(*i*Pr$_2$Im)$_4$][B(CN)$_4$]$_2$ (**2d**) in CD_3CN.

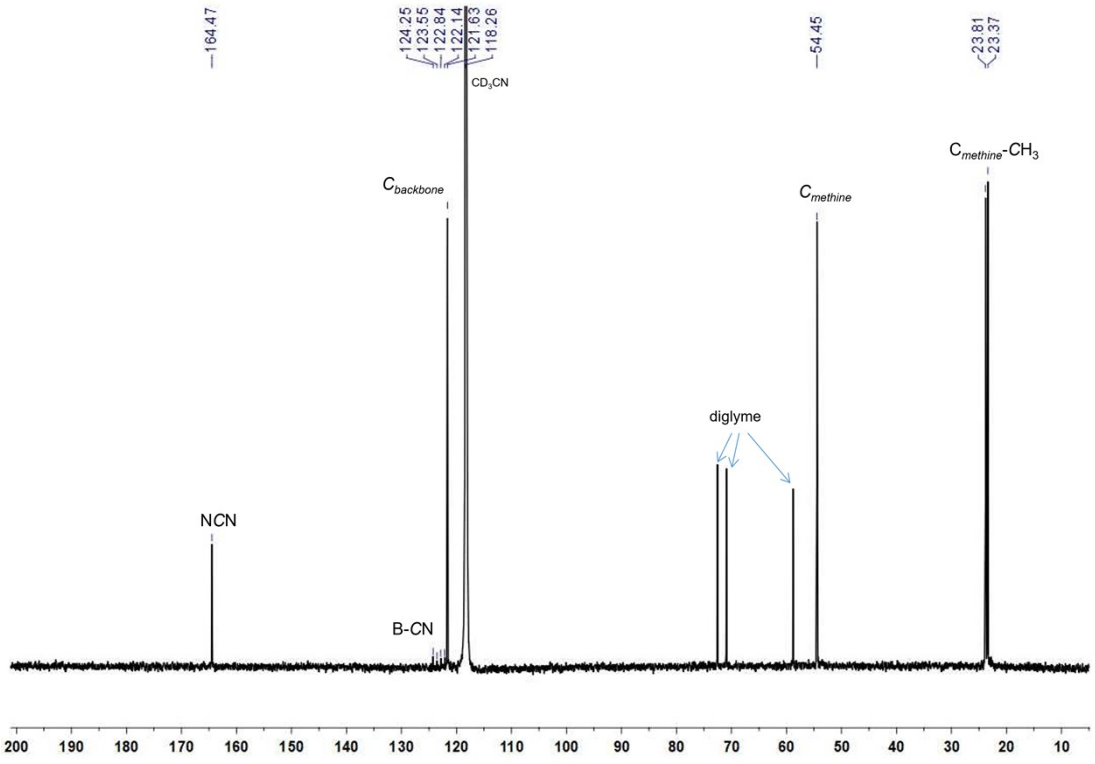

Figure S16. $^{13}C\{^{1}H\}$ NMR spectrum of $[Ni(i\text{Pr}_2\text{Im})_4][B(CN)_4]_2$ (**2d**) in CD_3CN.

$[Ni(i\text{Pr}_2\text{Im}^{Me})_3(NC\text{-}BH_2CN)][BH_2(CN)_2]$ (3b)

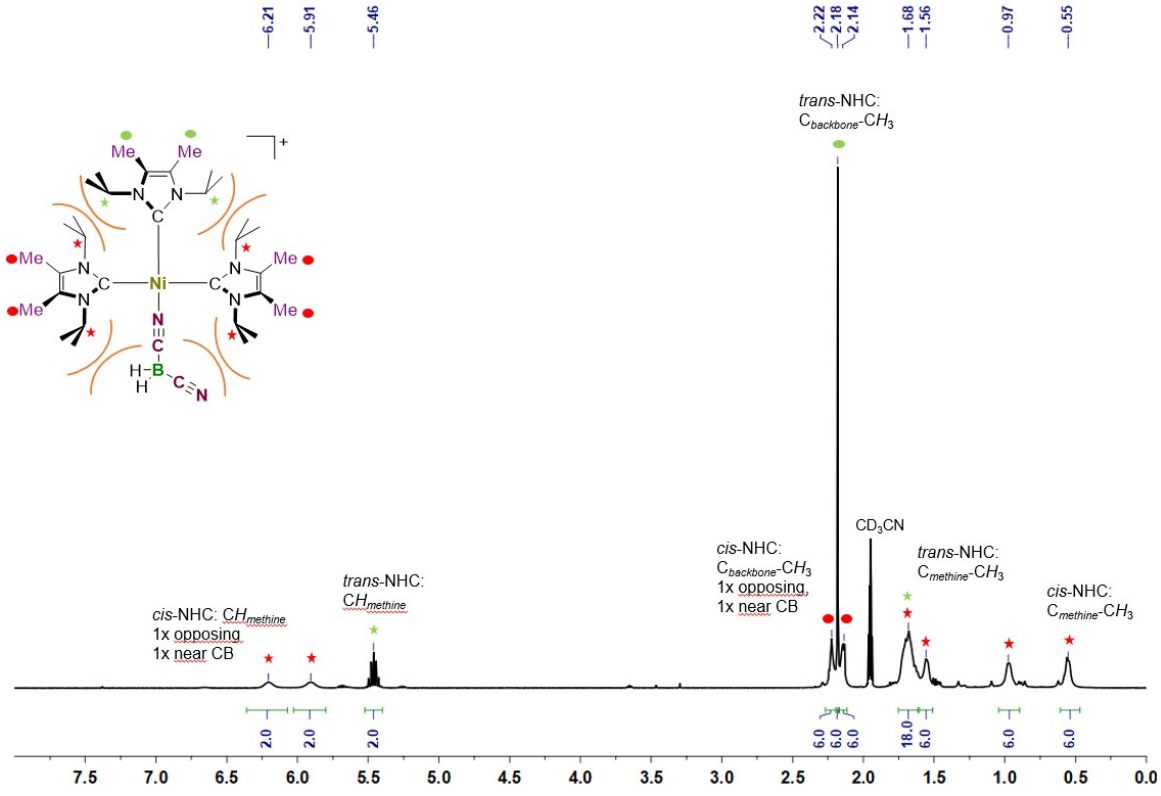

Figure S17. ^{1}H NMR spectrum of $[Ni(i\text{Pr}_2\text{Im}^{Me})_3(NC\text{-}BH_2CN)][BH_2(CN)_2]$ (**3b**) in CD_3CN. A detailed explanation of the NMR spectroscopic data of **3b** is given in the captions of Figure S23.

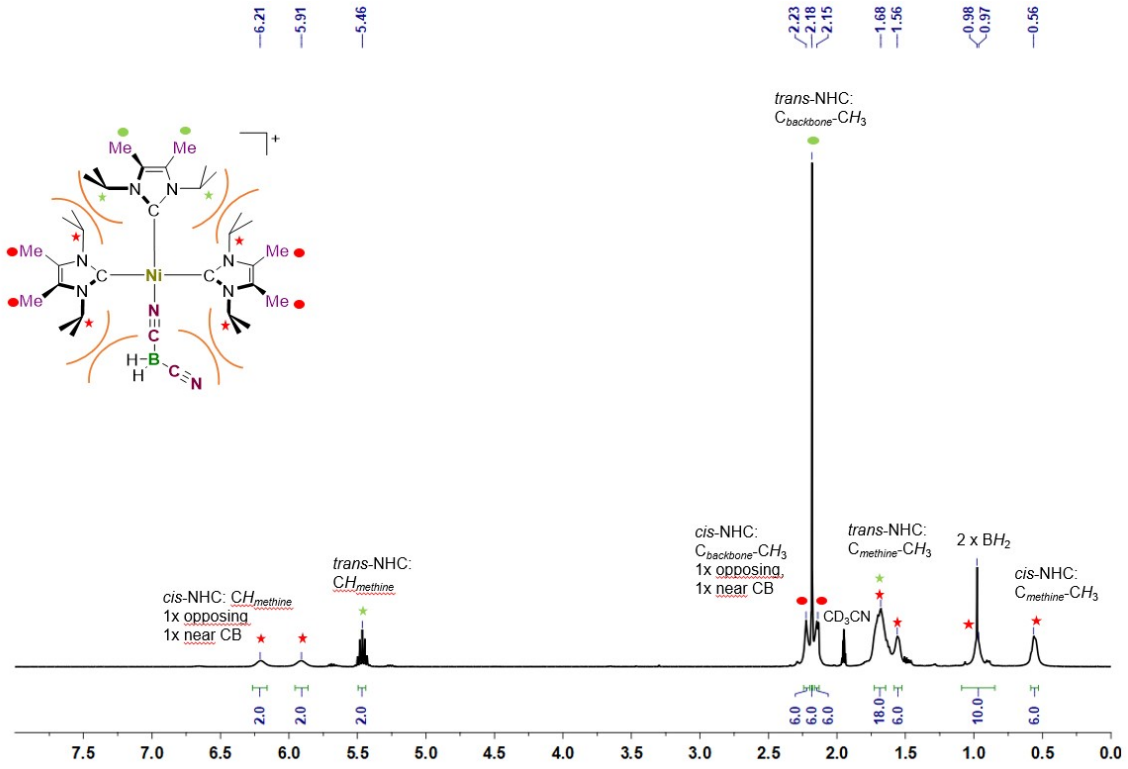

Figure S18. $^{1}H\{^{11}B\}$ NMR spectrum of $[Ni(iPr_2Im^{Me})_3(NC\text{-}BH_2CN)][BH_2(CN)_2]$ (**3b**) in CD_3CN. A detailed explanation of the NMR spectroscopic data of **3b** is given in the sub-captions below Figure S23.

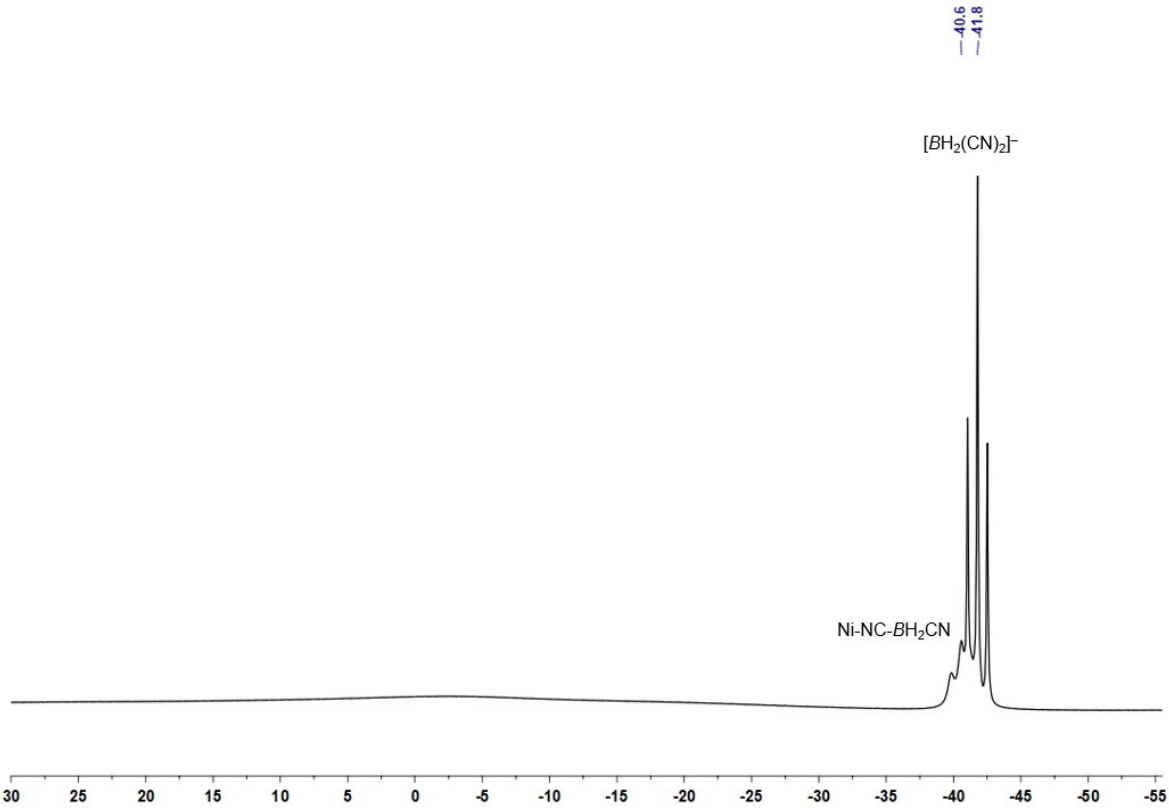

Figure S19. ^{11}B NMR spectrum of $[Ni(iPr_2Im^{Me})_3(NC\text{-}BH_2CN)][BH_2(CN)_2]$ (**3b**) in CD_3CN. A detailed explanation of the NMR spectroscopic data of **3b** is given in the sub-captions below Figure S23.

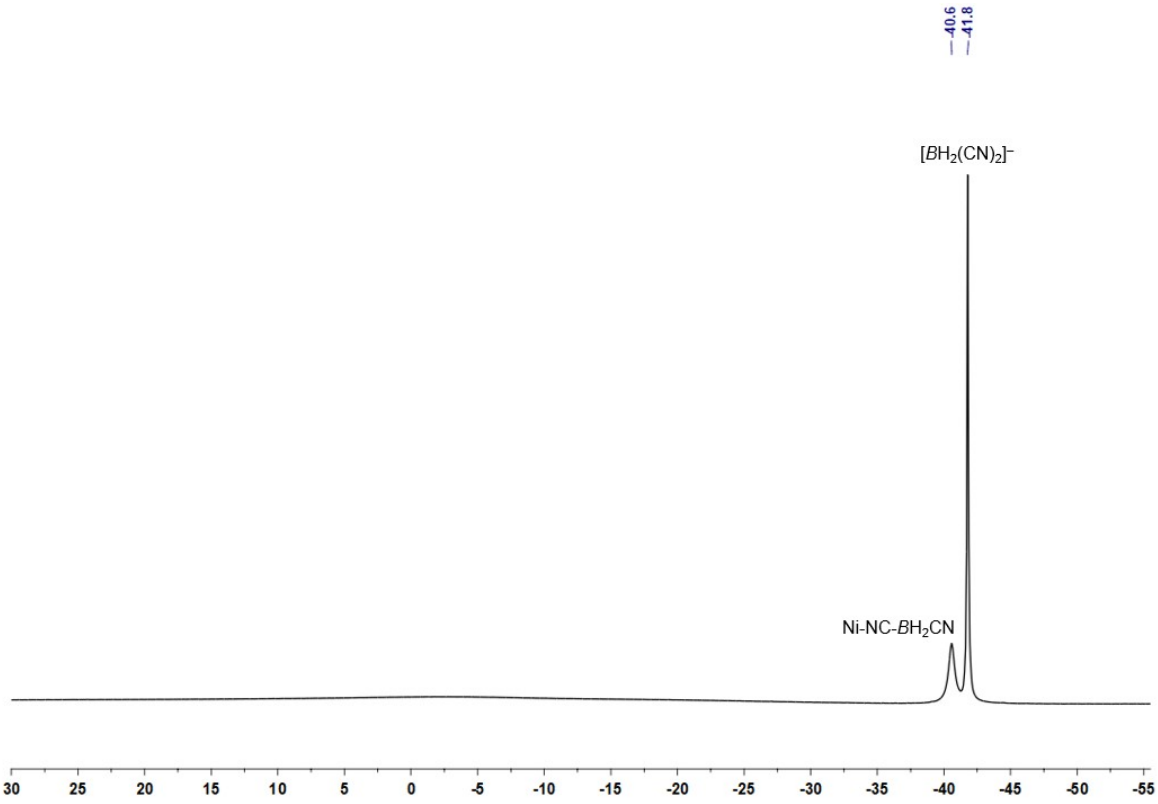

Figure S20. $^{11}B\{^{1}H\}$ NMR spectrum of [Ni(*i*Pr$_2$Im^{Me})$_3$(NC-BH$_2$CN)][BH$_2$(CN)$_2$] (**3b**) in CD$_3$CN. A detailed explanation of the NMR spectroscopic data of **3b** is given in the sub-captions below Figure S23.

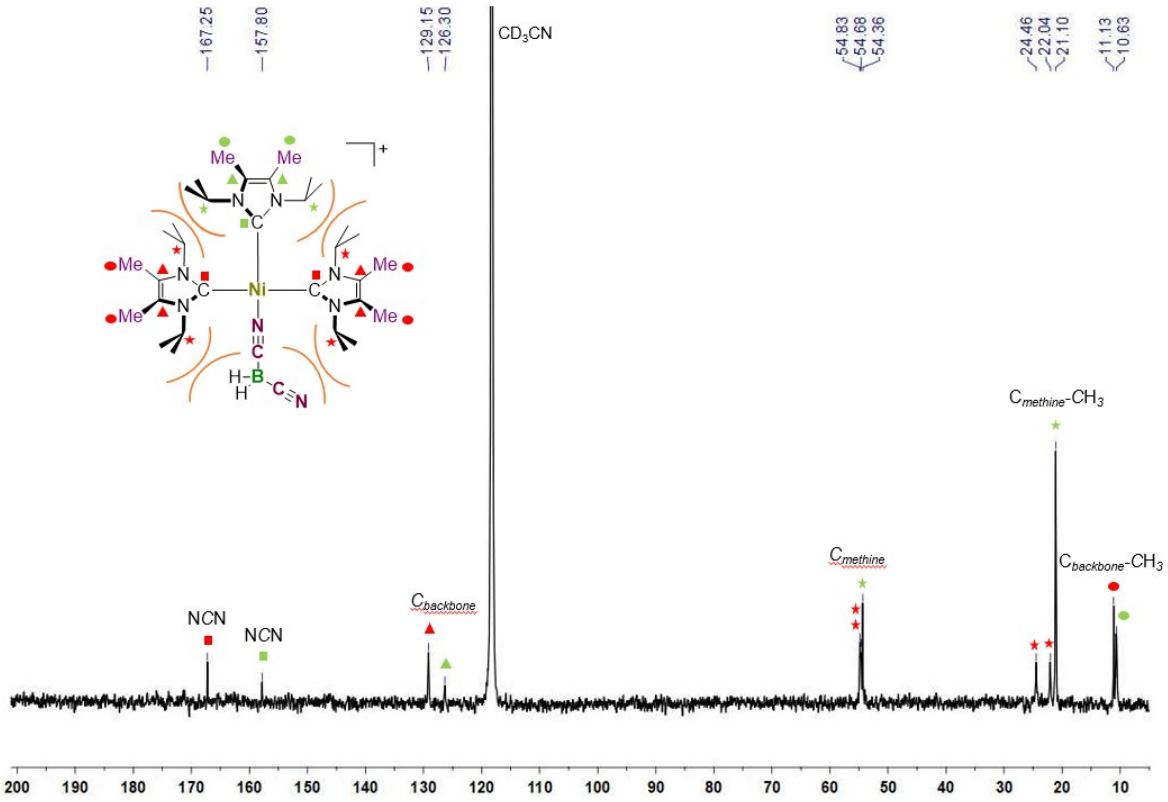

Figure S21. $^{13}C\{^{1}H\}$ NMR spectrum of [Ni(*i*Pr$_2$Im^{Me})$_3$(NC-BH$_2$CN)][BH$_2$(CN)$_2$] (**3b**) in CD$_3$CN. B-CN groups were not detected. A detailed explanation of the NMR spectroscopic data of **3b** is given in the sub-captions below Figure S23.

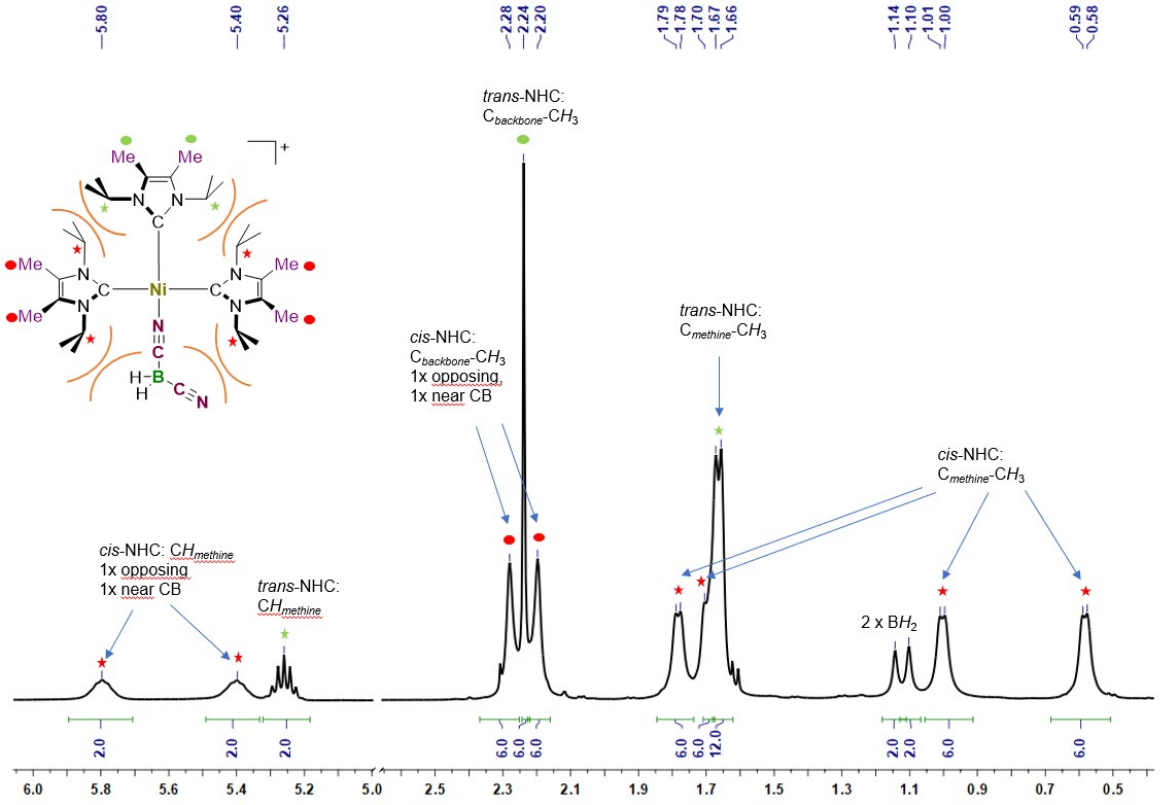

Figure S22. $^{1}H\{^{11}B\}$ NMR spectrum of $[Ni(i\mathrm{Pr}_2\mathrm{Im}^{Me})_3(NC\text{-}BH_2CN)][BH_2(CN)_2]$ (**3b**) in $CDCl_3$. A detailed explanation of the NMR spectroscopic data of **3b** is given in the sub-captions below Figure S23.

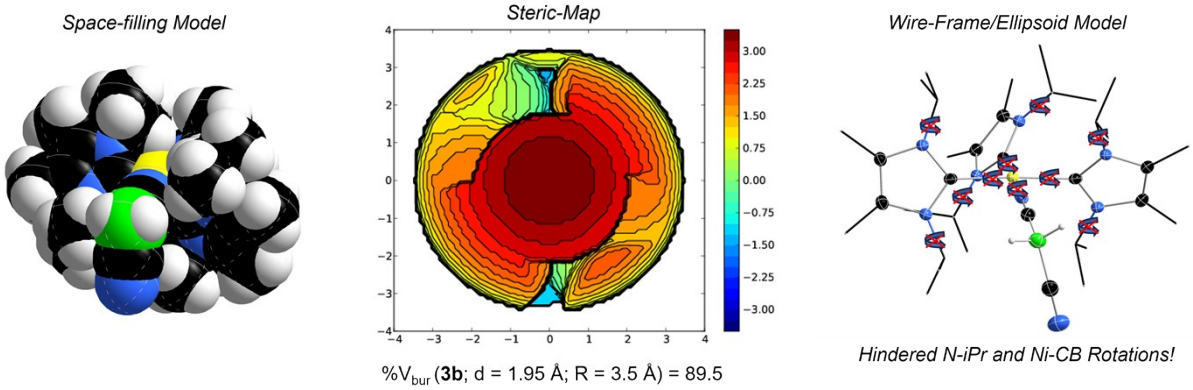

Figure S23. Molecular structure of **3b** (anion omitted for clarity) as space-filling (left) and wire-frame/ellipsoid model (right) and the calculated steric-map (middle) representing the high %Vbur[12–14] of the central nickel atom explaining the NMR signature of **3b** shown in Figures S17–S22 by hindered *N*-*i*Pr and Ni-CB rotations. As the square-planar complexes $[Ni(NHC)_3X]^+$ with N-*i*Pr substituted NHCs are sterically very crowded, especially for the $i\mathrm{Pr}_2\mathrm{Im}^{Me}$ ligand, which is sterically more demanding compared to the $i\mathrm{Pr}_2$Im ligand (%V_{Bur} (d = 1.99 Å; R = 3.5 Å) = 28.8)[15] a unique resonance pattern of the NHC ligands is observed. The sterically over-encumbered environment of the central nickel atom in $[Ni(i\mathrm{Pr}_2\mathrm{Im}^{Me})_3(NC\text{-}BH_2CN)]^+$ can be demonstrated in a space filling model, but also in a calculated buried

volume of the ligand sphere of 89.5%. Because of the steric hindrance, rotation of the NHC ligands, of the *N*-iPr substituents but also of the coordinated cyanoborate is hindered, which removes pseudo-C_{2v} symmetry of the molecule. Thus, many of the resonances are fairly broad in the NMR spectra. There are two different NHC ligands in the molecule, one *trans*- and two *cis*- to the anion, which leads to resonances for two different carbene carbon atoms. The *N-iso*-propyl and $C_{backbone}$-CH_3 groups are more influenced by steric interactions of the ligands compared to the $C_{backbone}$ and N*C*N groups, leading to the detection of only two $C_{backbone}$ resonances in a ratio of 1:2 and 3 $C_{backbone}$-CH_3 resonances in a 1:1:1 ratio. Concerning the $CH_{methine}$ resonances, those of the *trans*-NHC ligand are a relatively sharp resolved septet, whereas those of the *cis*-NHC ligands give two broad resonances, standing pairwise either towards or away from the coordinated cyanoborate ligand. And final, the $C_{methine}$-CH_3 resonances split into one set for the *trans*-NHC ligands (integration 12 protons) and 4 resonances for the *cis*-NHC ligands (either towards or away from the cyanoborate ligand as well as “inside” and “outside” of the NHC ligand).

***trans*-[Ni(Dipp$_2$Im)$_2$(NC-BH$_2$CN)$_2$] (*trans*-4b)**

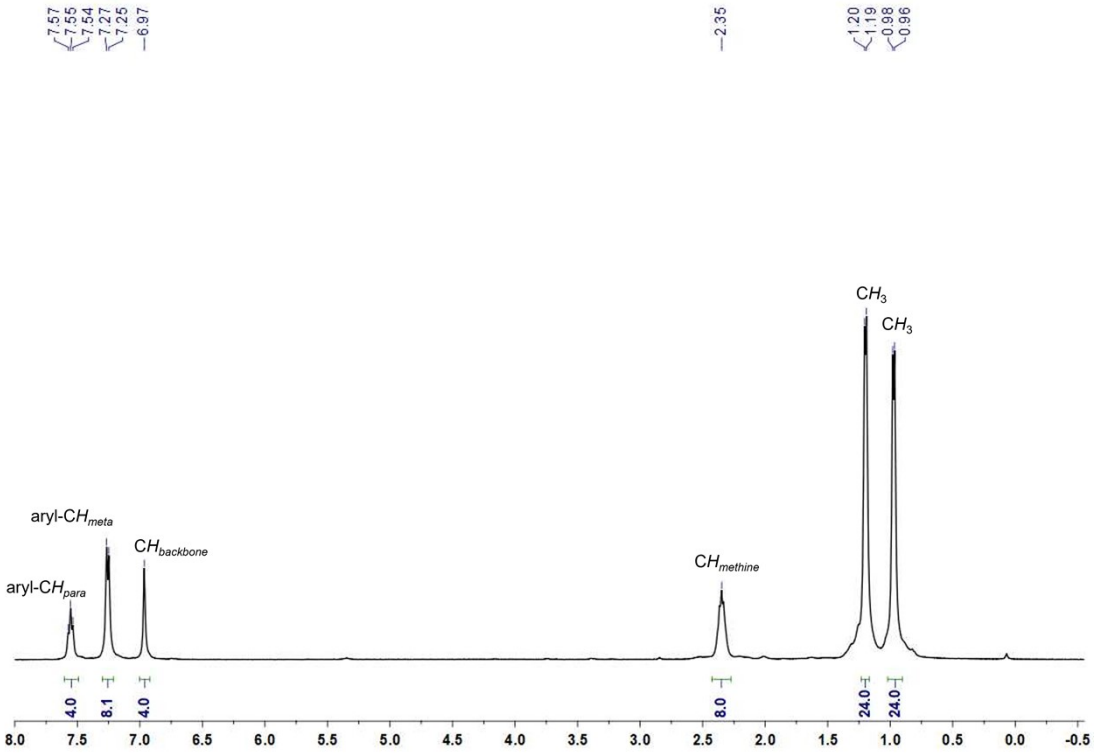

Figure S24. ^{1}H NMR spectrum of *trans*-[Ni(Dipp$_2$Im)$_2$(NC-BH$_2$CN)$_2$] (*trans*-**4b**) in $CDCl_3$. BH_2-groups were not detected.

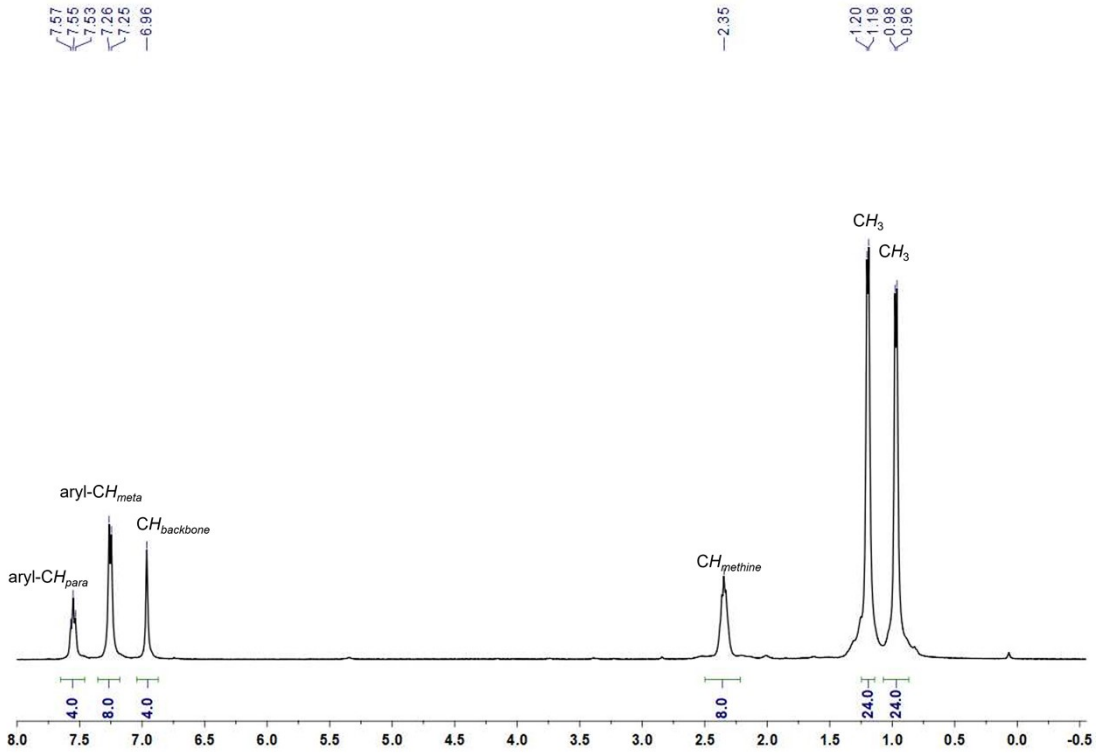

Figure S25. $^{1}H\{^{11}B\}$ NMR spectrum of *trans*-[Ni(Dipp$_2$Im)$_2$(NC-BH$_2$CN)$_2$] (*trans*-**4b**) in $CDCl_3$. BH_2-groups were not detected.

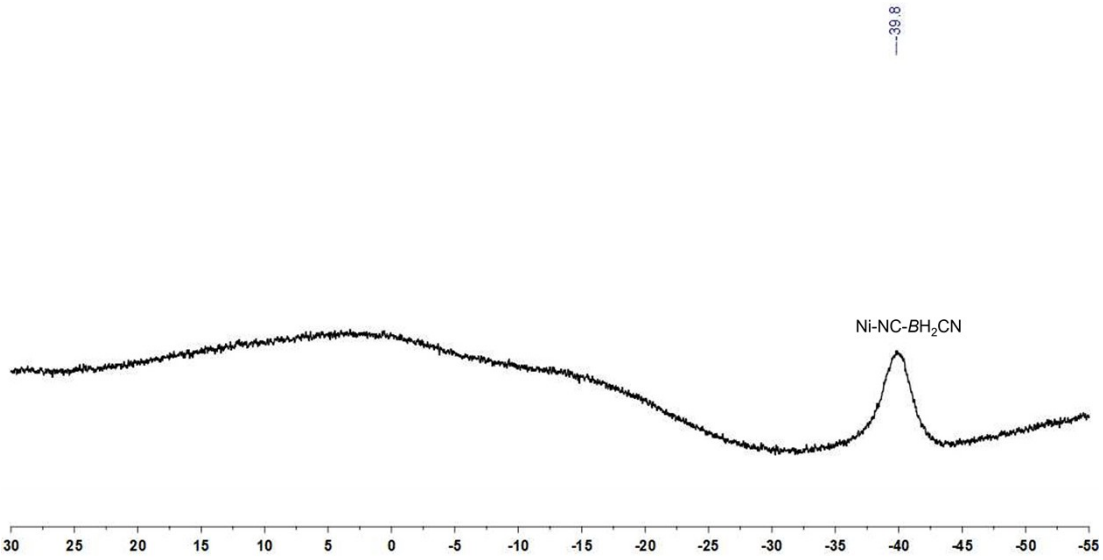

Figure S26. ^{11}B NMR spectrum of *trans*-[Ni(Dipp$_2$Im)$_2$(NC-BH$_2$CN)$_2$] (*trans*-**4b**) in $CDCl_3$.

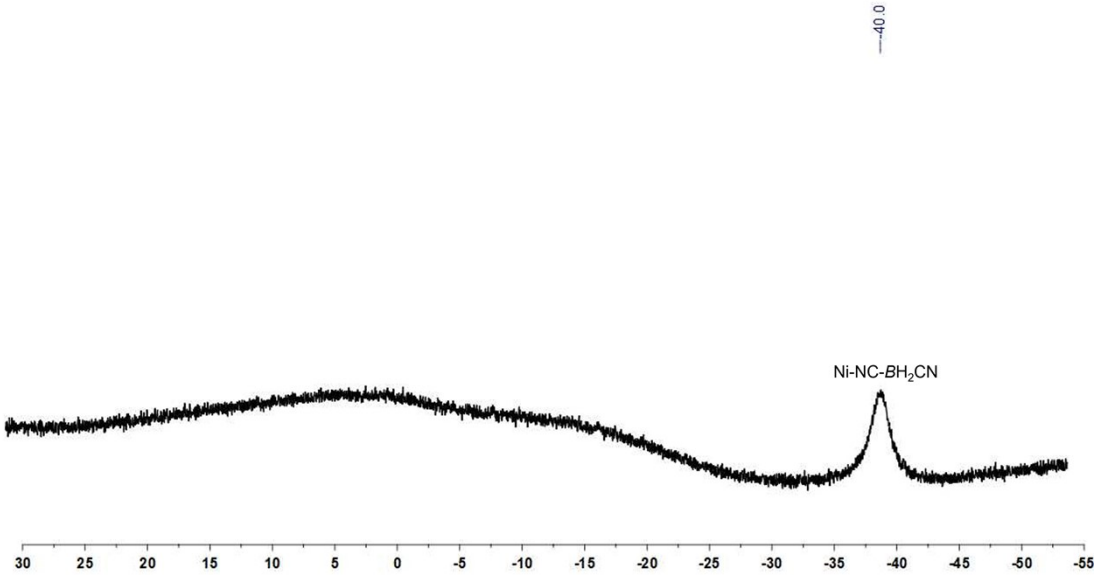

Figure S27. $^{11}B\{^{1}H\}$ NMR spectrum of *trans*-[Ni(Dipp$_2$Im)$_2$(NC-BH$_2$CN)$_2$] (*trans*-**4b**) in $CDCl_3$.

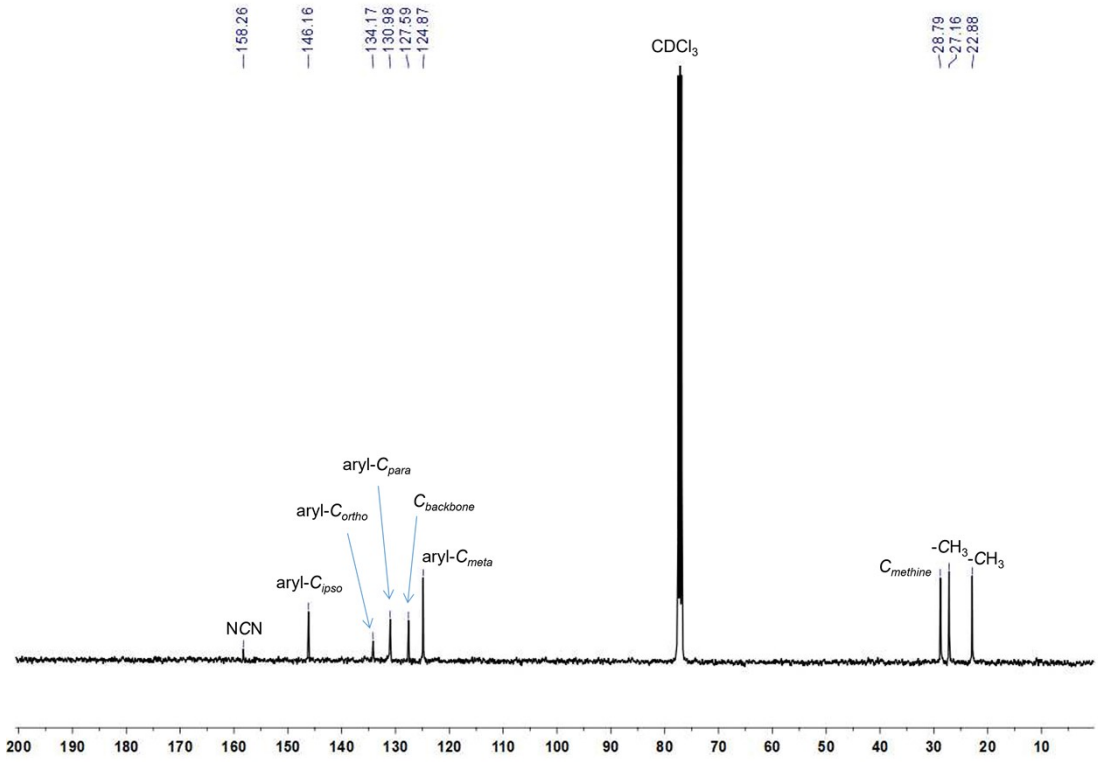

Figure S28. $^{13}C\{^{1}H\}$ NMR spectrum *trans*-[Ni(Dipp$_2$Im)$_2$(NC-BH$_2$CN)$_2$] (*trans*-**4b**) in $CDCl_3$. B-CN groups were not detected.

***trans*-[Ni(Mes$_2$Im)$_2$(NC-BH$_2$CN)$_2$] (*trans*-5b)**

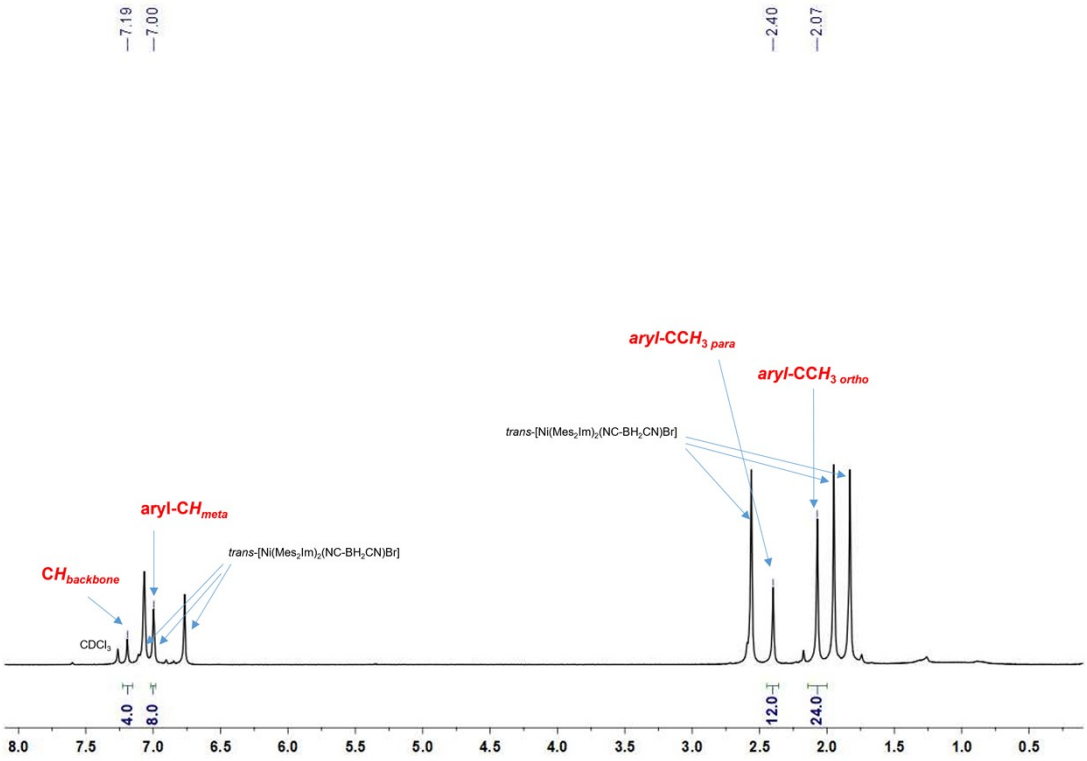

Figure S29. ^{1}H NMR spectrum of a mixture of *trans*-[Ni(Mes$_2$Im)$_2$(NC-BH$_2$CN)$_2$] (*trans*-**5b**) (marked herein with red) and *trans*-[Ni(Mes$_2$Im)$_2$(NC-BH$_2$CN)Br] (*trans*-**12b**) in CDCl$_3$.

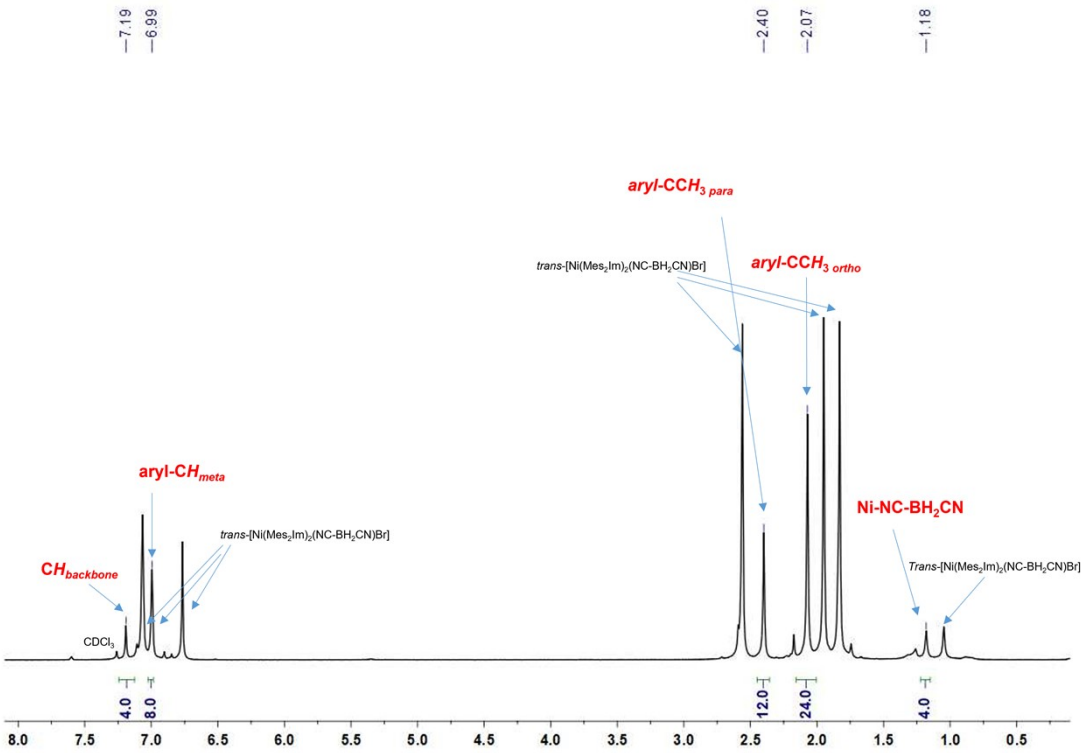

Figure S30. ^{1}H{^{11}B} NMR spectrum of a mixture of *trans*-[Ni(Mes$_2$Im)$_2$(NC-BH$_2$CN)$_2$] (*trans*-**5b**) (marked herein with red) and *trans*-[Ni(Mes$_2$Im)$_2$(NC-BH$_2$CN)Br] (*trans*-**12b**) in CDCl$_3$.

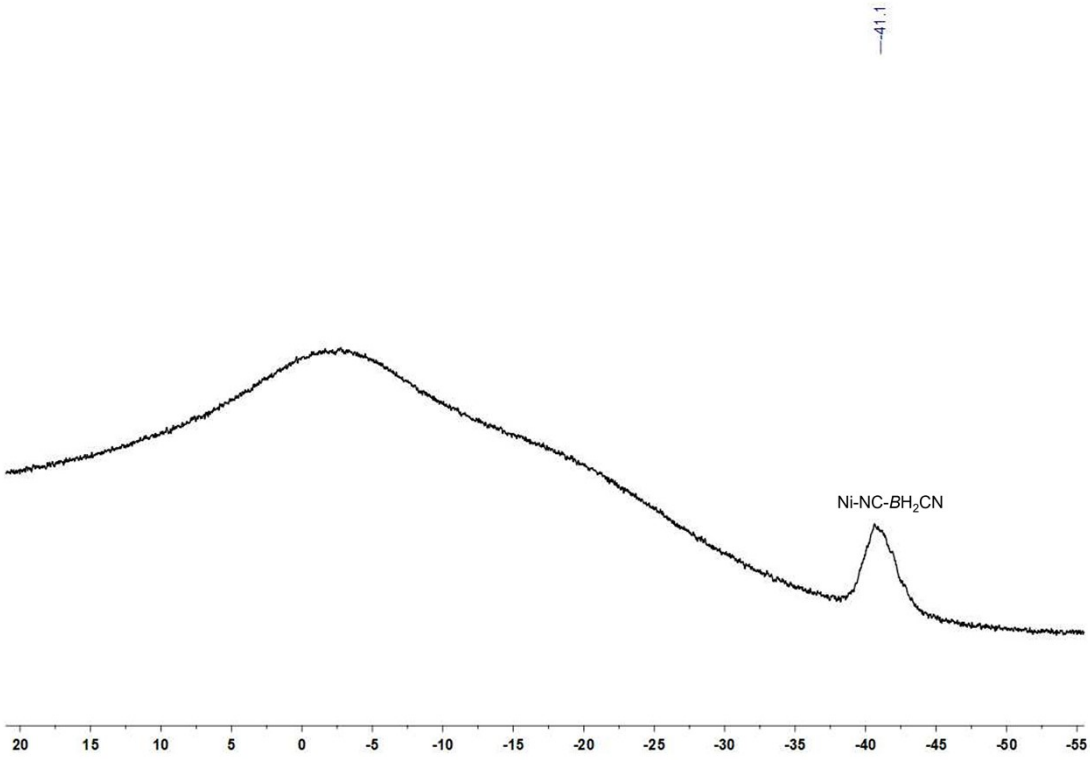

Figure S31. ^{11}B NMR spectrum of a mixture of *trans*-[Ni(Mes$_2$Im)$_2$(NC-BH$_2$CN)$_2$] (*trans*-**5b**) (marked herein with red) and *trans*-[Ni(Mes$_2$Im)$_2$(NC-BH$_2$CN)Br] (*trans*-**12b**) in CDCl$_3$.

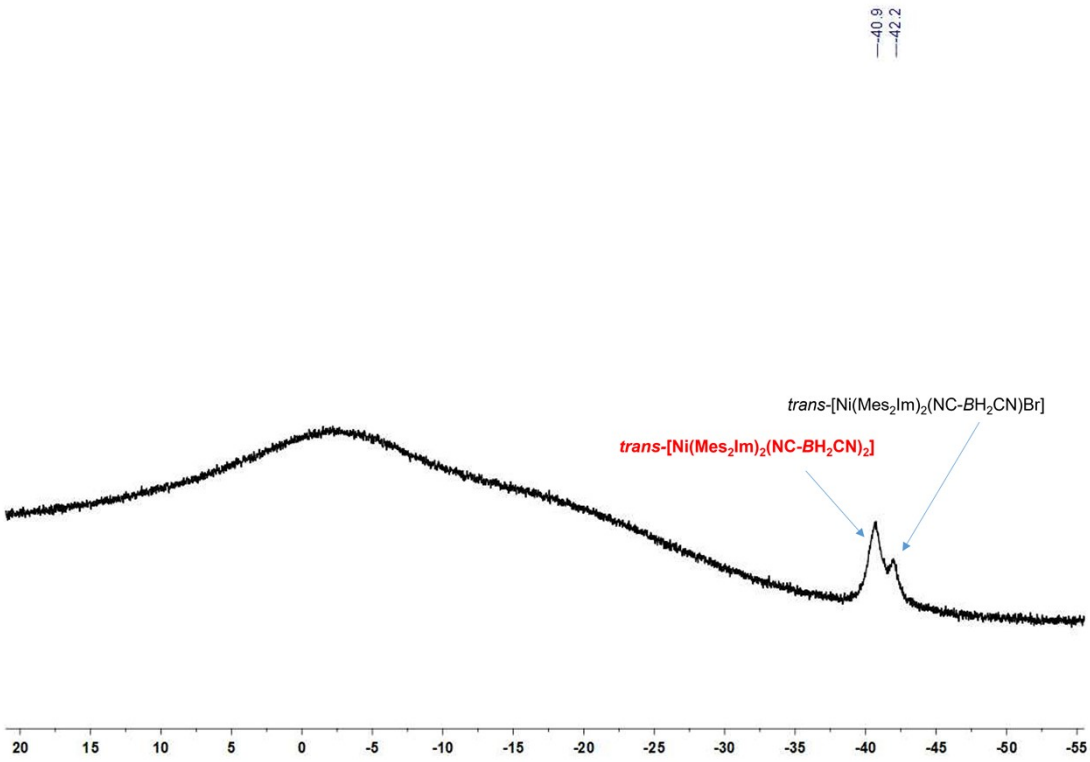

Figure S32. ^{11}B{^{1}H} NMR spectrum of a mixture of *trans*-[Ni(Mes$_2$Im)$_2$(NC-BH$_2$CN)$_2$] (*trans*-**5b**) (marked herein with red) and *trans*-[Ni(Mes$_2$Im)$_2$(NC-BH$_2$CN)Br] (*trans*-**12b**) in CDCl$_3$.

***trans*-[Ni(Mes$_2$Im)$_2${NC-BH(CN)$_2$}$_2$] (*trans*-5c)**

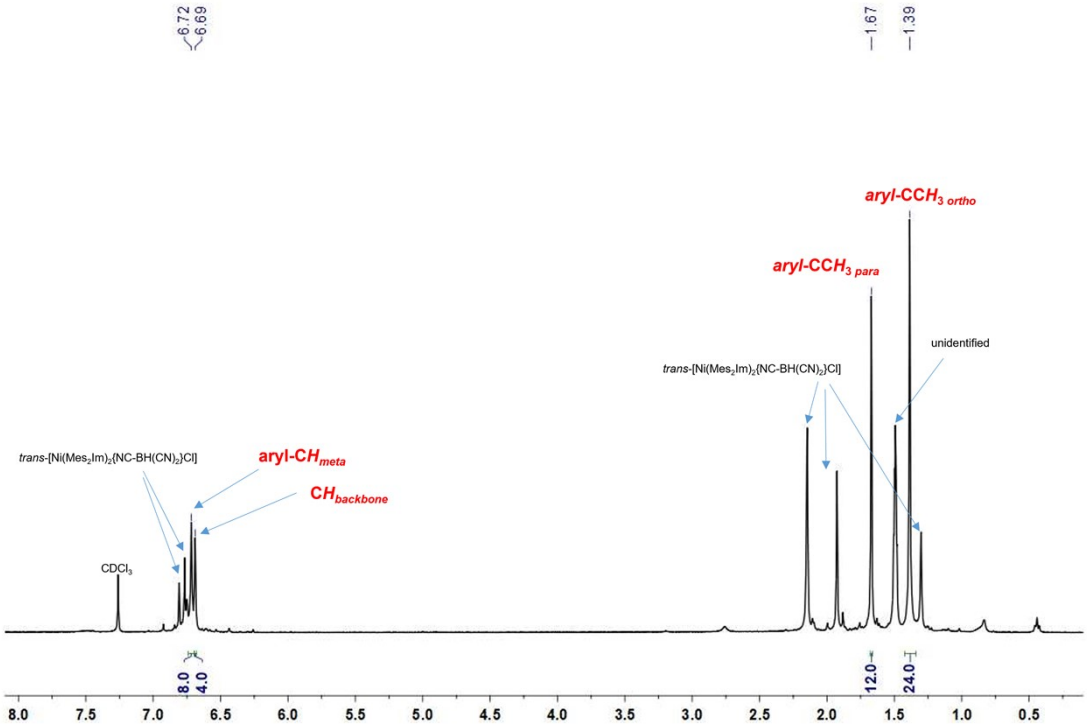

Figure S33. ^{1}H NMR spectrum of a mixture of *trans*-[Ni(Mes$_2$Im)$_2${NC-BH(CN)$_2$}$_2$] (*trans*-**5c**) (marked red), *trans*-[Ni(Mes$_2$Im)$_2${NC-BH(CN)$_2$}Cl] (*trans*-**6c**) in $CDCl_3$.

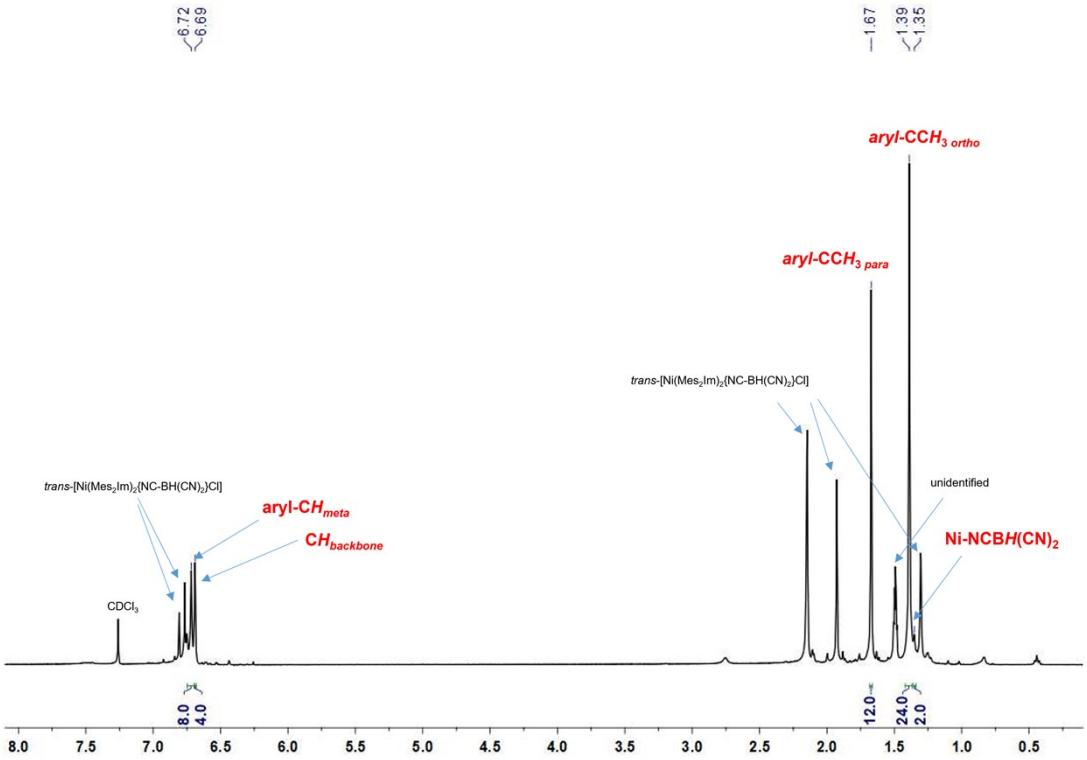

Figure S34. ^{1}H{^{11}B} NMR spectrum of a mixture of *trans*-[Ni(Mes$_2$Im)$_2${NC-BH(CN)$_2$}$_2$] (*trans*-**5c**) (marked red), *trans*-[Ni(Mes$_2$Im)$_2${NC-BH(CN)$_2$}Cl] (*trans*-**6c**) in $CDCl_3$.

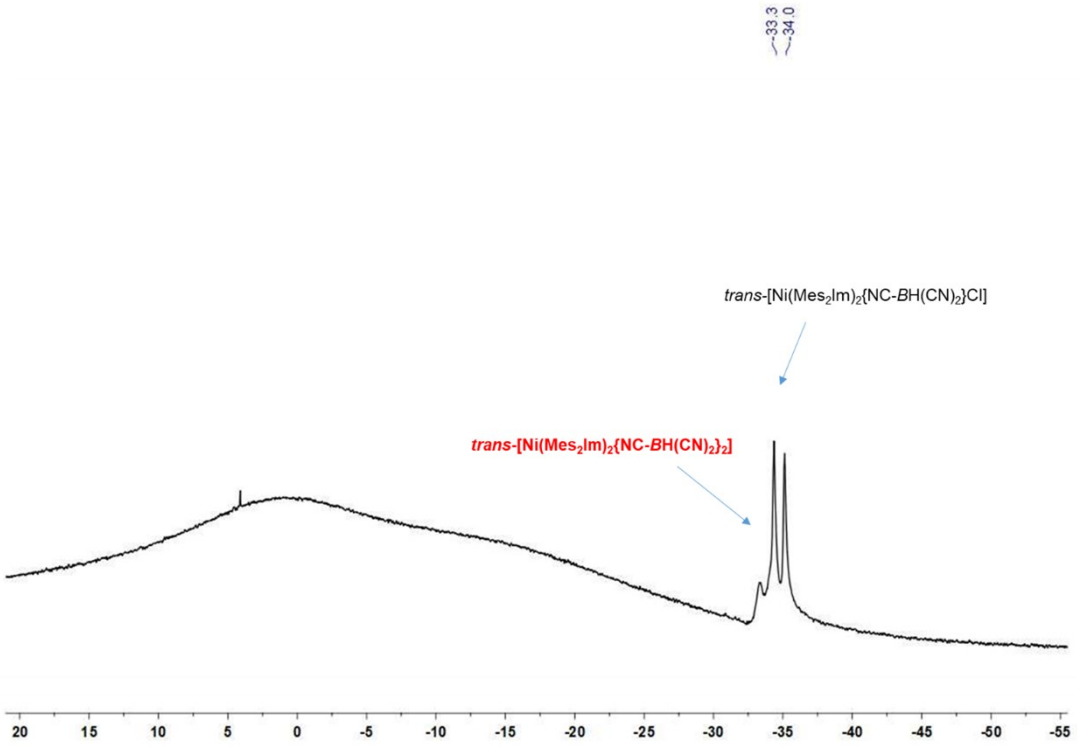

Figure S35. ^{11}B NMR spectrum of a mixture of *trans*-[Ni(Mes_2Im)$_2${NC-BH$(CN)_2$}$_2$] (*trans*-**5c**) (marked red), *trans*-[Ni(Mes_2Im)$_2${NC-BH$(CN)_2$}Cl] (*trans*-**6c**) in $CDCl_3$.

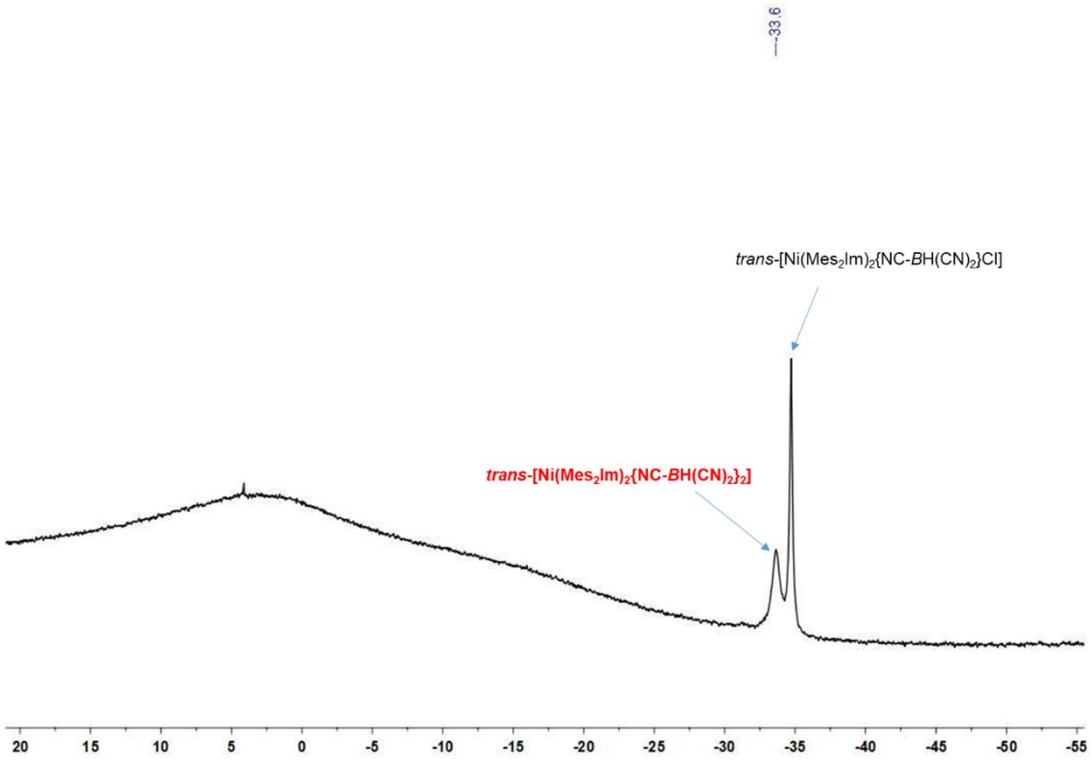

Figure S36. $^{11}B\{^1H\}$ NMR spectrum of a mixture of *trans*-[Ni(Mes_2Im)$_2${NC-BH$(CN)_2$}$_2$] (*trans*-**5c**) (marked red), *trans*-[Ni(Mes_2Im)$_2${NC-BH$(CN)_2$}Cl] (*trans*-**6c**) in $CDCl_3$.

***trans*-[Ni(Mes$_2$Im)$_2${NC-BH(CN)$_2$}Cl] (*trans*-6c)**

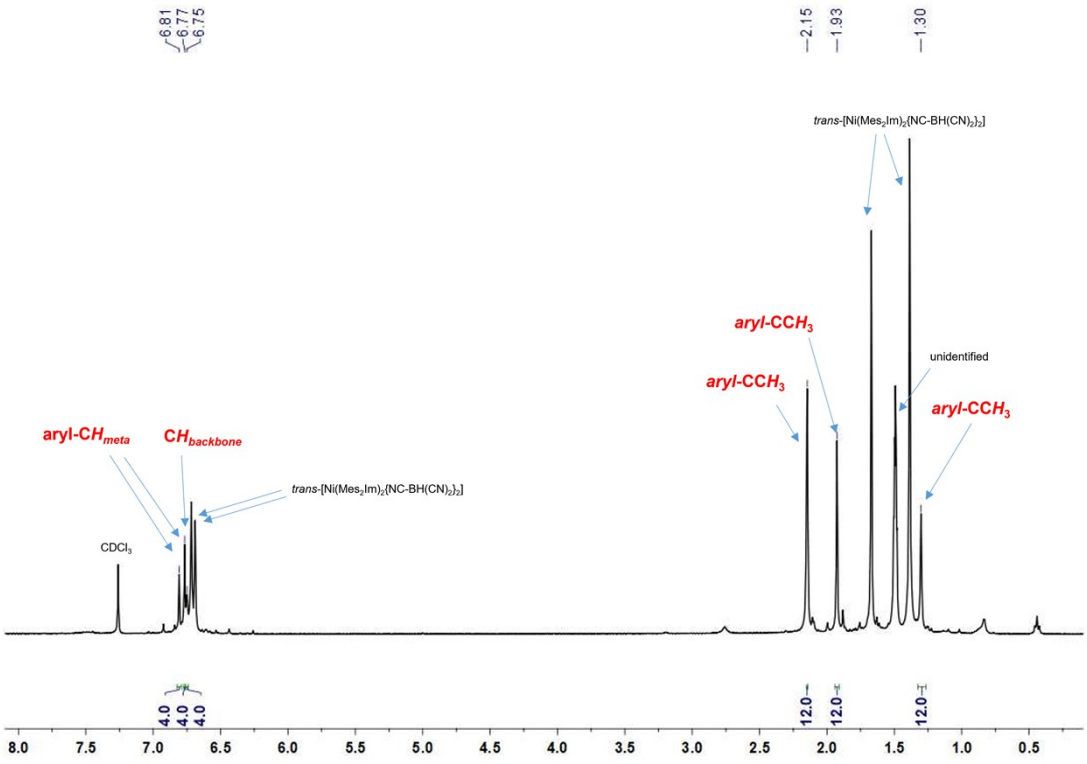

Figure S37. ^{1}H NMR spectrum of a mixture of *trans*-[Ni(Mes$_2$Im)$_2${NC-BH(CN)$_2$}Cl] (*trans*-**6c**) (marked red), *trans*-[Ni(Mes$_2$Im)$_2${NC-BH(CN)$_2$}$_2$] (*trans*-**5c**) in $CDCl_3$.

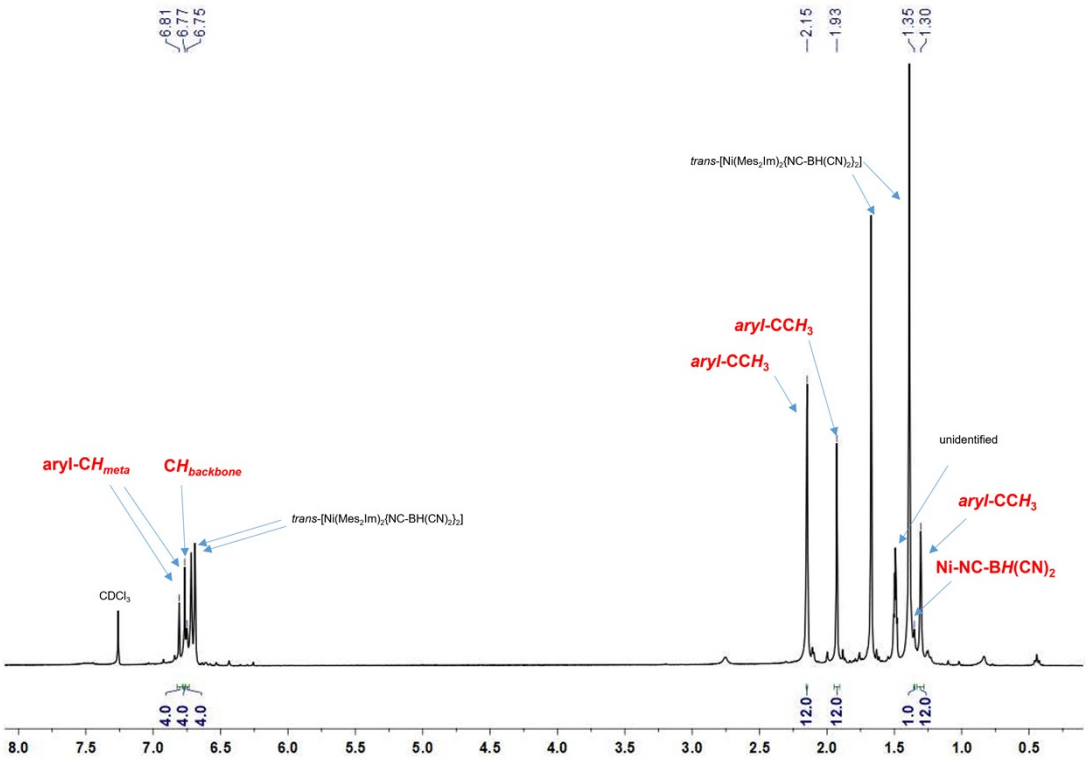

Figure S38. ^{1}H{^{11}B} NMR spectrum of a mixture of *trans*-[Ni(Mes$_2$Im)$_2${NC-BH(CN)$_2$}Cl] (*trans*-**6c**) (marked red), *trans*-[Ni(Mes$_2$Im)$_2${NC-BH(CN)$_2$}$_2$] (*trans*-**5c**) in $CDCl_3$.

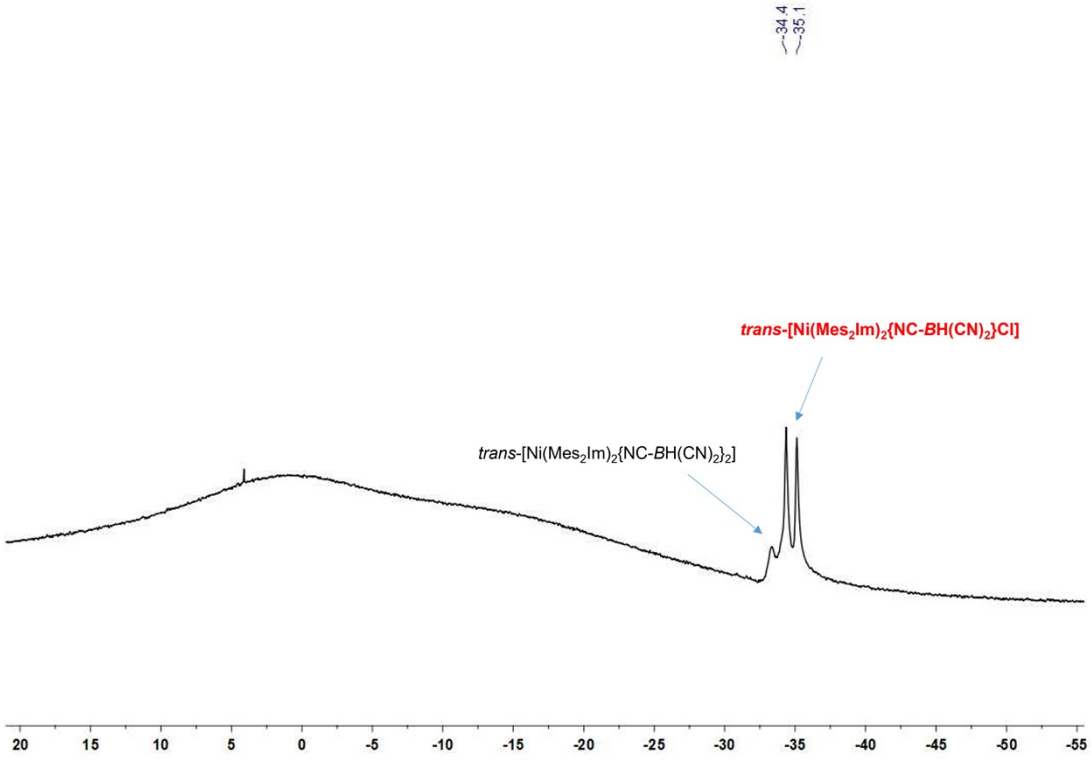

Figure S39. ^{11}B NMR spectrum of a mixture of *trans*-[Ni(Mes$_2$Im)$_2${NC-BH(CN)$_2$}Cl] (*trans*-**6c**) (marked red), *trans*-[Ni(Mes$_2$Im)$_2${NC-BH(CN)$_2$}$_2$] (*trans*-**5c**) in $CDCl_3$.

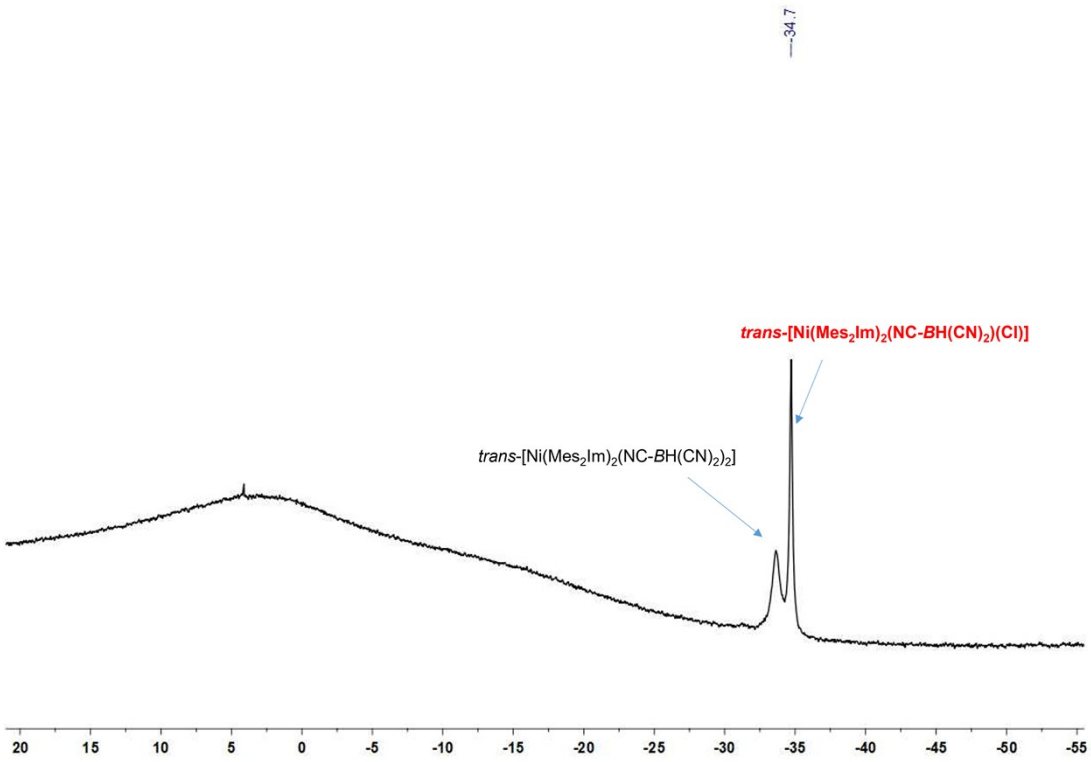

Figure S40. $^{11}B\{^1H\}$ NMR spectrum of a mixture of *trans*-[Ni(Mes$_2$Im)$_2${NC-BH(CN)$_2$}Cl] (*trans*-**6c**) (marked red), *trans*-[Ni(Mes$_2$Im)$_2${NC-BH(CN)$_2$}$_2$] (*trans*-**5c**) in $CDCl_3$.

[Ni(*i*Pr$_2$Im)$_3$(OH)][B(CN)$_4$] (7d)

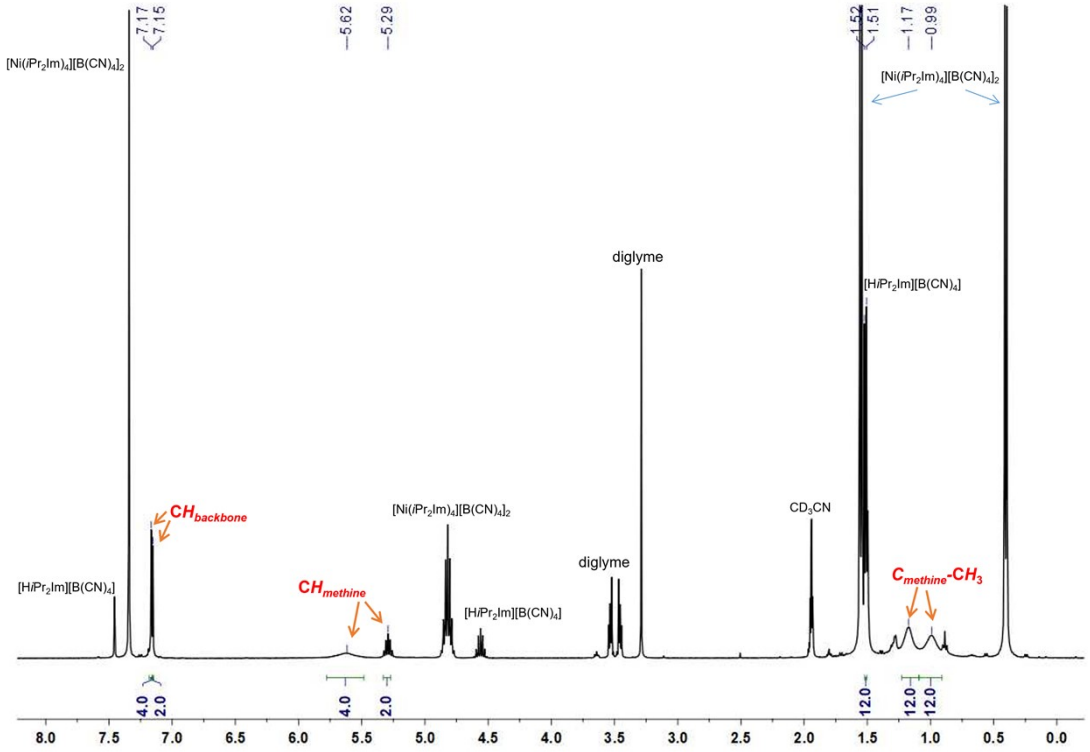

Figure S41. ^{1}H NMR spectrum of a mixture containing the side product [Ni(*i*Pr$_2$Im)$_3$(OH)][B(CN)$_4$] (**7d**) (red marks) in CD$_3$CN. Other compounds in the mixture are [Ni(*i*Pr$_2$Im)$_4$][B(CN)$_4$]$_2$ (**2d**), [H*i*Pr$_2$Im][B(CN)$_4$] and diglyme.

***cis*-[Ni(Me$_2$Im^{Me})$_2${NC-BH(CN)$_2$}Br] (*cis*-15c)**

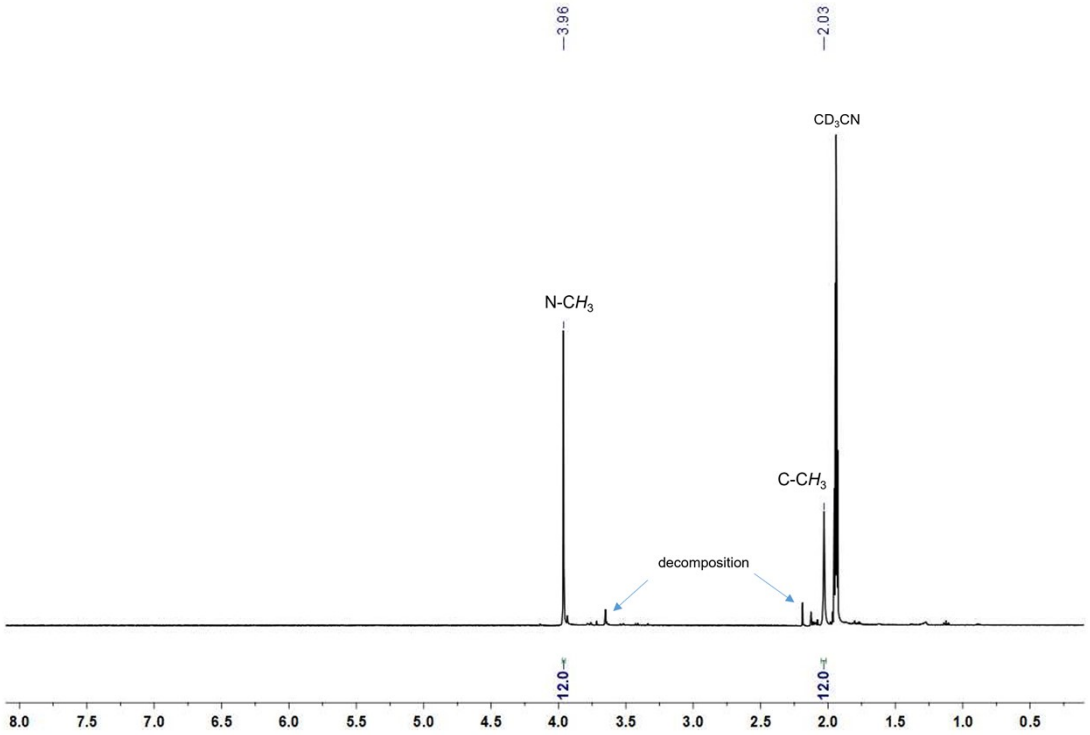

Figure S42. ^{1}H NMR spectrum of *cis*-[Ni(Me$_2$Im^{Me})$_2${NC-BH(CN)$_2$}Br] (*cis*-**10c**) in CD$_3$CN.

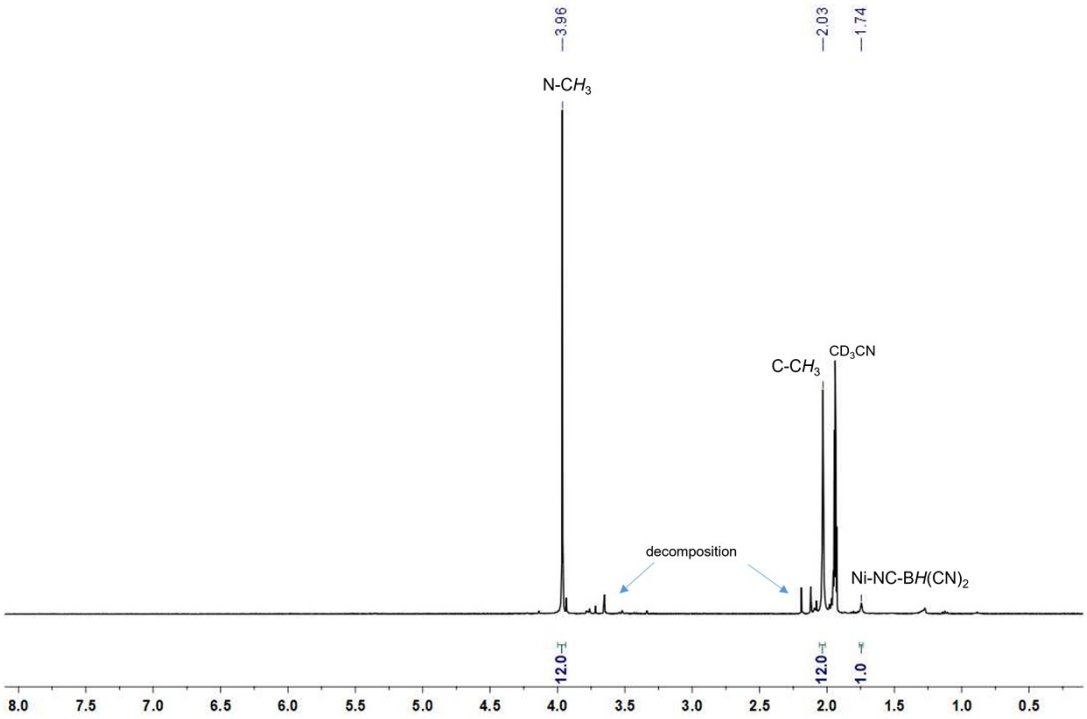

Figure S43. $^{1}H\{^{11}B\}$ NMR spectrum of *cis*-[Ni(Me_2Im^{Me})$_2${NC-BH(CN)$_2$}Br] (*cis*-**10c**) in CD_3CN.

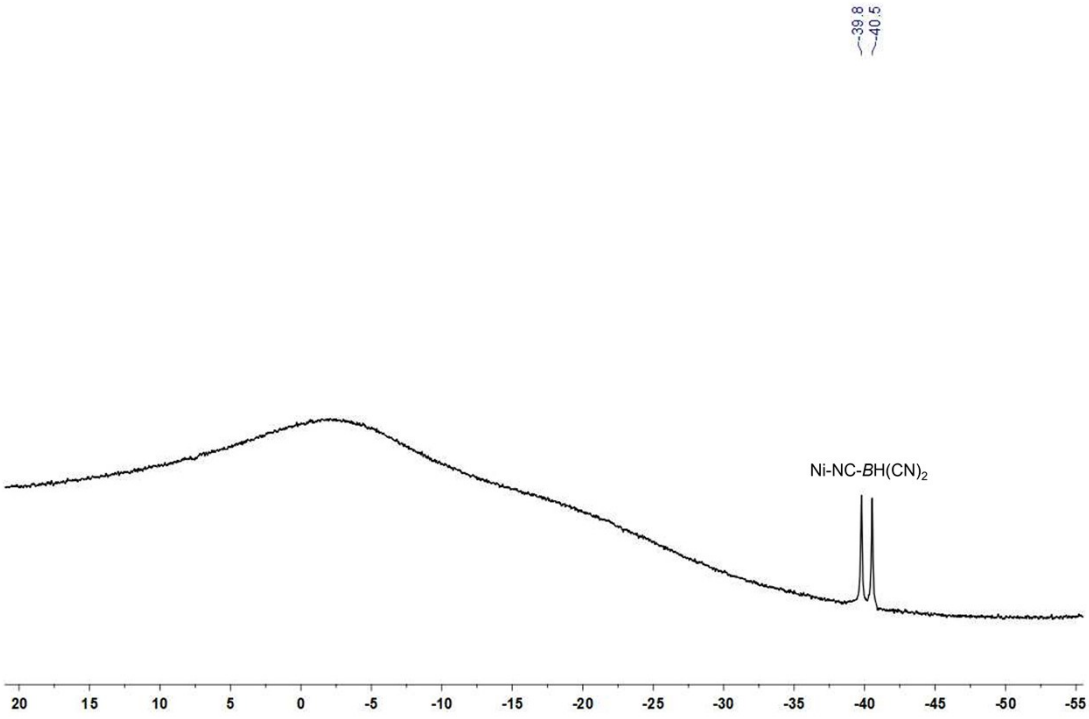

Figure S44. ^{11}B NMR spectrum of *cis*-[Ni(Me_2Im^{Me})$_2${NC-BH(CN)$_2$}Br] (*cis*-**10c**) in CD_3CN.

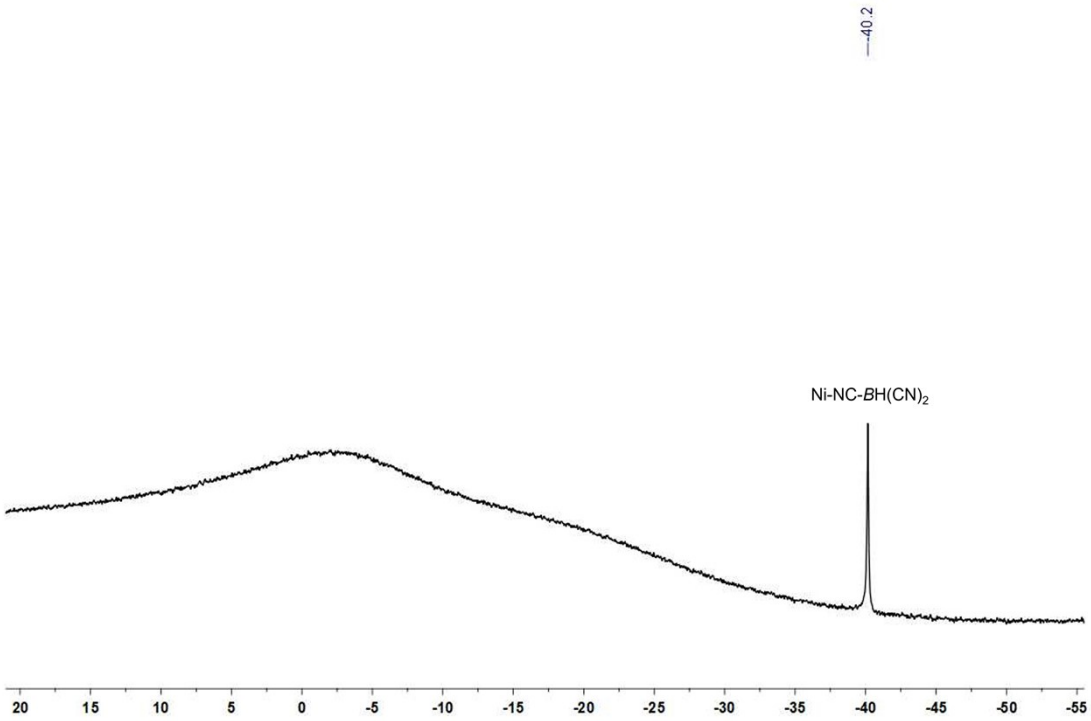

Figure S45. $^{11}B\{^{1}H\}$ NMR spectrum of *cis*-[Ni(Me_2Im^{Me})$_2${NC-BH(CN)$_2$}Br] (*cis*-**10c**) in CD_3CN.

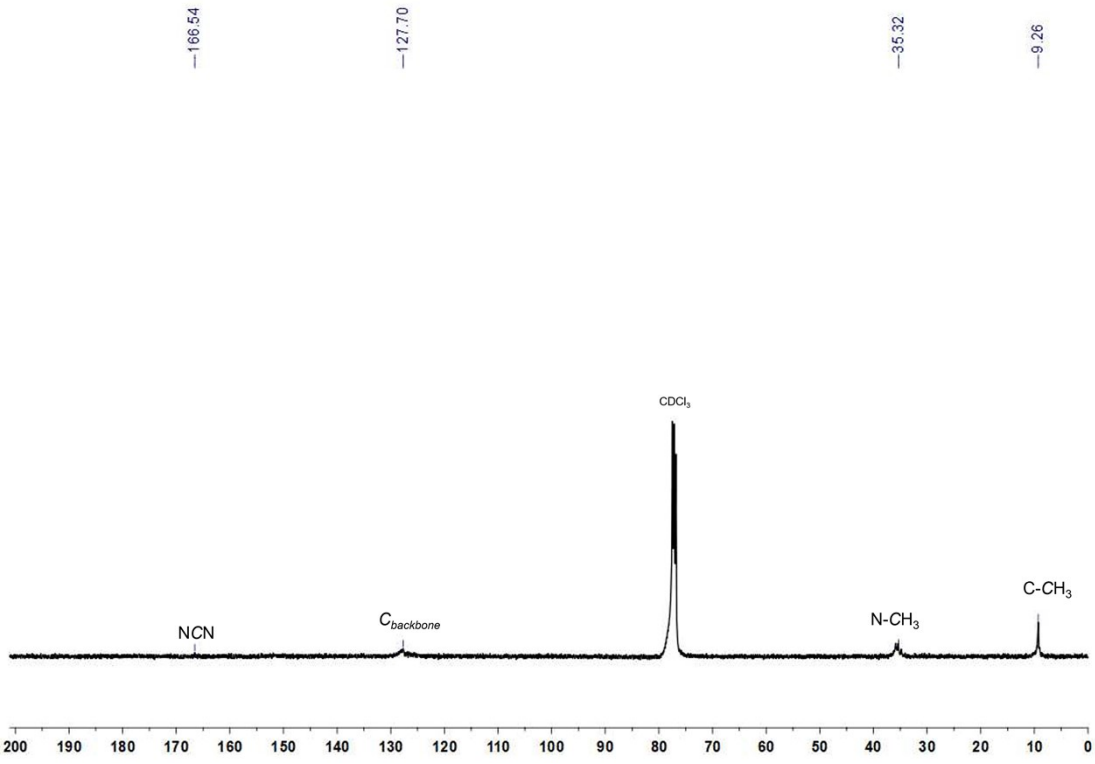

Figure S46. $^{13}C\{^{1}H\}$ NMR spectrum of *cis*-[Ni(Me_2Im^{Me})$_2${NC-BH(CN)$_2$}Br] (*cis*-**10c**) in $CDCl_3$.

***trans*-[Ni(Mes$_2$Im)$_2$(NC-BH$_2$CN)Br] (*trans*-12b)**

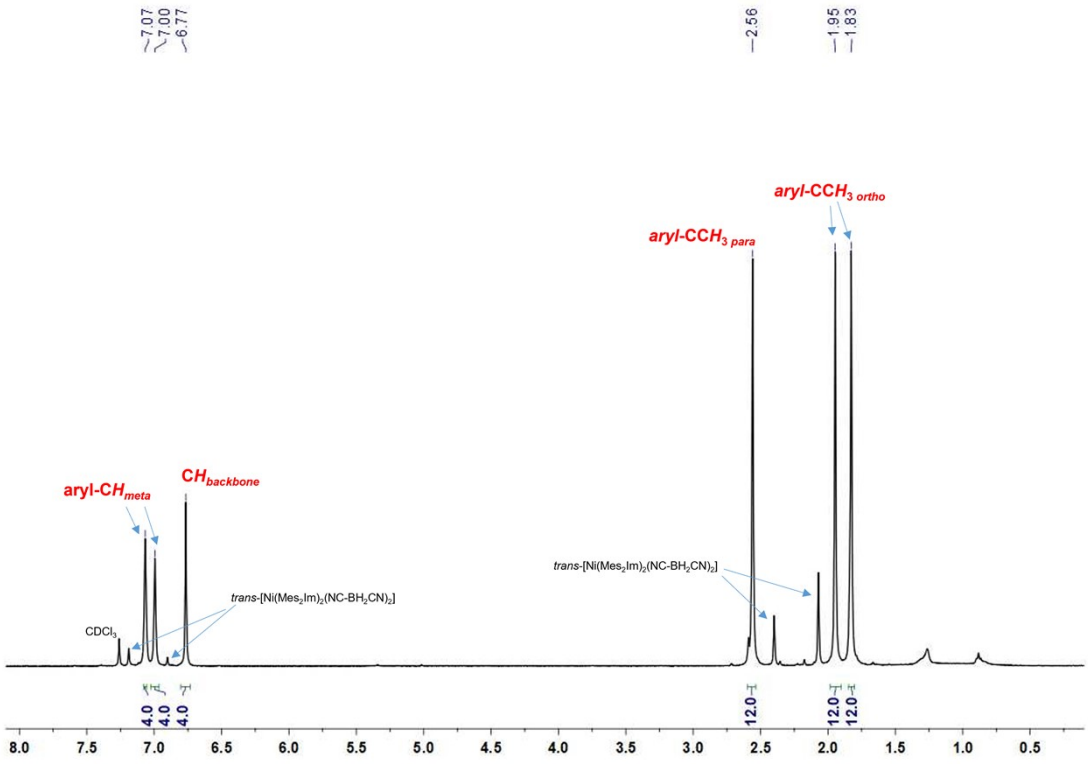

Figure S47. ^{1}H NMR spectrum of a mixture of *trans*-[Ni(Mes$_2$Im)$_2$(NC-BH$_2$CN)Br] (*trans*-**12b**) (marked herein with red) and *trans*-[Ni(Mes$_2$Im)$_2$(NC-BH$_2$CN)$_2$] (*trans*-**5b**) in $CDCl_3$.

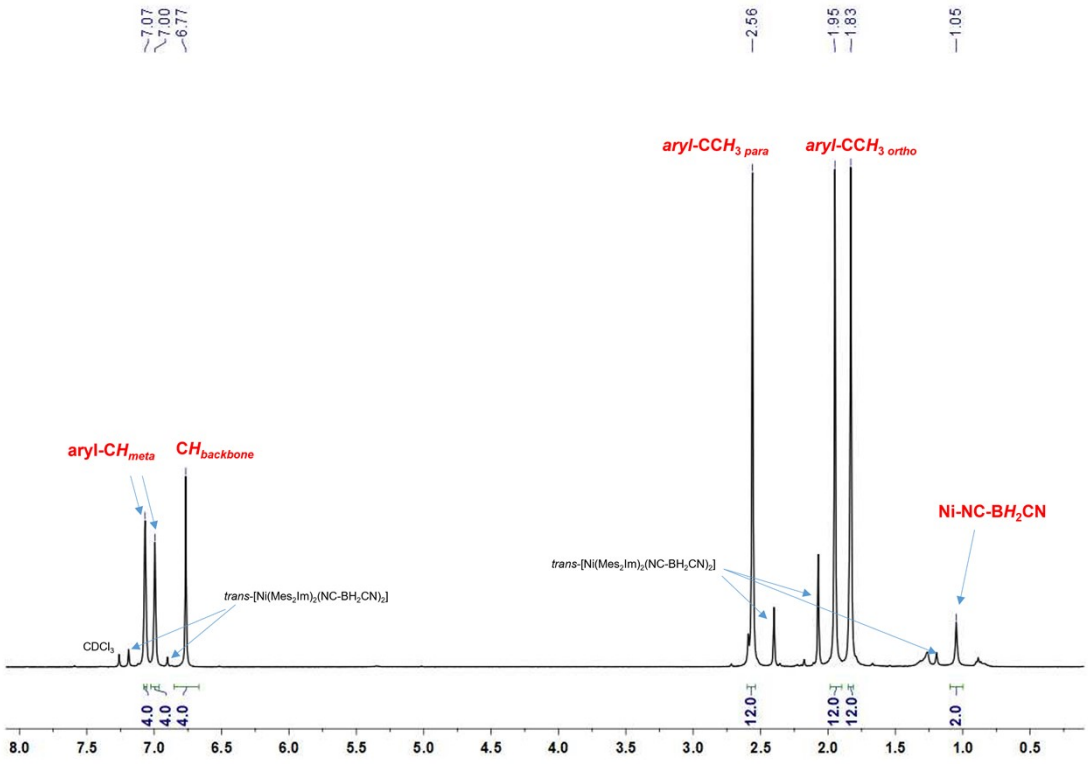

Figure S48. ^{1}H{^{11}B} NMR spectrum of a mixture of *trans*-[Ni(Mes$_2$Im)$_2$(NC-BH$_2$CN)Br] (*trans*-**12b**) (marked herein with red) and *trans*-[Ni(Mes$_2$Im)$_2$(NC-BH$_2$CN)$_2$] (*trans*-**5b**) in $CDCl_3$.

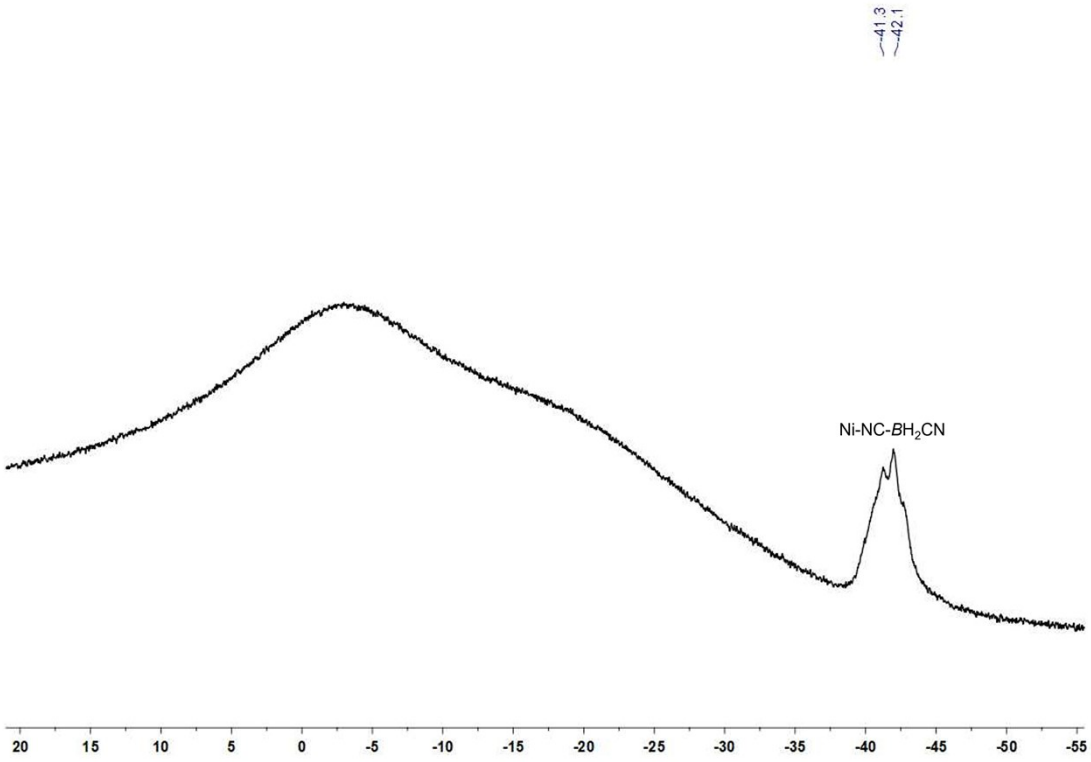

Figure S49. ^{11}B NMR spectrum of a mixture of *trans*-[Ni(Mes_2Im)$_2$(NC-BH_2CN)Br] (*trans*-**12b**) and *trans*-[Ni(Mes_2Im)$_2$(NC-BH_2CN)$_2$] (*trans*-**5b**) in $CDCl_3$.

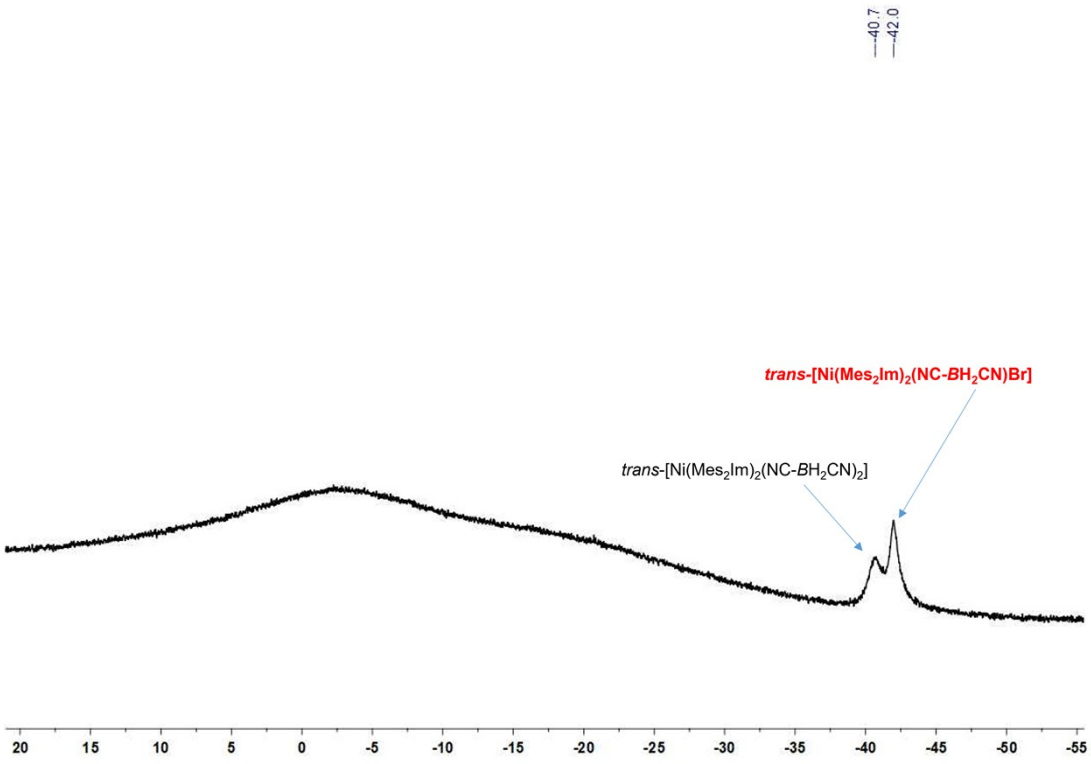

Figure S50. $^{11}B\{^1H\}$ NMR spectrum of a mixture of *trans*-[Ni(Mes_2Im)$_2$(NC-BH_2CN)Br] (*trans*-**12b**) (marked herein with red) and *trans*-[Ni(Mes_2Im)$_2$(NC-BH_2CN)$_2$] (*trans*-**5b**) in $CDCl_3$.

***cis*-[Ni(Me$_2$Im^{Me})$_2$(NC-BH$_2$CN)$_2$] (*cis*-13b)**

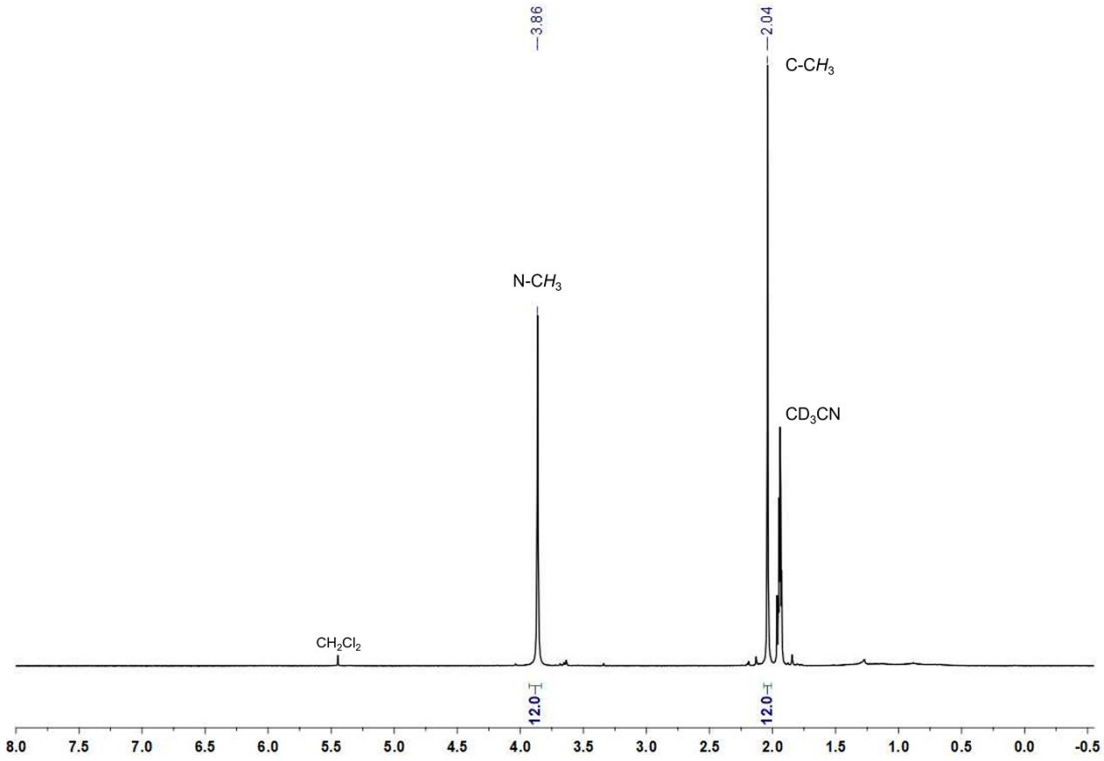

Figure S51. $^{1}H\{^{11}B\}$ NMR spectrum of *cis*-[Ni(Me$_2$Im^{Me})$_2$(NC-BH$_2$CN)$_2$] (*cis*-**13b**) in CD_3CN.

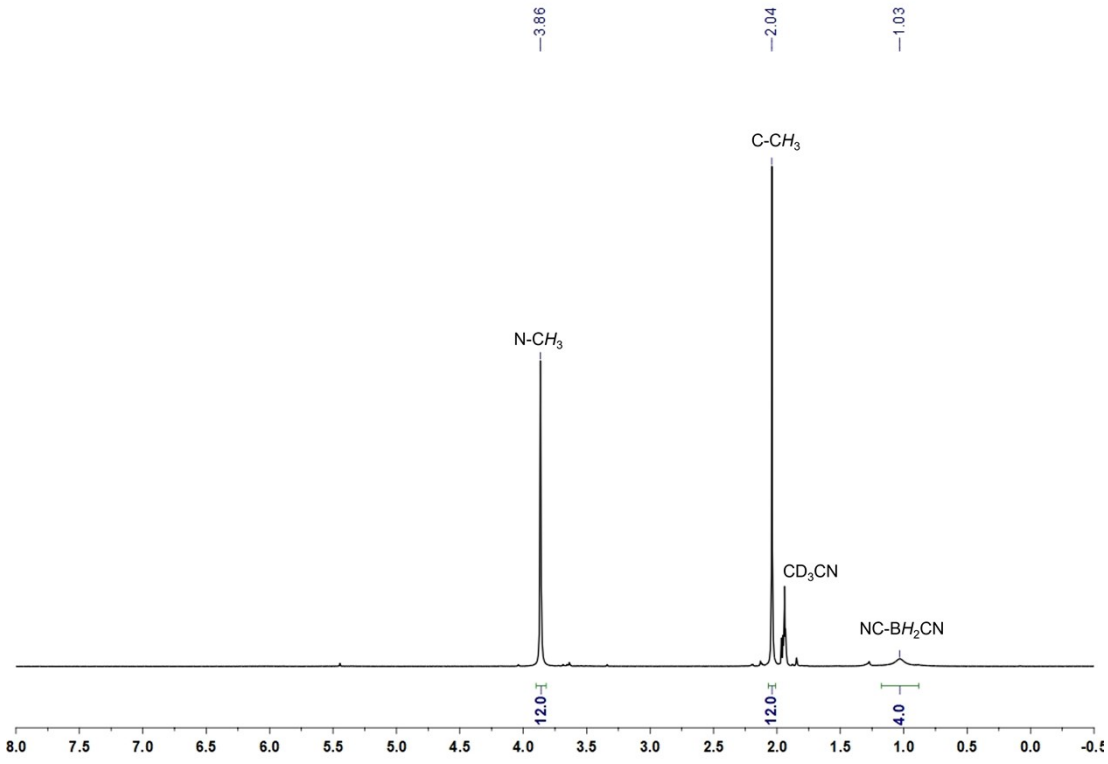

Figure S52. ^{1}H NMR spectrum of *cis*-[Ni(Me$_2$Im^{Me})$_2$(NC-BH$_2$CN)$_2$] (*cis*-**13b**) in CD_3CN.

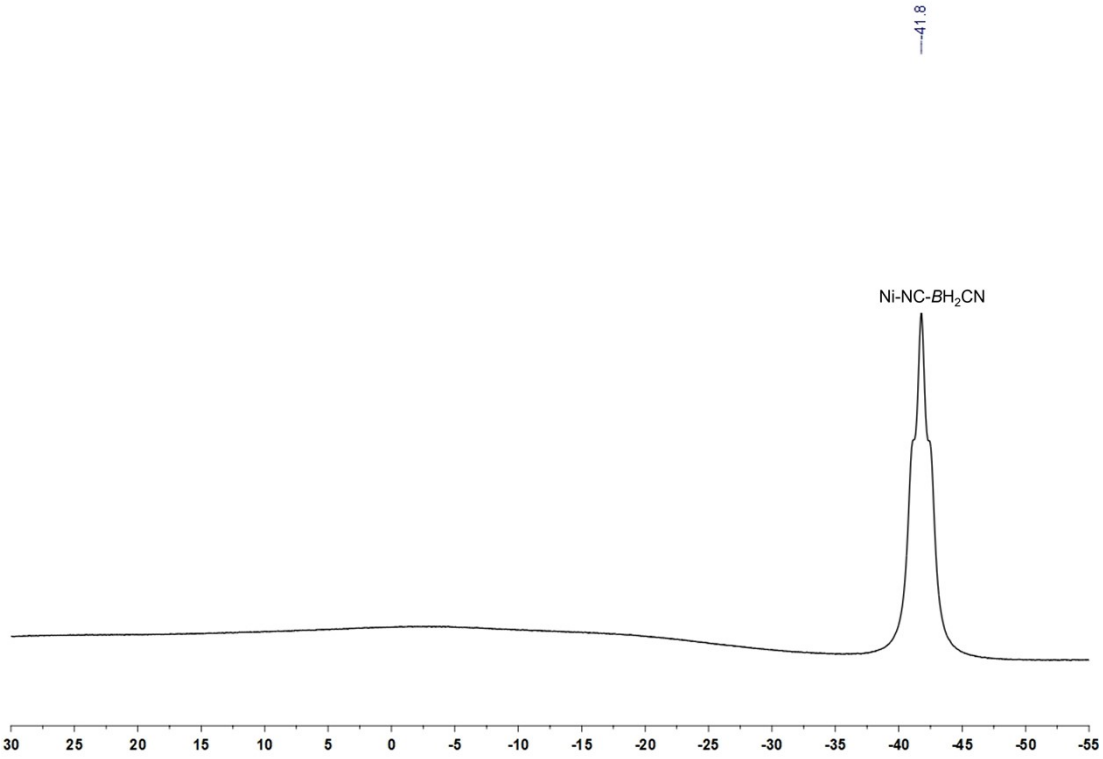

Figure S53. ^{11}B NMR spectrum of *cis*-[Ni(Me_2Im^{Me})$_2$(NC-BH_2CN)$_2$] (*cis*-**13b**) in CD_3CN.

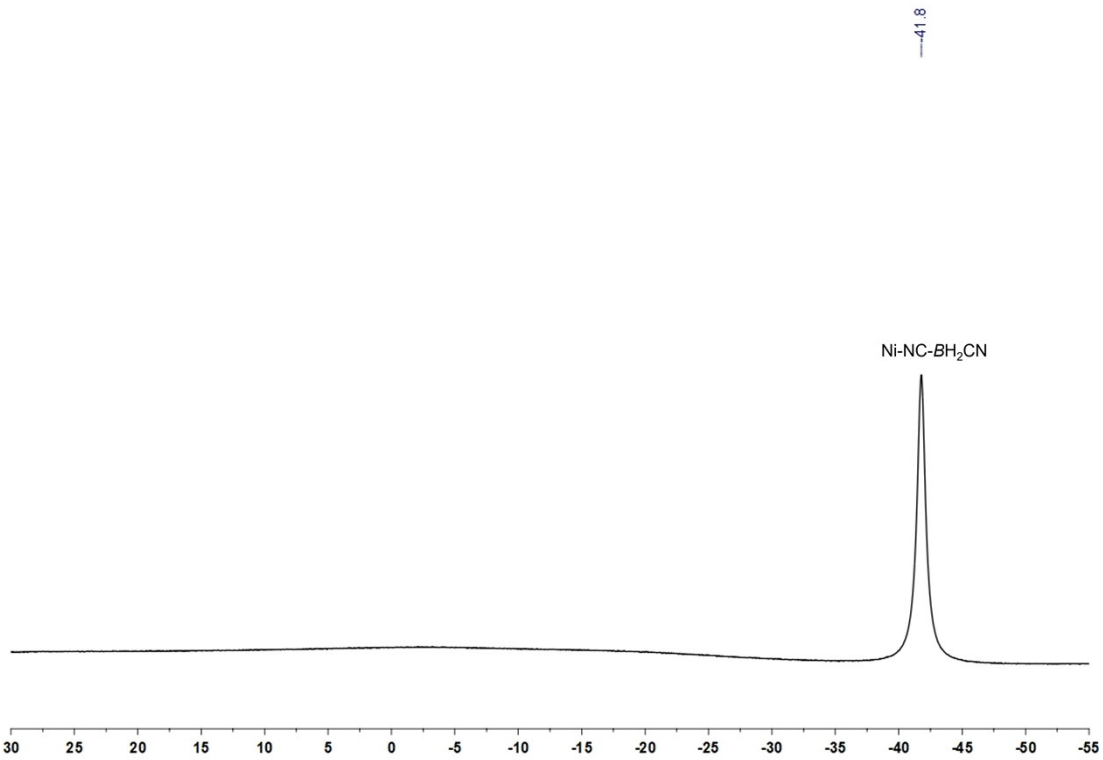

Figure S54. ^{11}B {^{1}H} NMR spectrum of *cis*-[Ni(Me_2Im^{Me})$_2$(NC-BH_2CN)$_2$] (*cis*-**13b**) in CD_3CN.

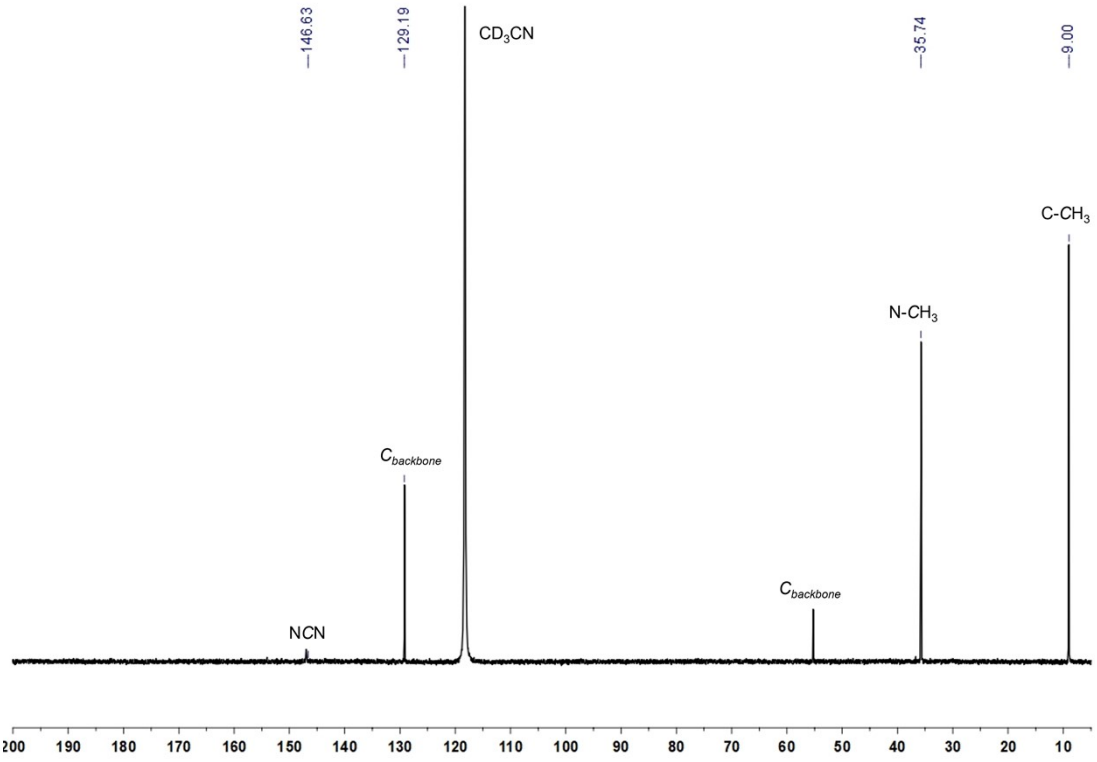

Figure S55. $^{13}C\{^{1}H\}$ NMR spectrum of *cis*-[Ni(Me_2Im^{Me})$_2$(NC-BH_2CN)$_2$] (*cis*-**13b**) in CD_3CN. B–CN groups were not detected.

trans-[Ni(*i*Pr_2Im)$_2$(NC-BH_3)$_2$] (*trans*-14a)

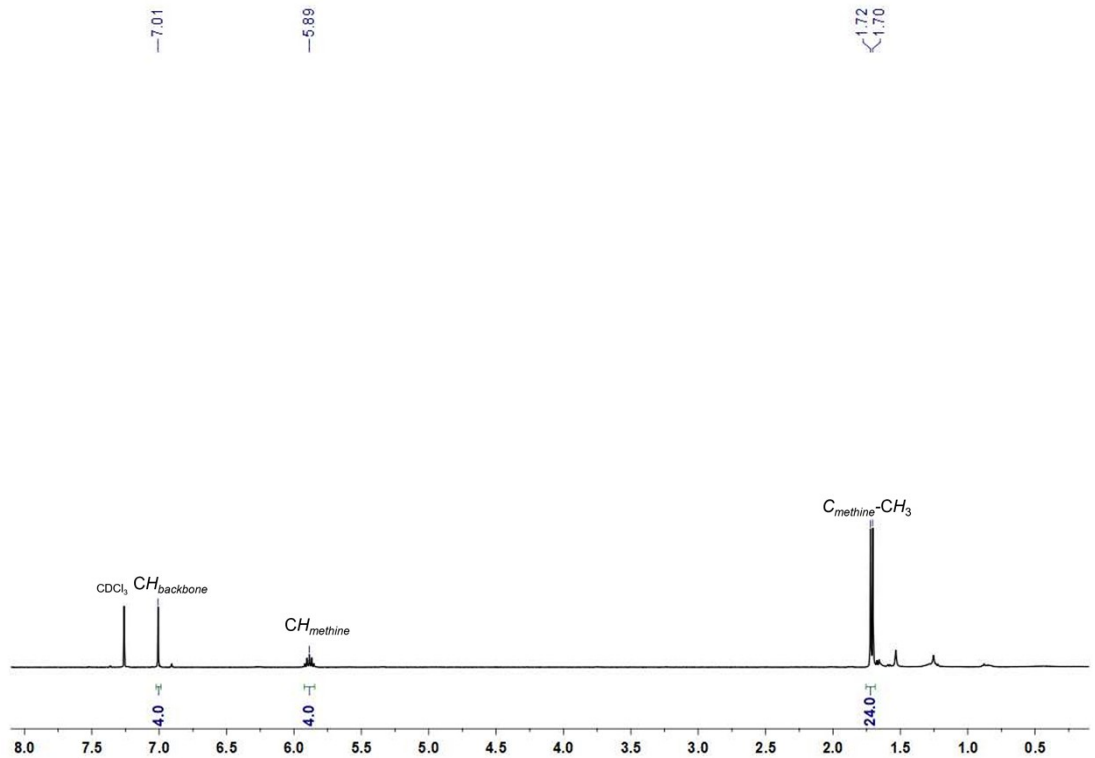

Figure S56. ^{1}H NMR spectrum of *trans*-[Ni(*i*Pr_2Im)$_2$(NC-BH_3)$_2$] (*trans*-**14a**) in $CDCl_3$.

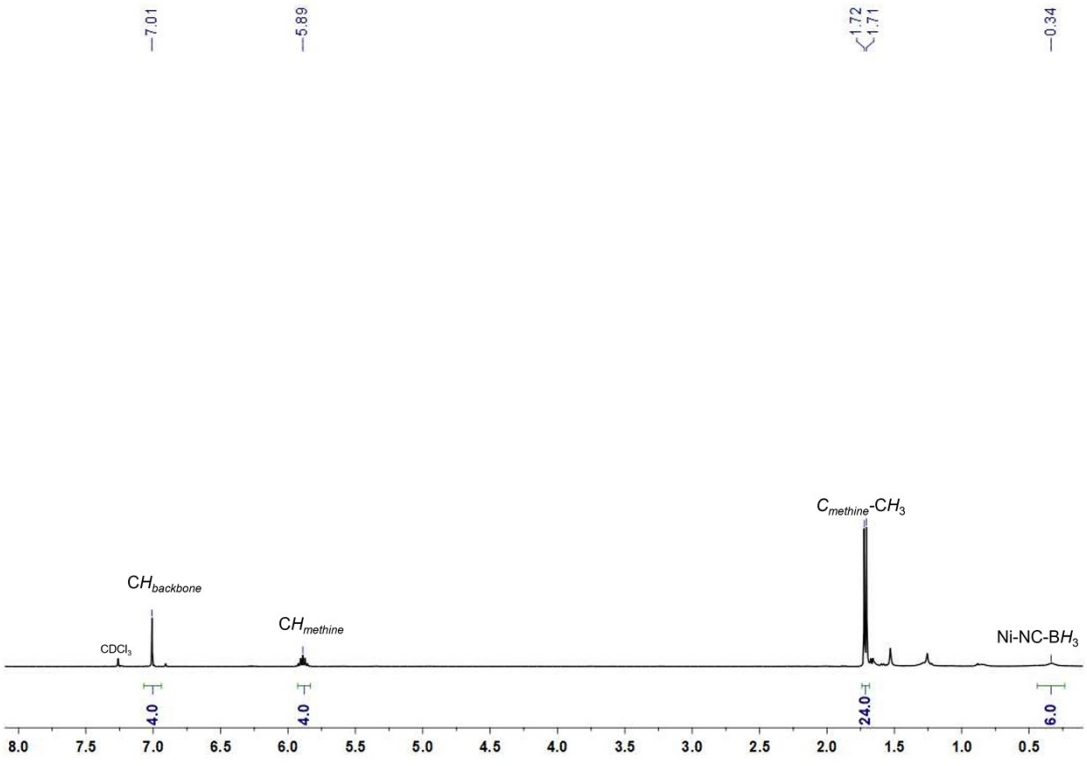

Figure S57. $^{1}H\{^{11}B\}$ NMR spectrum of *trans*-[Ni(*i*Pr_2Im)$_2$(NC-BH_3)$_2$] (*trans*-**14a**) in $CDCl_3$.

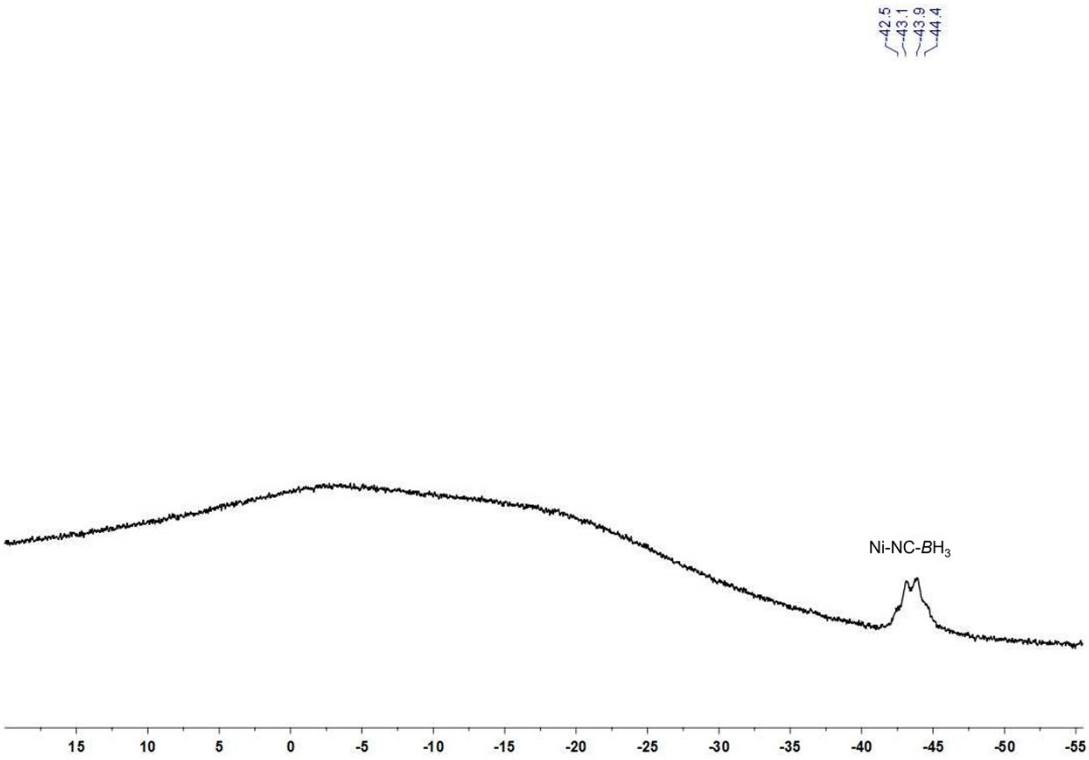

Figure S58. ^{11}B NMR spectrum of *trans*-[Ni(*i*Pr_2Im)$_2$(NC-BH_3)$_2$] (*trans*-**14a**) in $CDCl_3$.

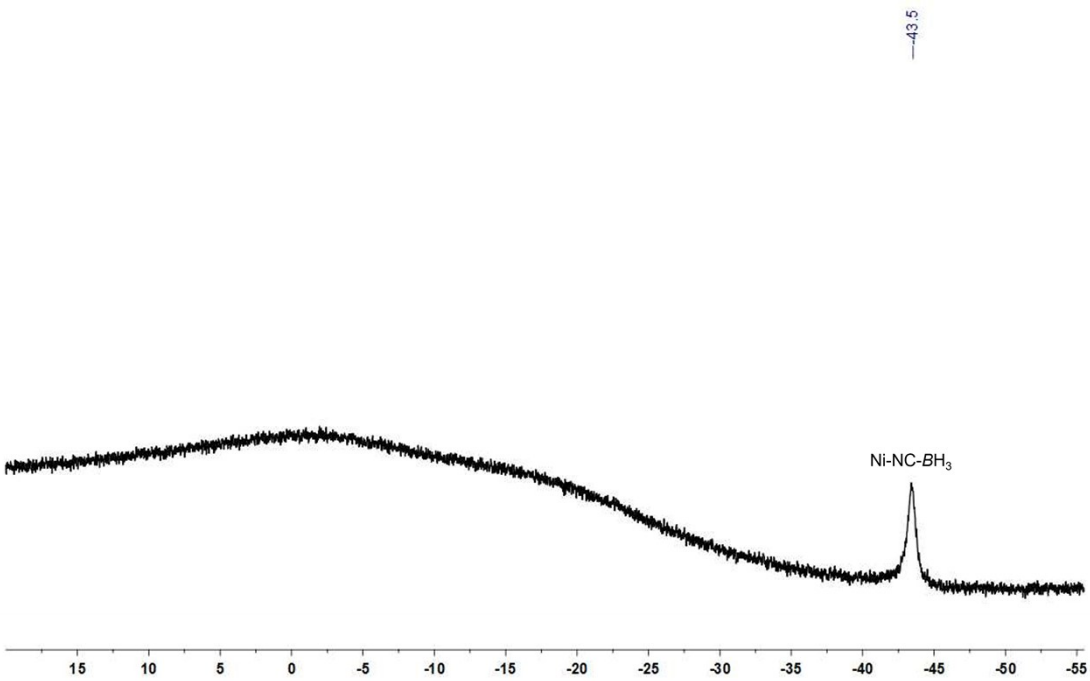

Figure S59. $^{11}B\{^{1}H\}$ NMR spectrum of *trans*-[Ni(*i*Pr_2Im)$_2$(NC-BH_3)$_2$] (*trans*-**14a**) in $CDCl_3$.

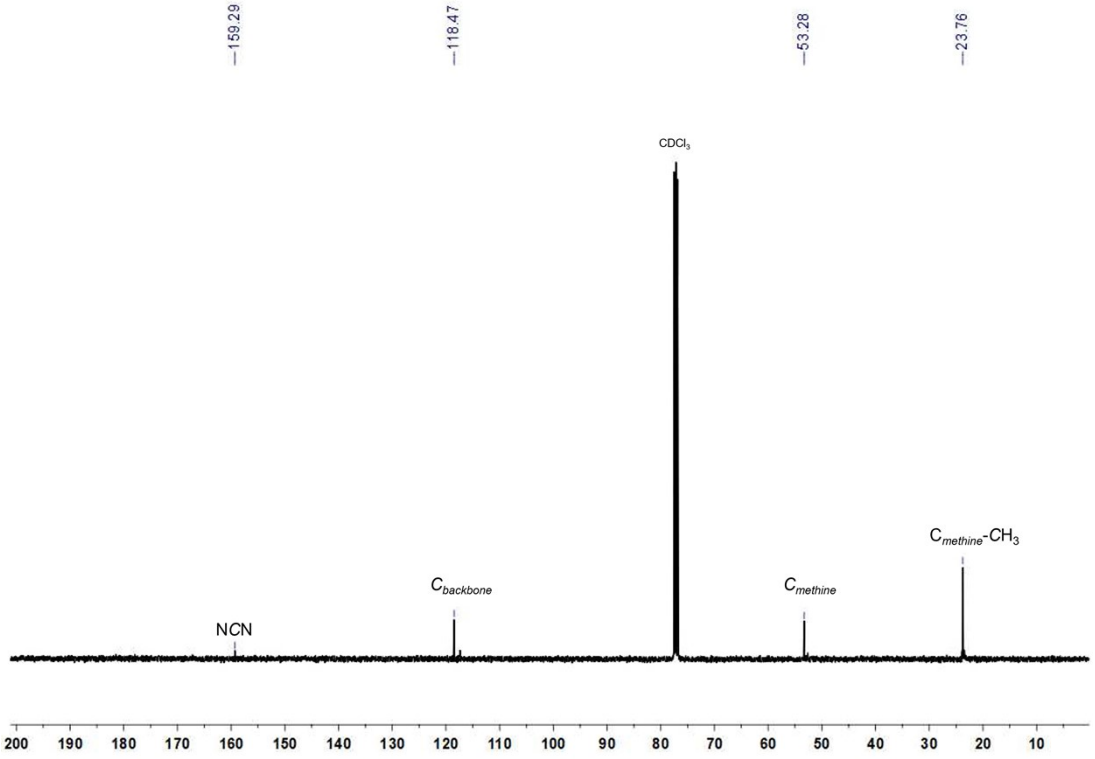

Figure S60. $^{13}C\{^{1}H\}$ NMR spectrum of *trans*-[Ni(*i*Pr_2Im)$_2$(NC-BH_3)$_2$] (*trans*-**14a**) in $CDCl_3$. B-CN signals were not detected.

***cis*-[Ni(*i*Pr$_2$Im)$_2$(NC-BH$_3$)$_2$] (*cis*-14a)**

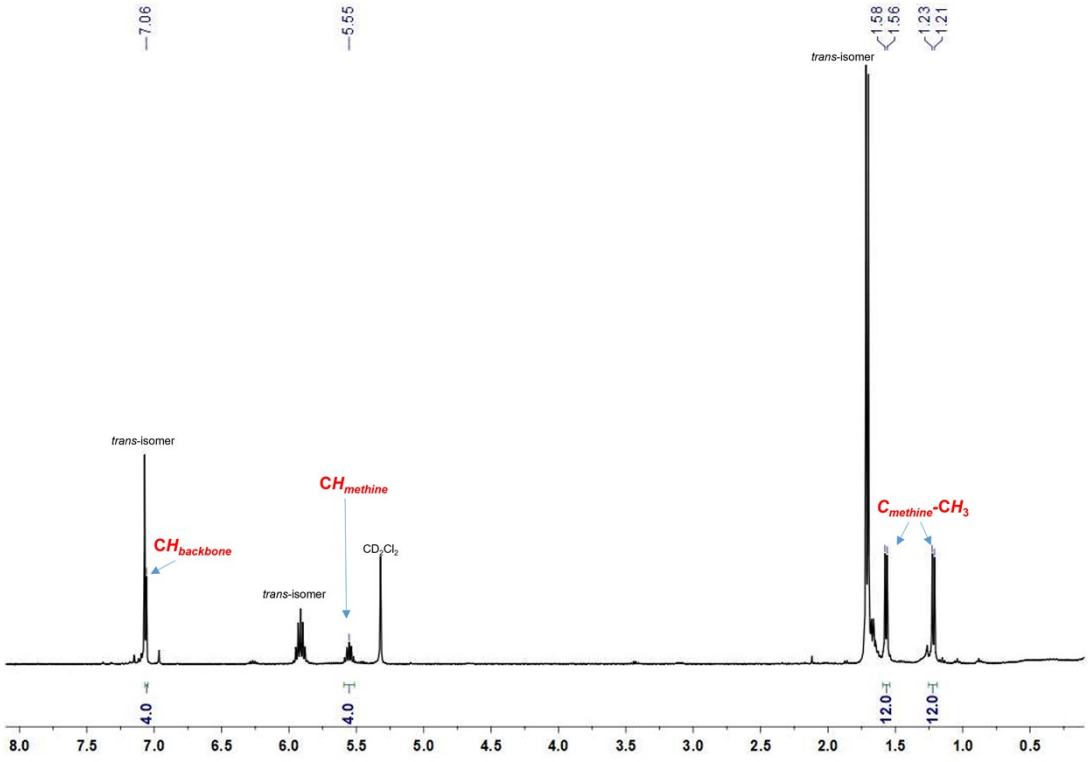

Figure S61. ^{1}H NMR spectrum of a ***cis*-** (marked herein) and trans- mixture of [Ni(*i*Pr$_2$Im)$_2$(NC-BH$_3$)] (*cis*-/*trans*-**14a**) in CD_2Cl_2.

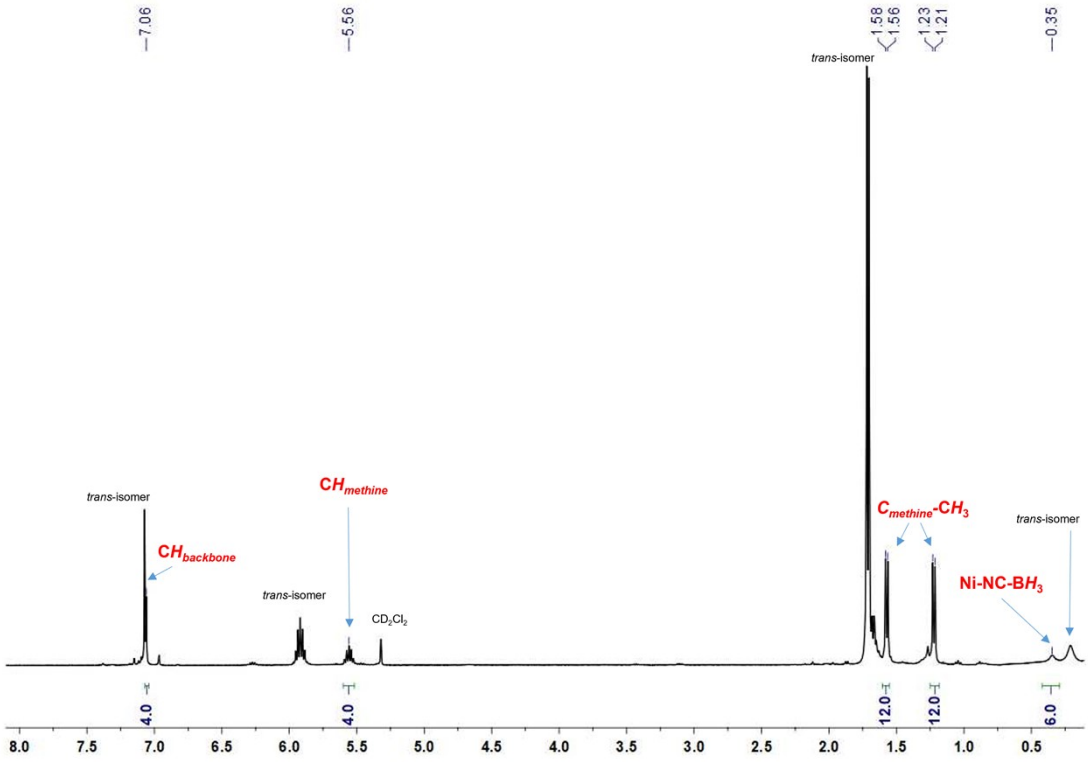

Figure S62. ^{1}H{^{11}B} NMR spectrum of a ***cis*-** (marked herein) and *trans*- mixture of [Ni(*i*Pr$_2$Im)$_2$(NC-BH$_3$)] (*cis*-/*trans*-**14a**) in CD_2Cl_2.

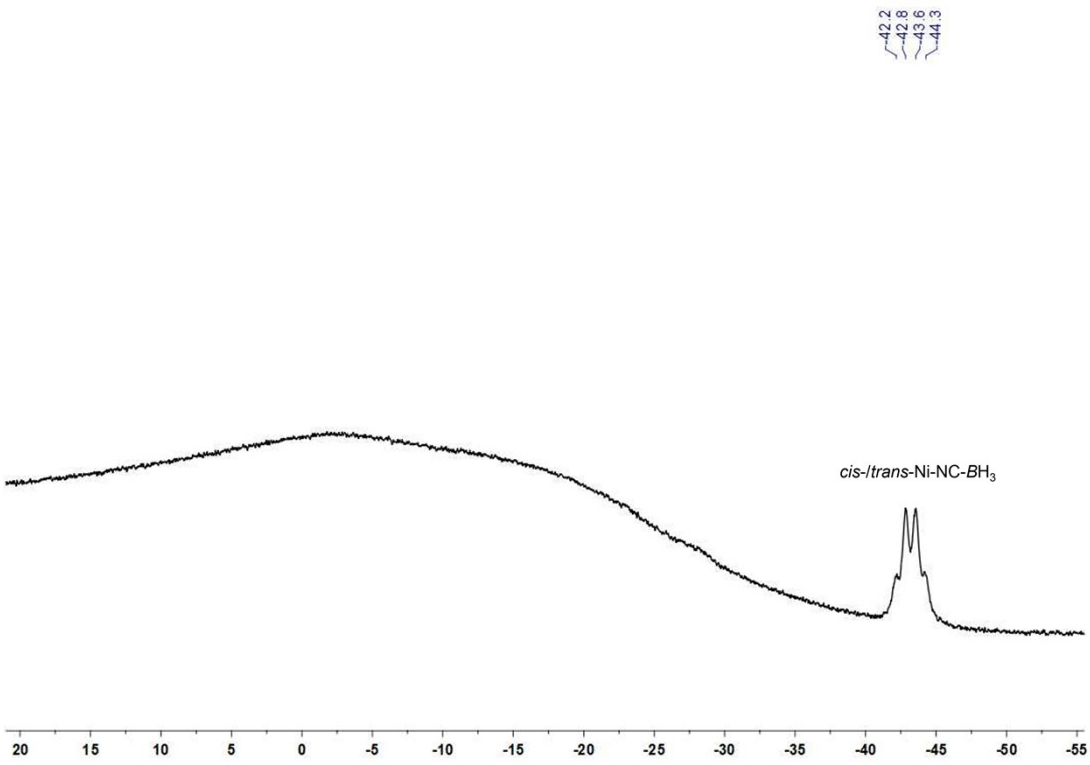

Figure S63. ^{11}B NMR spectrum of a *cis*- and *trans*- mixture of [Ni(*i*Pr$_2$Im)$_2$(NC-BH$_3$)] (*cis*-/*trans*-**14a**) in CD_2Cl_2.

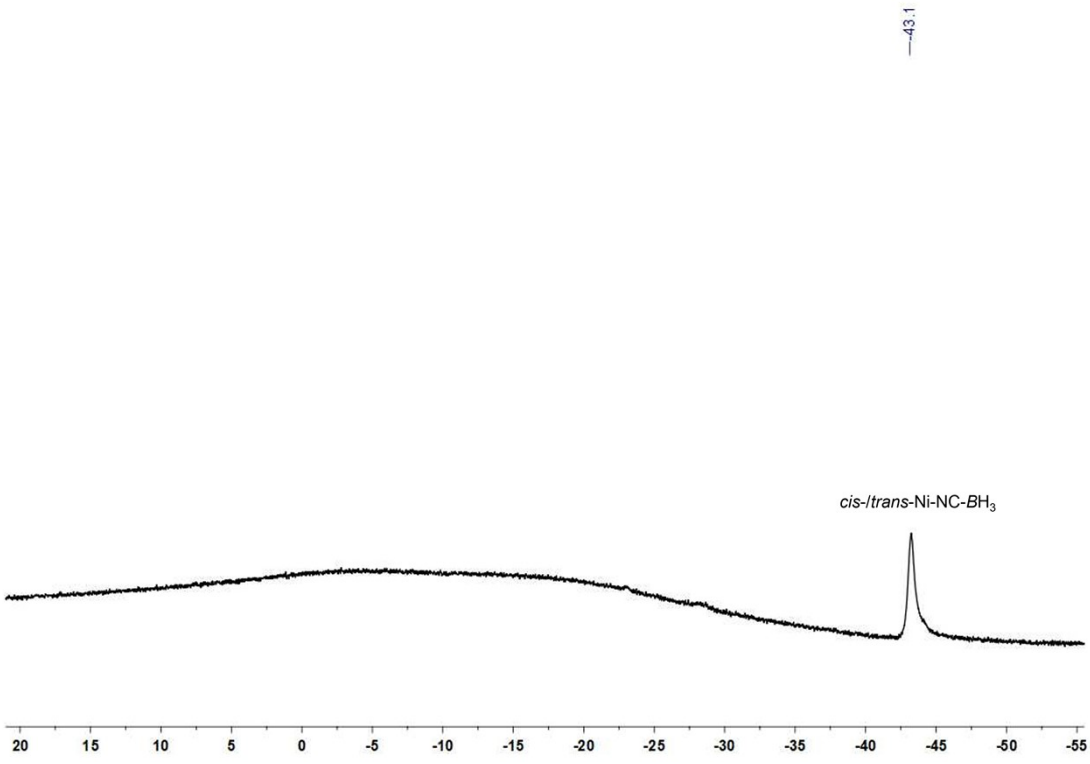

Figure S64. $^{11}B\{^1H\}$ NMR spectrum of a *cis*- and *trans*- mixture of [Ni(*i*Pr$_2$Im)$_2$(NC-BH$_3$)] (*cis*-/*trans*-**14a**) in CD_2Cl_2.

***cis- /trans-* mixture of [Ni(*i*Pr$_2$Im)$_2$(NC-BH$_2$(CN))$_2$] (*cis-*/*trans*-14b)**

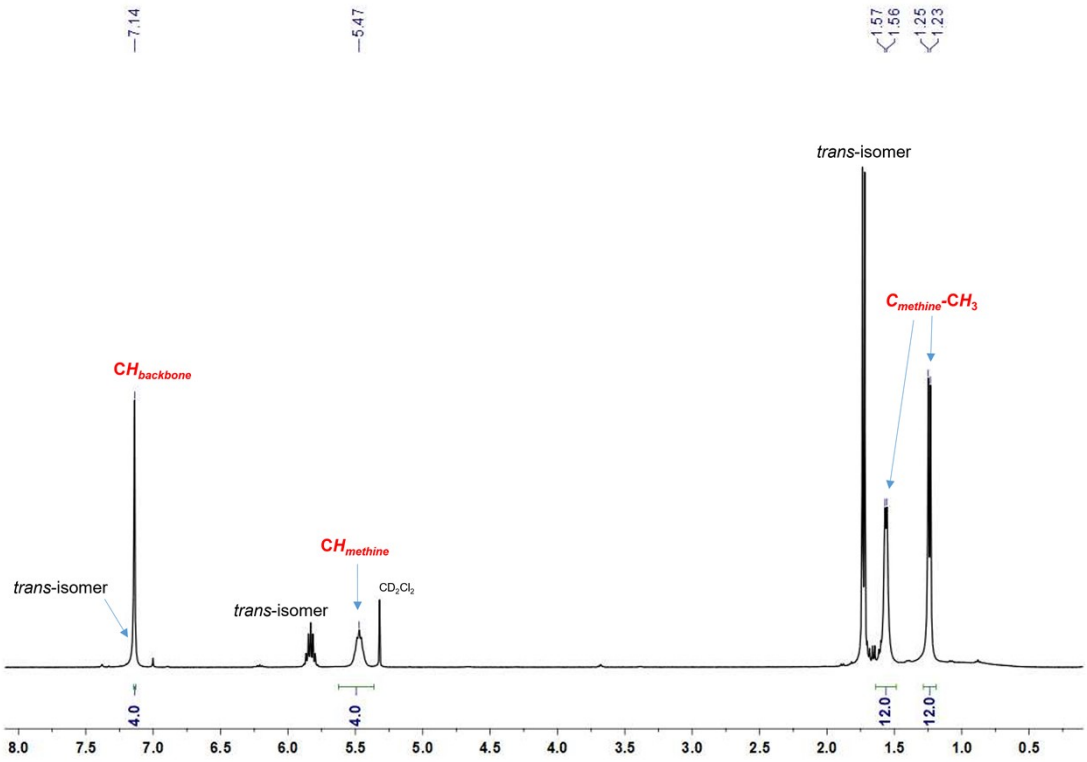

Figure S65. ^{1}H NMR spectrum of a ***cis-*** (marked herein) and *trans*- mixture of [Ni(*i*Pr$_2$Im)$_2$(NC-BH$_2$CN)$_2$] (*cis-*/*trans*-**14b**) in CD_2Cl_2.

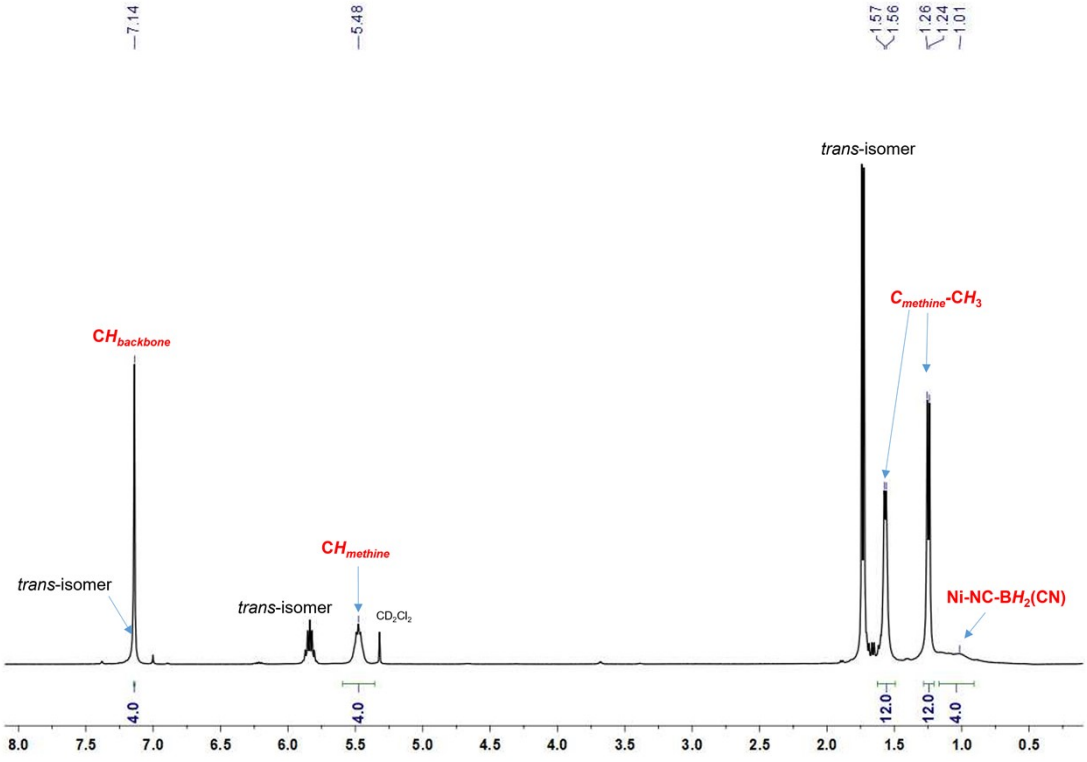

Figure S66. ^{1}H{^{11}B} NMR spectrum of a ***cis-*** (marked herein) and *trans*- mixture of [Ni(*i*Pr$_2$Im)$_2$(NC-BH$_2$CN)$_2$] (*cis-*/*trans*-**14b**) in CD_2Cl_2.

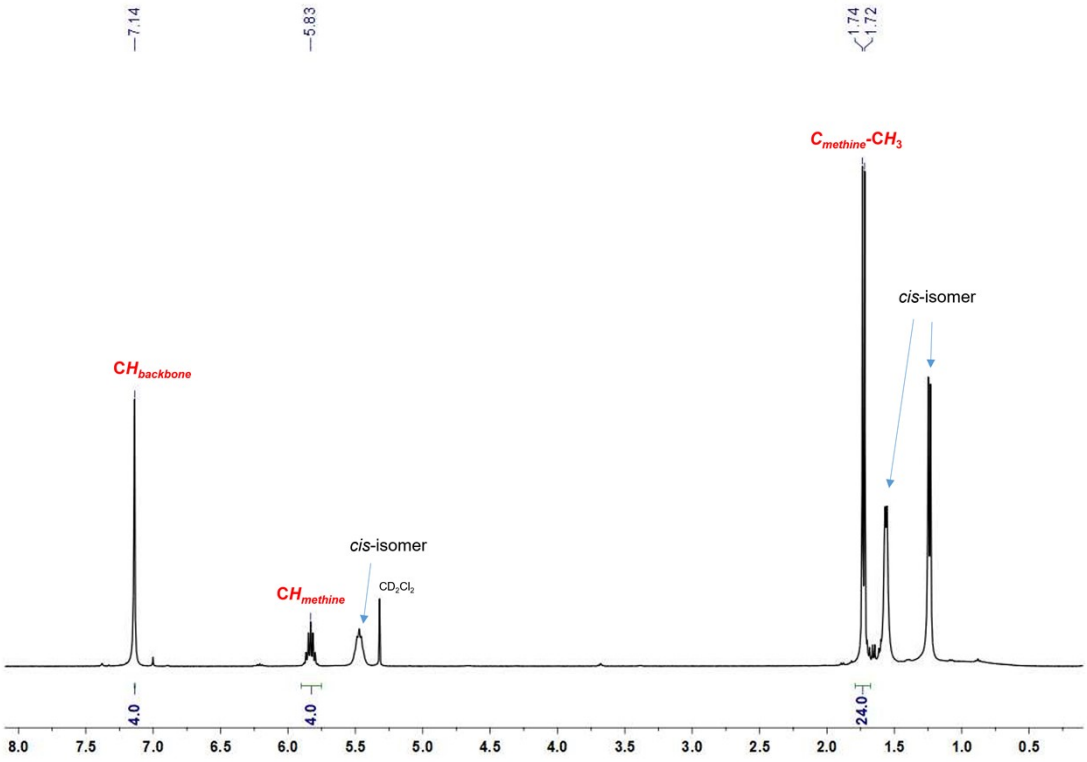

Figure S67. ^{1}H NMR spectrum of a *cis*- and ***trans*-** (marked herein) mixture of [Ni(*i*Pr$_2$Im)$_2$(NC-BH$_2$CN)$_2$] (*cis*-/*trans*-**14b**) in CD_2Cl_2.

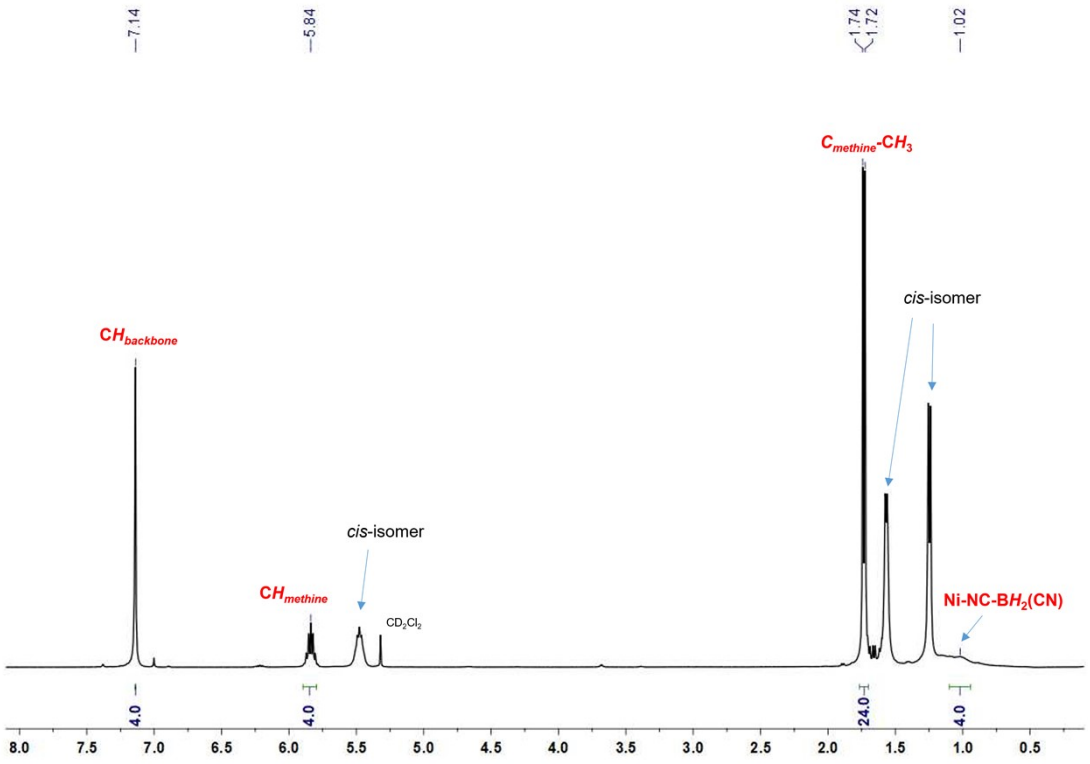

Figure S68. ^{1}H{^{11}B} NMR spectrum of a *cis*- and ***trans*-** (marked herein) mixture of [Ni(*i*Pr$_2$Im)$_2$(NC-BH$_2$CN)$_2$] (*cis*-/*trans*-**14b**) in CD_2Cl_2.

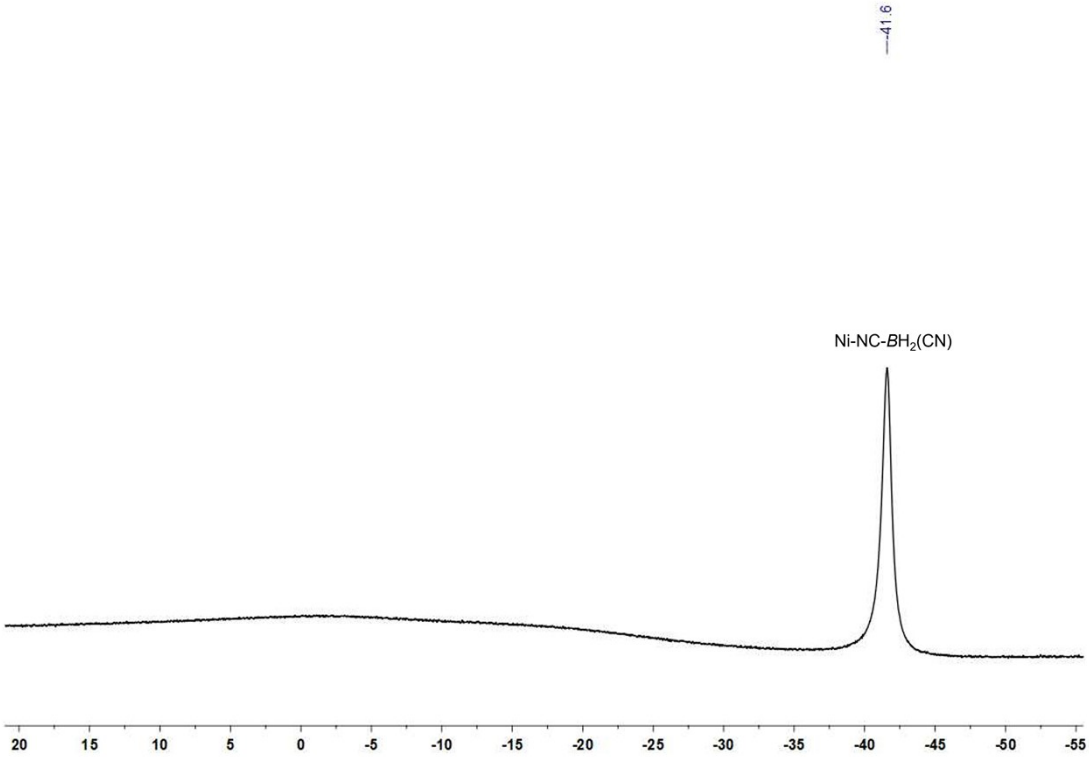

Figure S69. $^{11}B\{^{1}H\}$ NMR spectrum of a *cis*- and *trans*- (marked herein) mixture of $[Ni(i Pr_2Im)_2(NC\text{-}BH_2CN)_2]$ (*cis*-/*trans*-**14b**) in CD_2Cl_2.

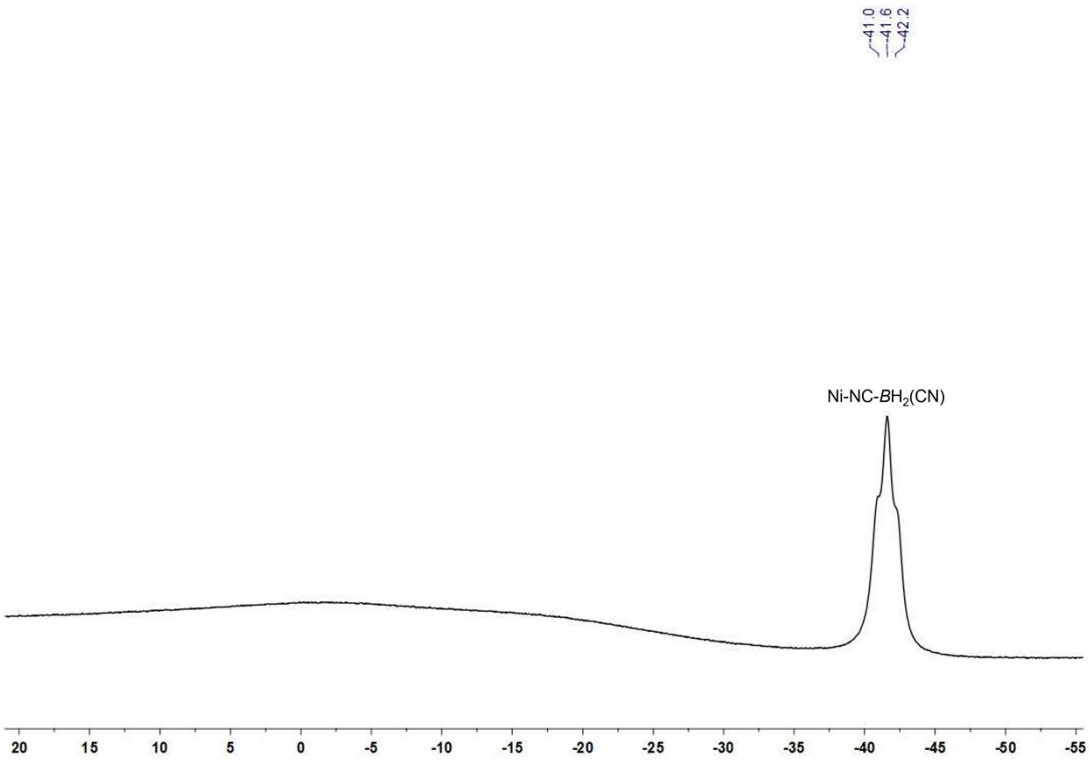

Figure S70. ^{11}B NMR spectrum of a *cis*- and *trans*- (marked herein) mixture of $[Ni(i Pr_2Im)_2(NC\text{-}BH_2CN)_2]$ (*cis*-/*trans*-**14b**) in CD_2Cl_2.

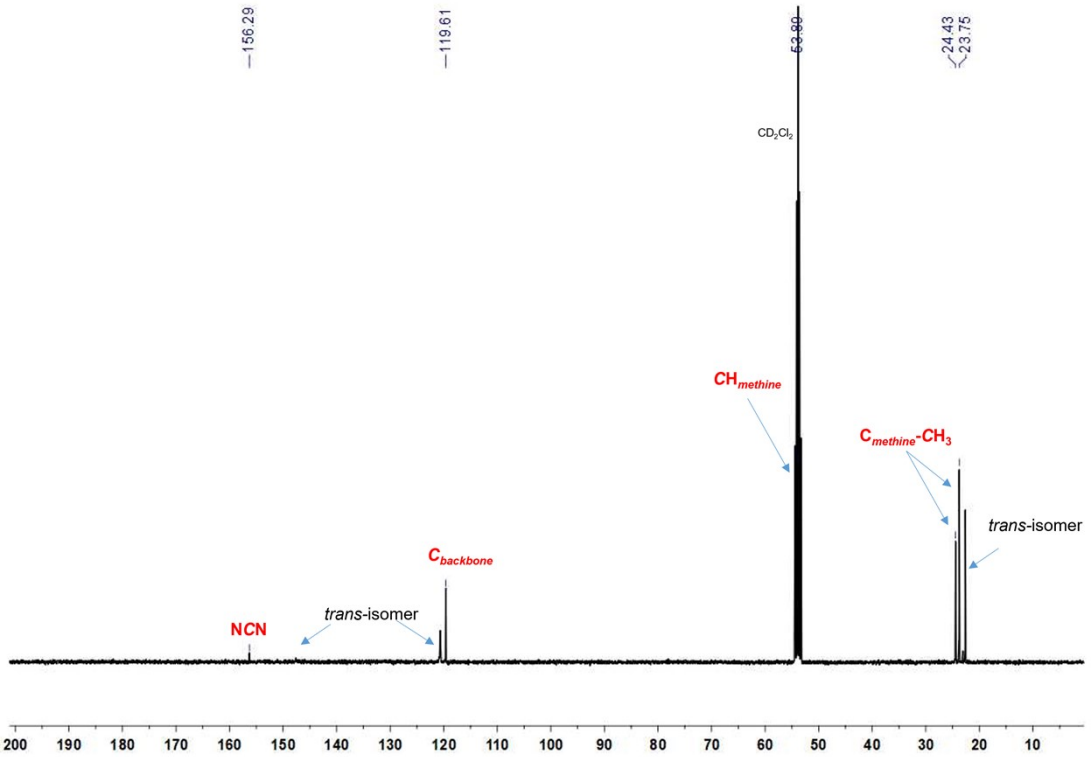

Figure S71. $^{13}C\{^{1}H\}$ NMR spectrum of a ***cis***- (marked herein) and *trans*- mixture of [Ni(*i*Pr$_2$Im)$_2$(NC-BH$_2$CN)$_2$] (*cis*-/*trans*-**14b**) in CD_2Cl_2.

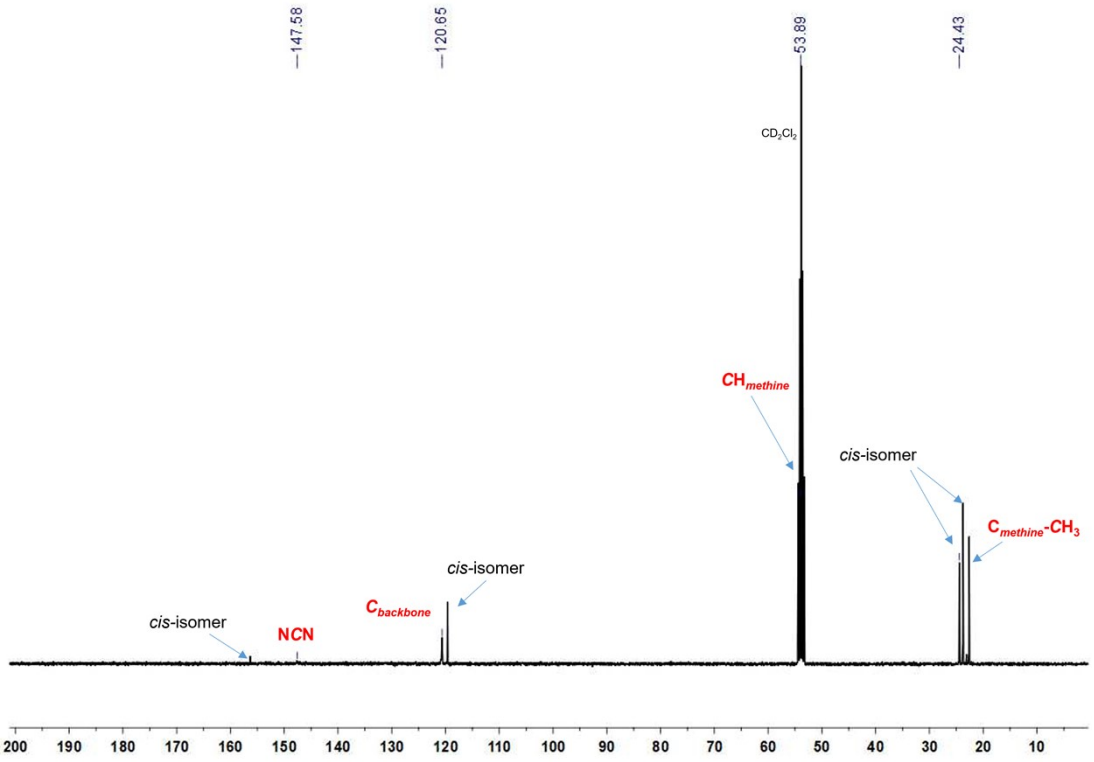

Figure S72. $^{13}C\{^{1}H\}$ NMR spectrum of a *cis*- and ***trans***-(marked herein) mixture of [Ni(*i*Pr$_2$Im)$_2$(NC-BH$_2$CN)$_2$] (*cis*-/*trans*-**14b**) in CD_2Cl_2.

***cis*-[Ni(*i*Pr$_2$Im)$_2${NC-BH(CN)$_2$}$_2$] (*cis*-14c)**

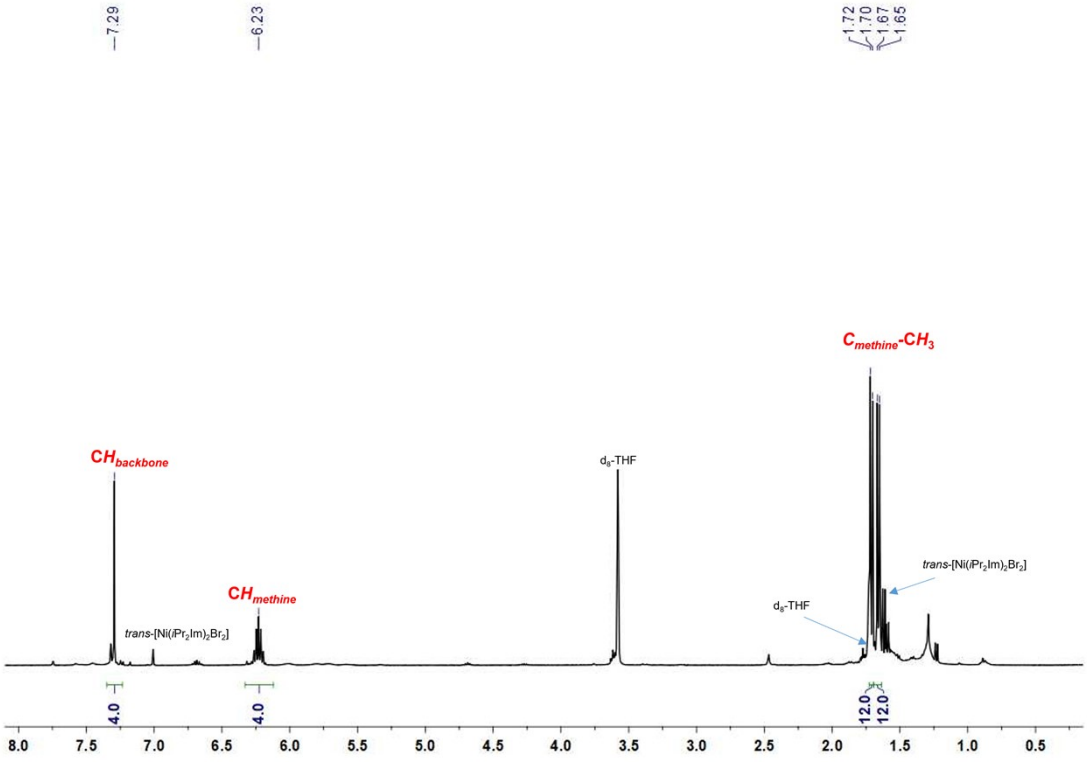

Figure S73. ^{1}H NMR spectrum of *cis*-[Ni(*i*Pr$_2$Im)$_2${NC-BH(CN)$_2$}$_2$] (*cis*-**14c**) in d$_8$-THF.

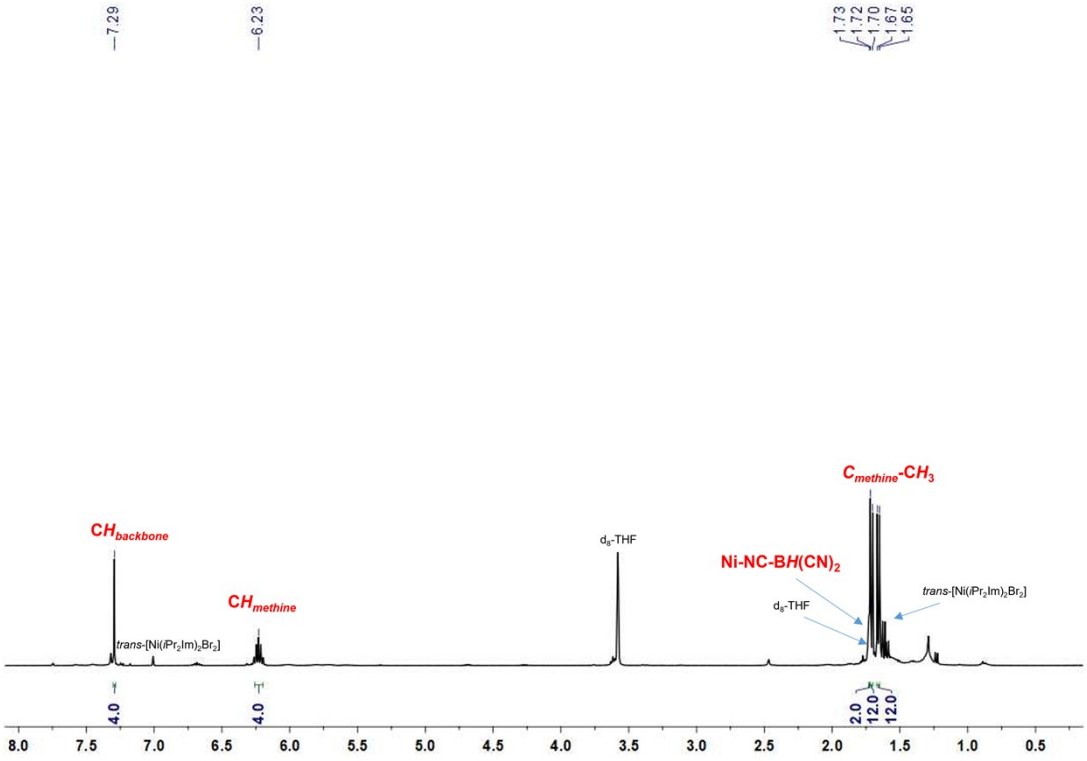

Figure S74. ^{1}H{^{11}B} NMR spectrum of *cis*-[Ni(*i*Pr$_2$Im)$_2${NC-BH(CN)$_2$}$_2$] (*cis*-**14c**) in d$_8$-THF.

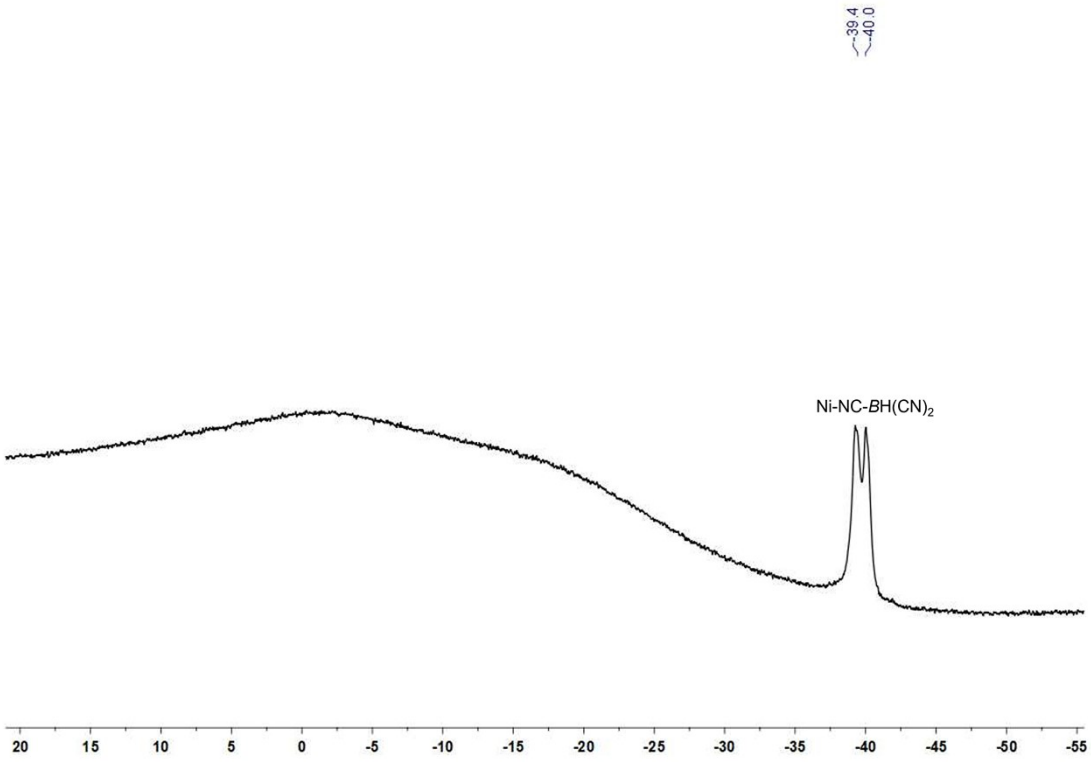

Figure S75. ^{11}B NMR spectrum of *cis*-[Ni(*i*Pr$_2$Im)$_2${NC-BH(CN)$_2$}$_2$] (*cis*-**14c**) in d$_8$-THF.

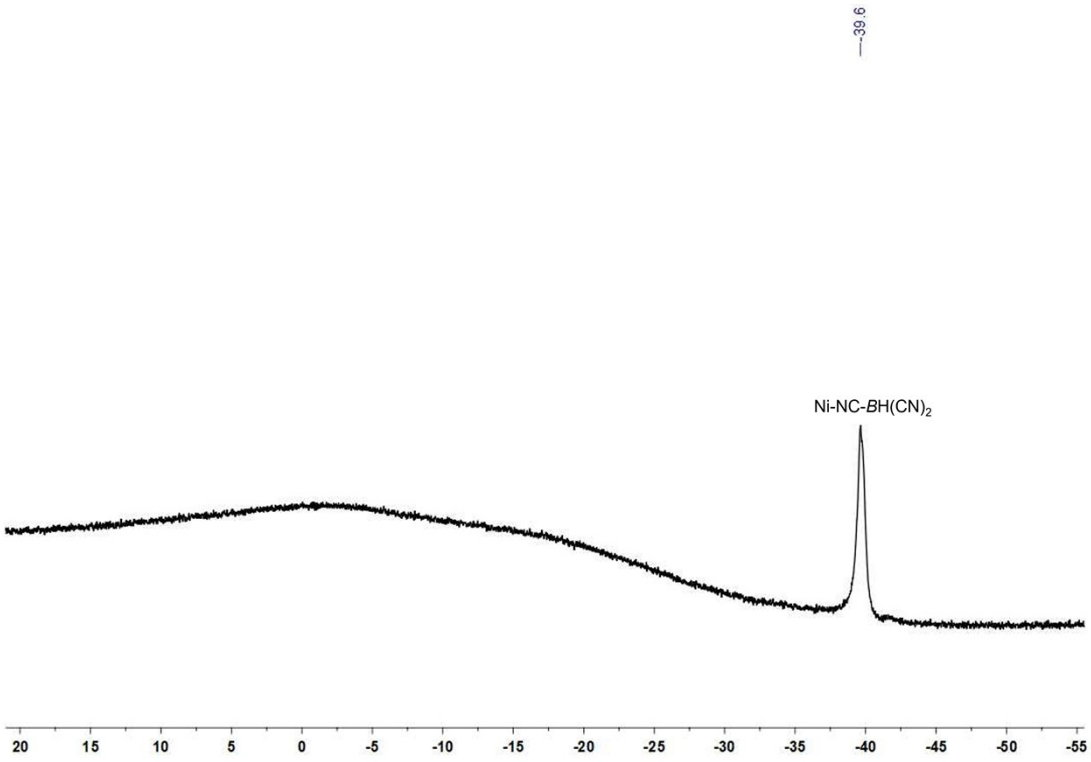

Figure S76. $^{11}B\{^1H\}$ NMR spectrum of *cis*-[Ni(*i*Pr$_2$Im)$_2${NC-BH(CN)$_2$}$_2$] (*cis*-**14c**) in d$_8$-THF.

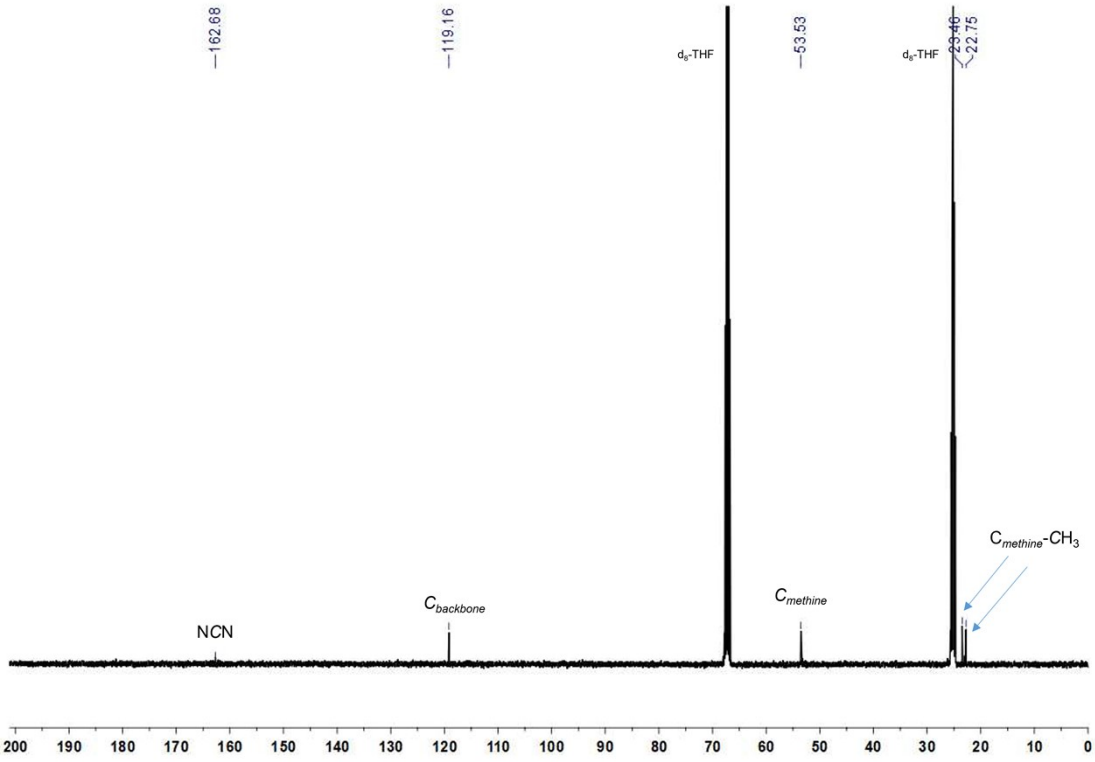

Figure S77. $^{13}C\{^{1}H\}$ NMR spectrum of *cis*-[Ni(*i*Pr_2Im)$_2${NC-BH(CN)$_2$}$_2$] (*cis*-**14c**) in d_8-THF. B-CN signals were not detected.

trans-[Ni(*i*Pr_2Im^{Me})$_2$(NC-BH_2(CN)$_2$] (*trans*-15b)

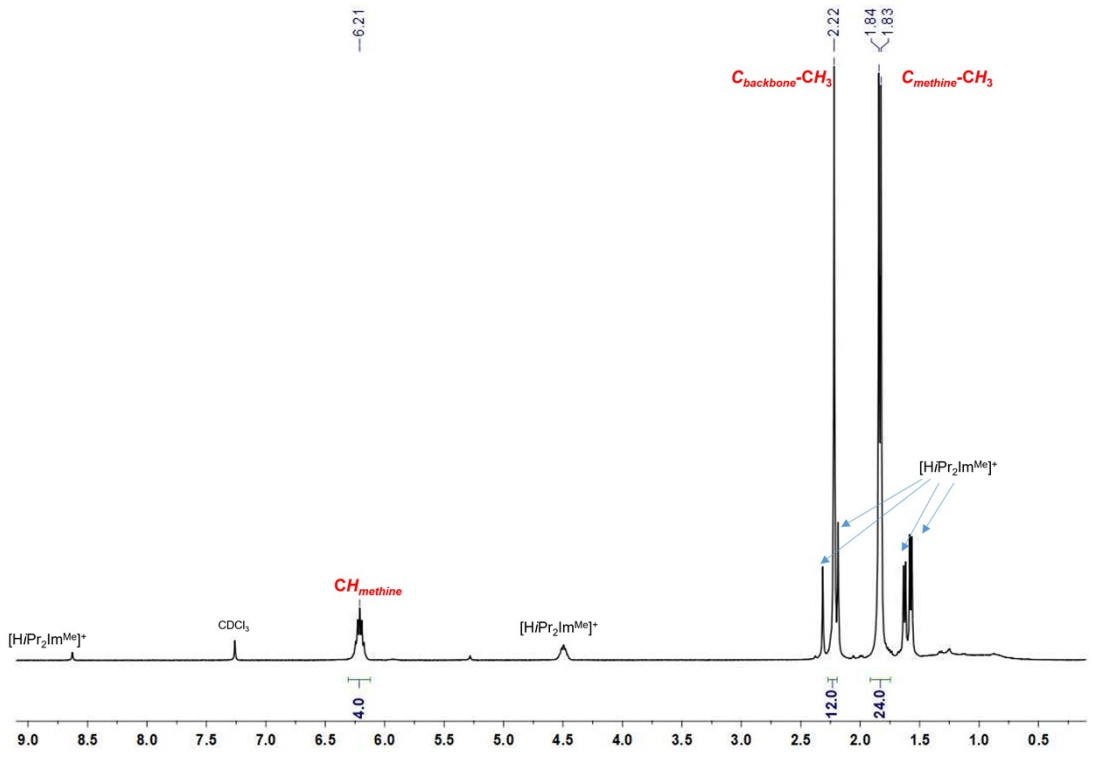

Figure S78. ^{1}H NMR spectrum of *trans*-[Ni(*i*Pr_2Im^{Me})$_2$(NC-BH_2CN)$_2$] (*trans*-**15b**) in $CDCl_3$.

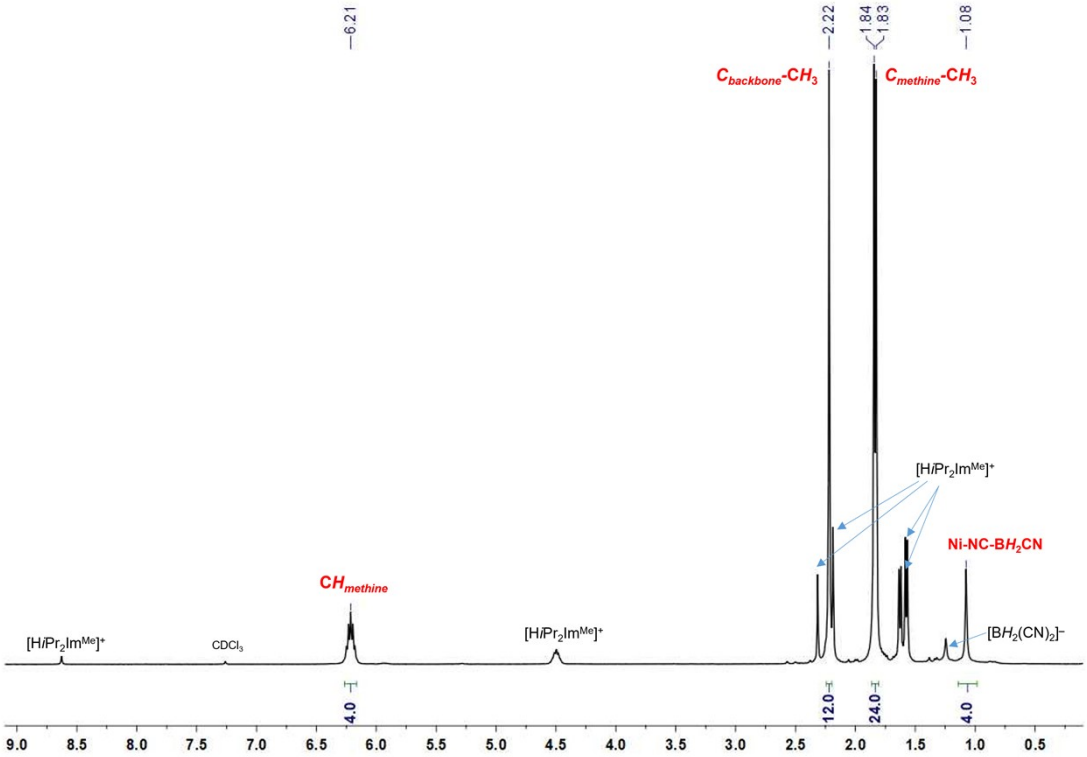

Figure S79. $^1H\{^{11}B\}$ NMR spectrum of *trans*-[Ni(*i*Pr$_2$Im^{Me})$_2$(NC-BH$_2$CN)$_2$] (*trans*-**15b**) in $CDCl_3$.

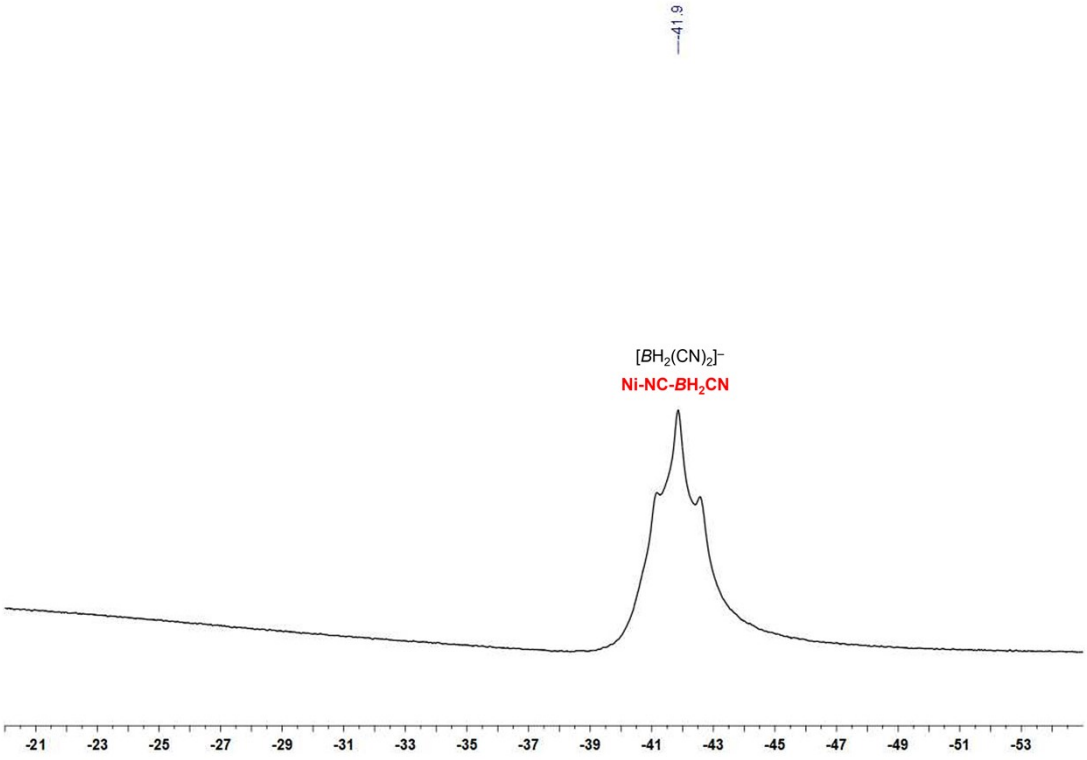

Figure S80. ^{11}B NMR spectrum of *trans*-[Ni(*i*Pr$_2$Im^{Me})$_2$(NC-BH$_2$CN)$_2$] (*trans*-**15b**) in $CDCl_3$.

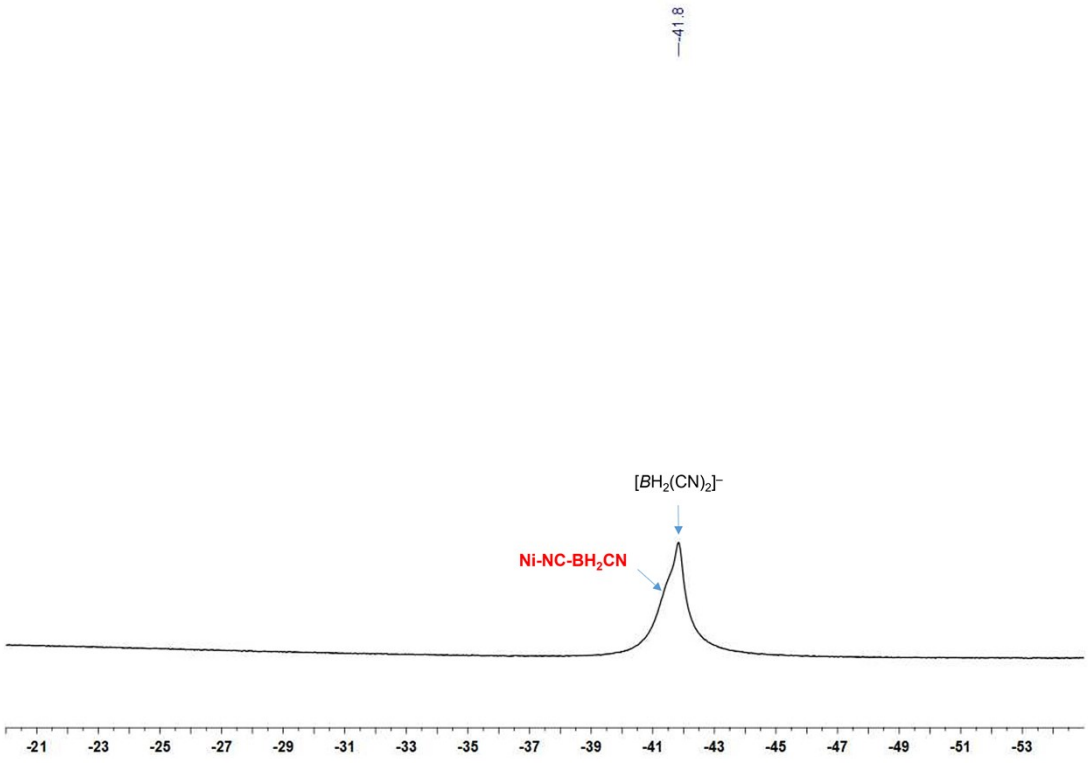

Figure S81. $^{11}B\{^{1}H\}$ NMR spectrum of *trans*-[Ni(*i*Pr$_2$Im^{Me})$_2$(NC-BH$_2$CN)$_2$] (*trans*-**15b**) in $CDCl_3$.

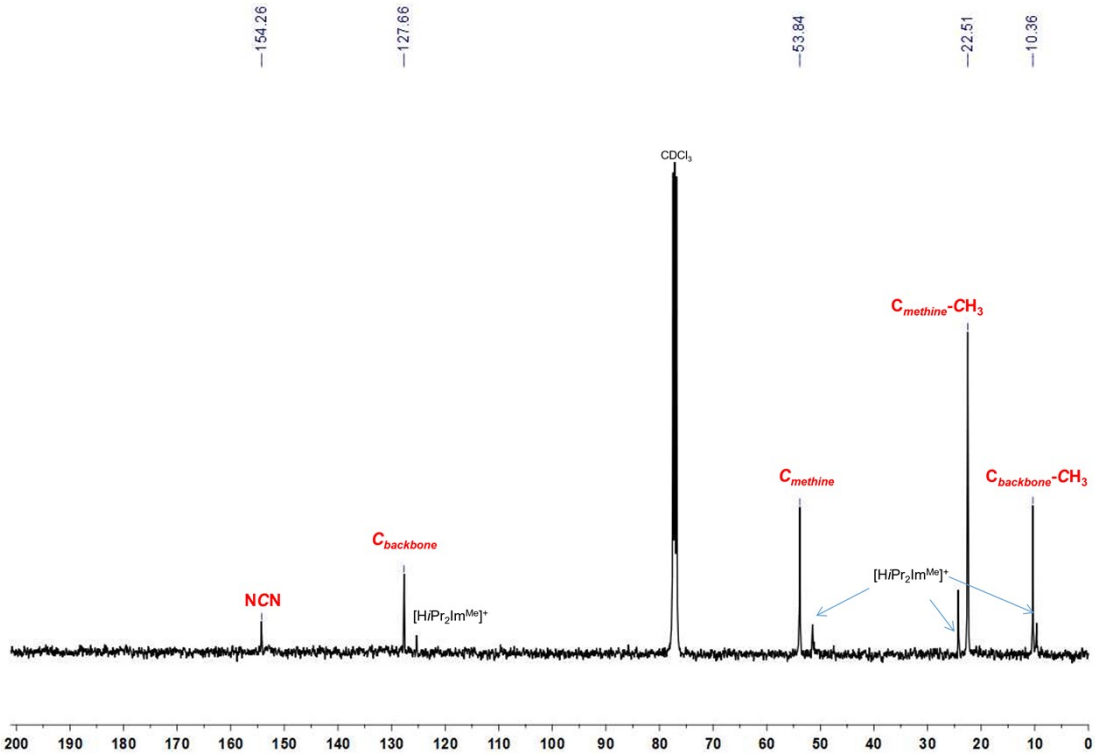

Figure S82. $^{13}C\{^{1}H\}$ NMR spectrum of *trans*-[Ni(*i*Pr$_2$Im^{Me})$_2$(NC-BH$_2$CN)$_2$] (*trans*-**15b**) in $CDCl_3$.

[Ni(*i*Pr$_2$Im)$_3${NC-BH(CN)$_2$}][BH(CN)$_3$] (16c)

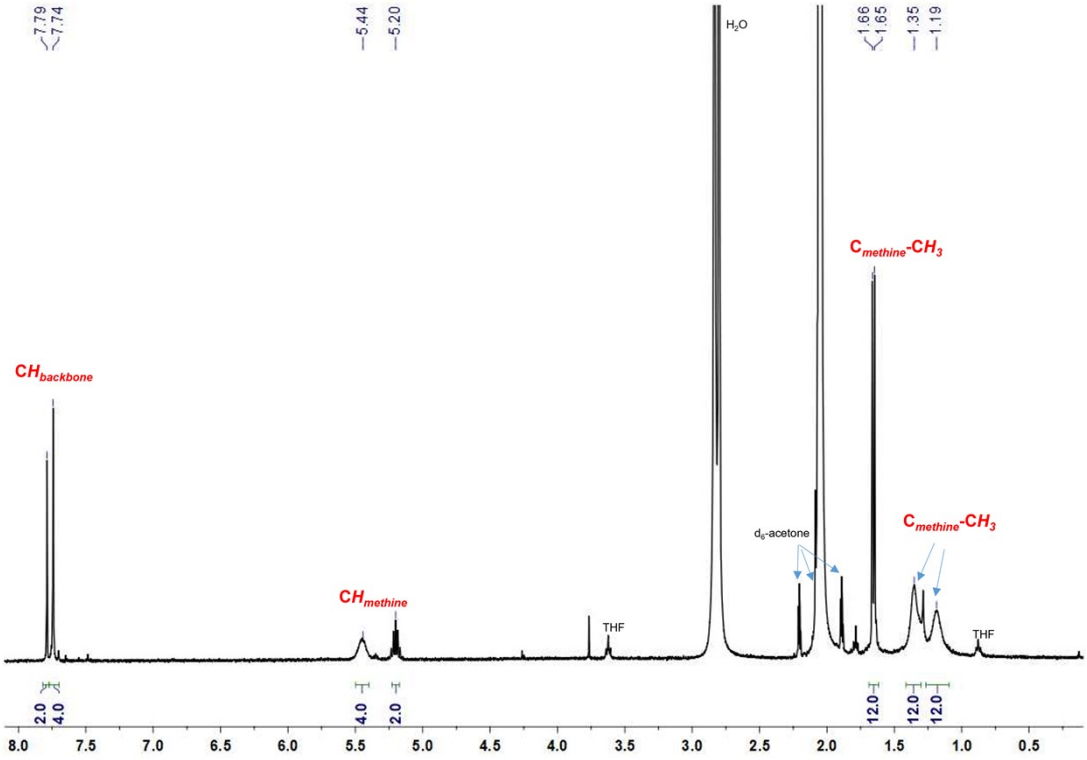

Figure S83. ^{1}H NMR spectrum of [Ni(*i*Pr$_2$Im)$_3${NC-BH(CN)$_2$}][BH(CN)$_3$] (**16c**) in d$_6$-acetone.

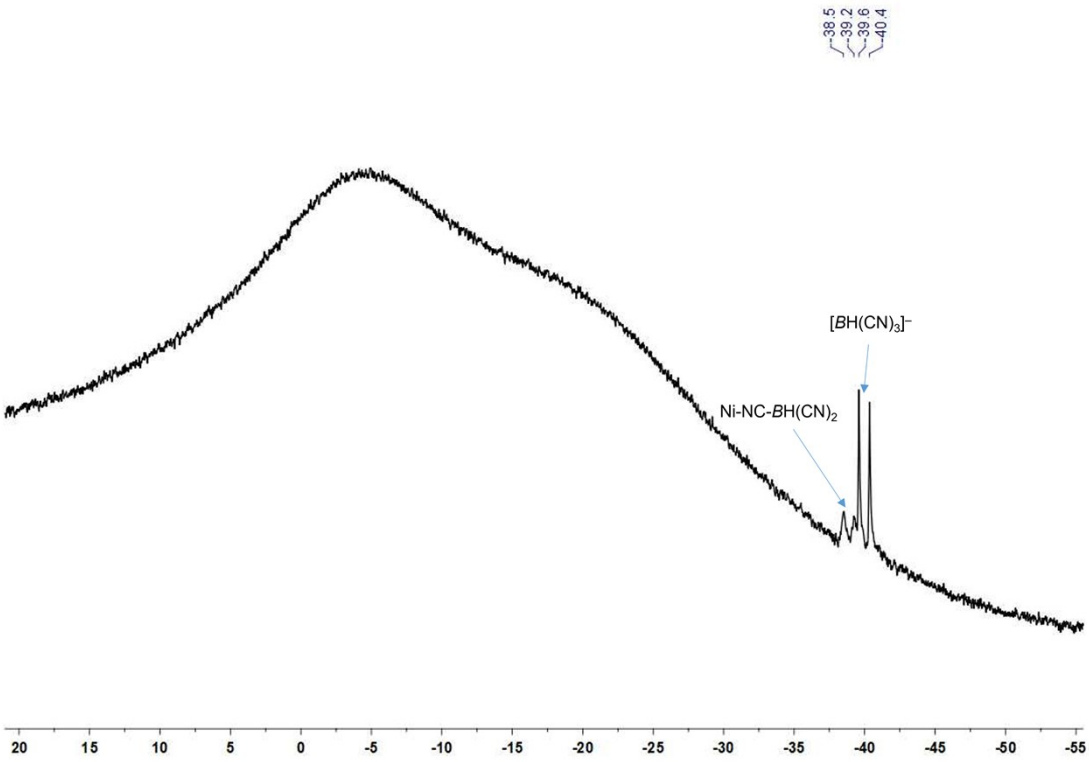

Figure S84. ^{11}B NMR spectrum of [Ni(*i*Pr$_2$Im)$_3${NC-BH(CN)$_2$}][BH(CN)$_3$] (**16c**) in d$_6$-acetone.

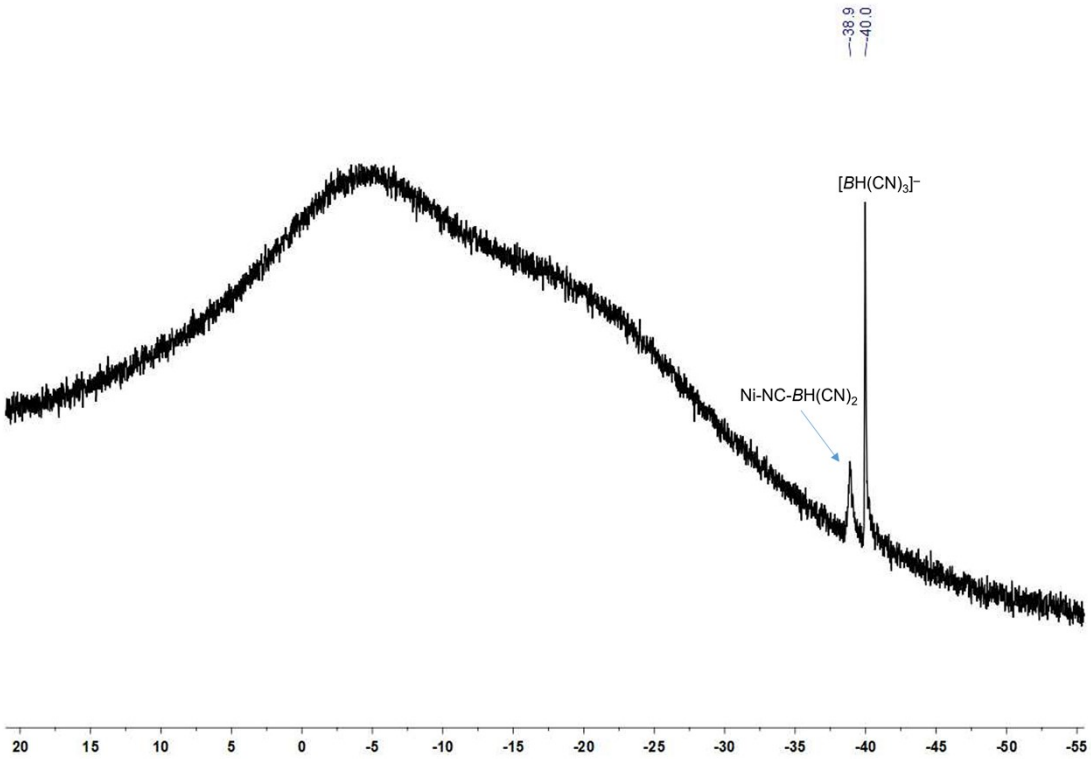

Figure S85. $^{11}B\{^{1}H\}$ NMR spectrum of $[Ni(iPr_2Im)_3\{NC\text{-}BH(CN)_2\}][BH(CN)_3]$ (**16c**) in d_6-acetone.

4 Infrared Spectroscopy Section

4.1 General Information

Infrared spectra were recorded on a Bruker Alpha II spectrometer as solids by using an ATR unit and plotted using the OPUS software package.

4.2 IR Spectra

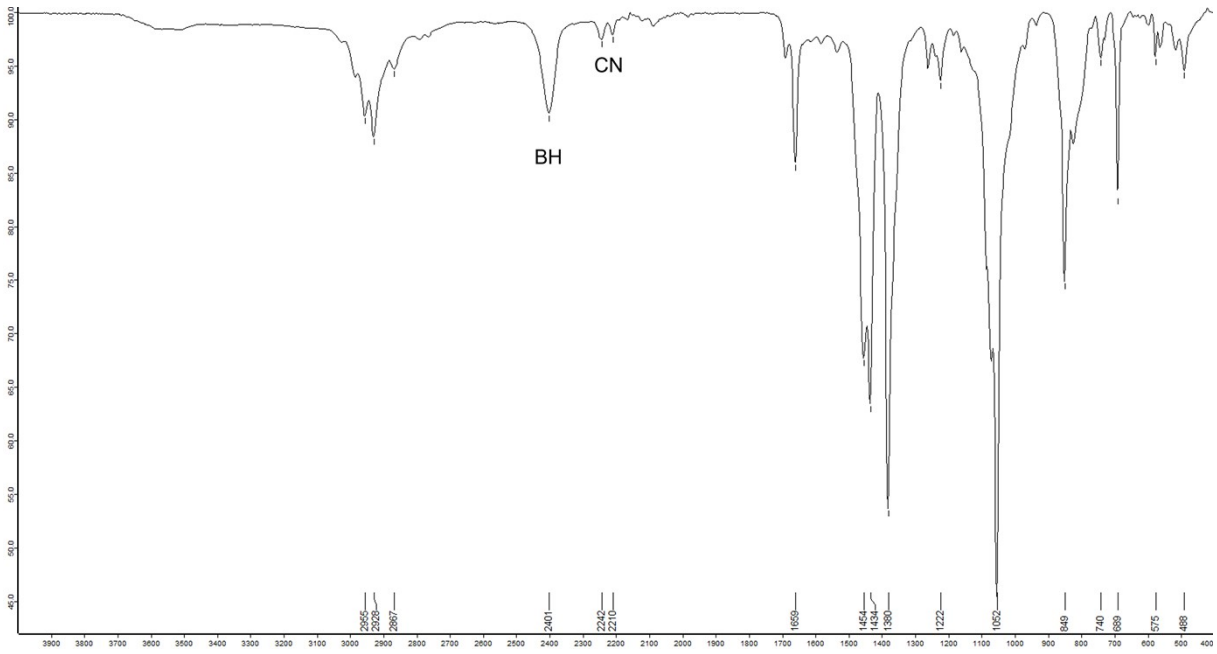

Figure S86. FT-IR spectrum (ATR) of $[Ni(Me_2Im^{Me})_4][BH(CN)_3]_2$ (**1c**).

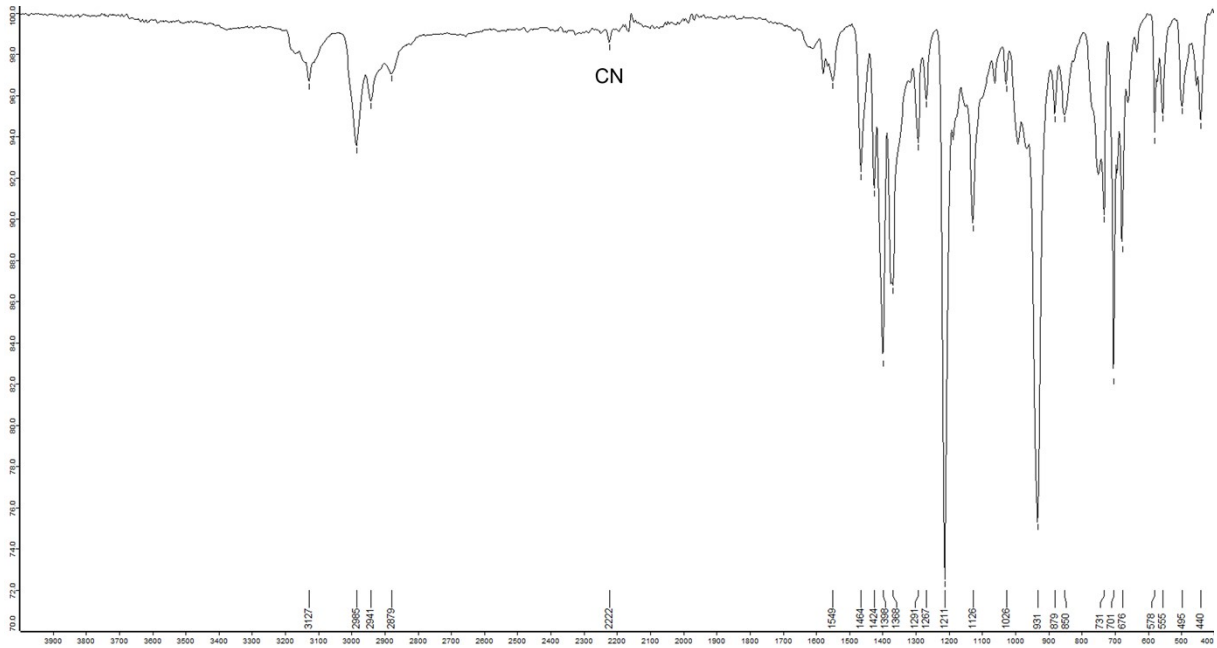

Figure S87. FT-IR spectrum (ATR) of $[Ni(i Pr_2Im)_4][B(CN)_4]_2$ (**2d**).

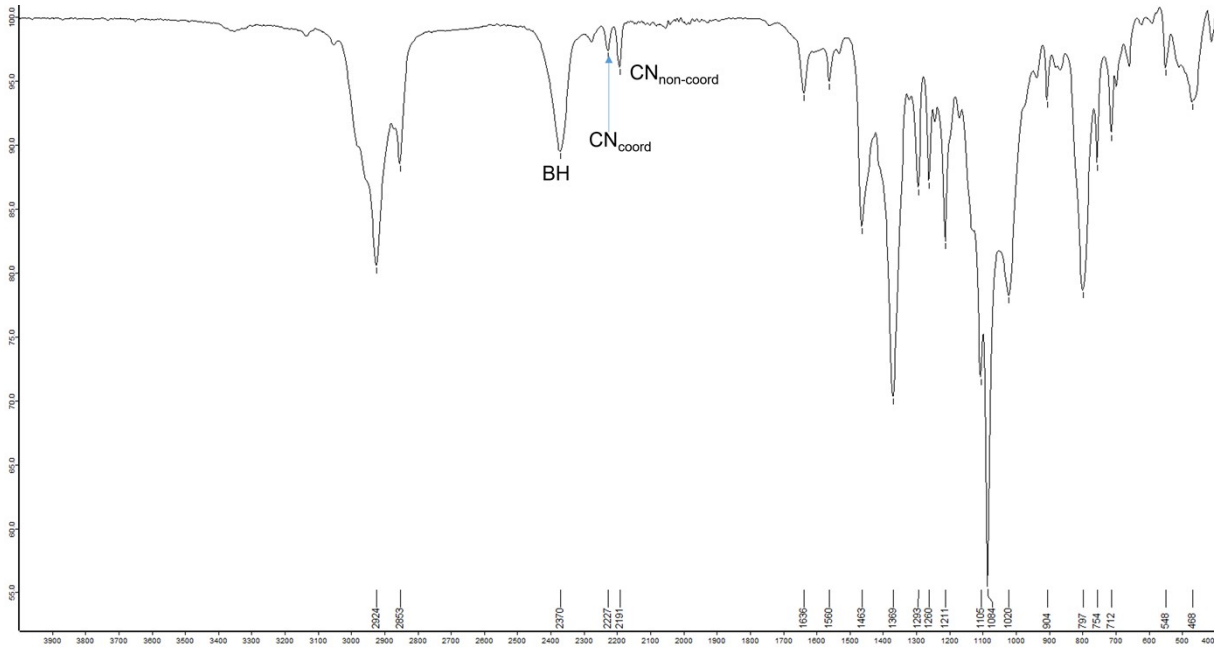

Figure S88. FT-IR spectrum (ATR) of [Ni(*i*Pr$_2$Im^{Me})$_3$(NC-BH$_2$CN)][BH$_2$(CN)$_2$] (**3b**).

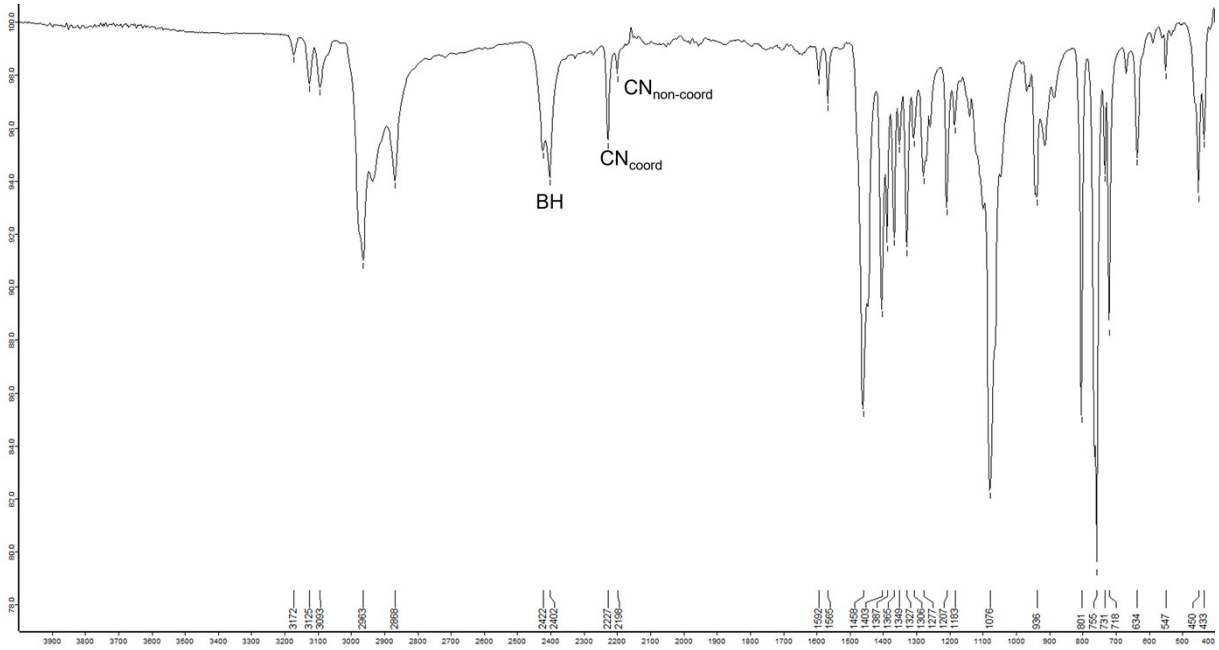

Figure S89. FT-IR spectrum (ATR) of *trans*-[Ni(Dipp$_2$Im)$_2$(NC-BH$_2$CN)$_2$] (*trans*-**4b**).

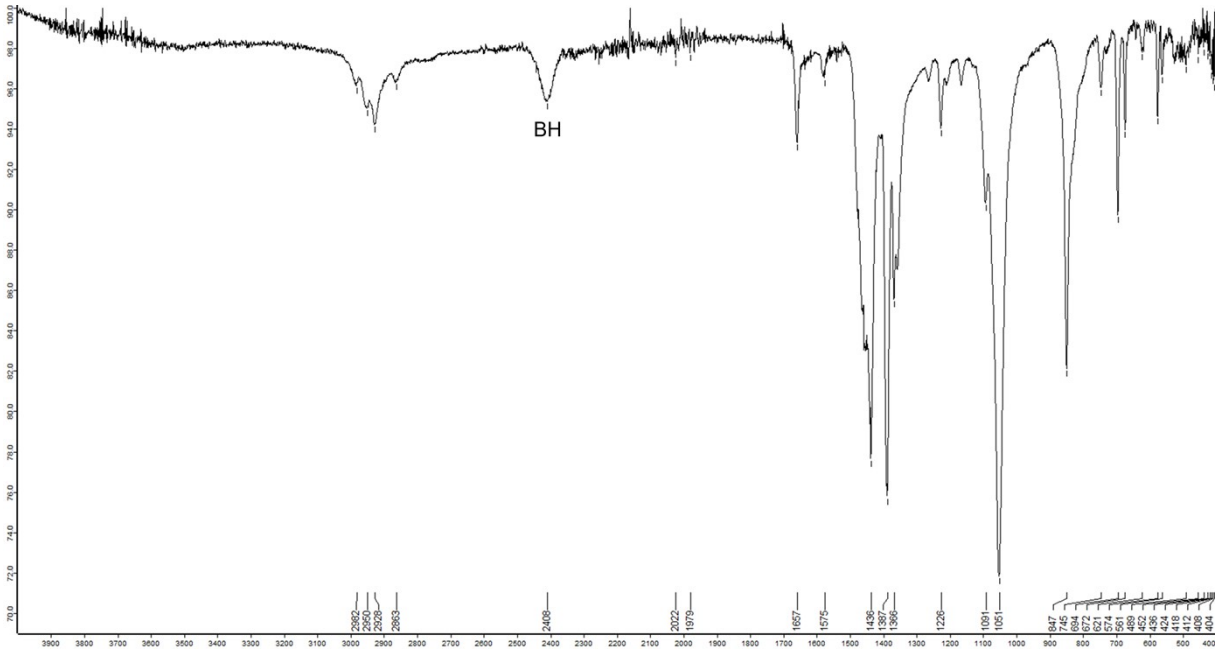

Figure S90. FT-IR spectrum (ATR) of *cis*-[Ni(Me_2Im^{Me})$_2${NC-BH$(CN)_2$}Br] (*cis*-**10c**). CN-bands were not detected.

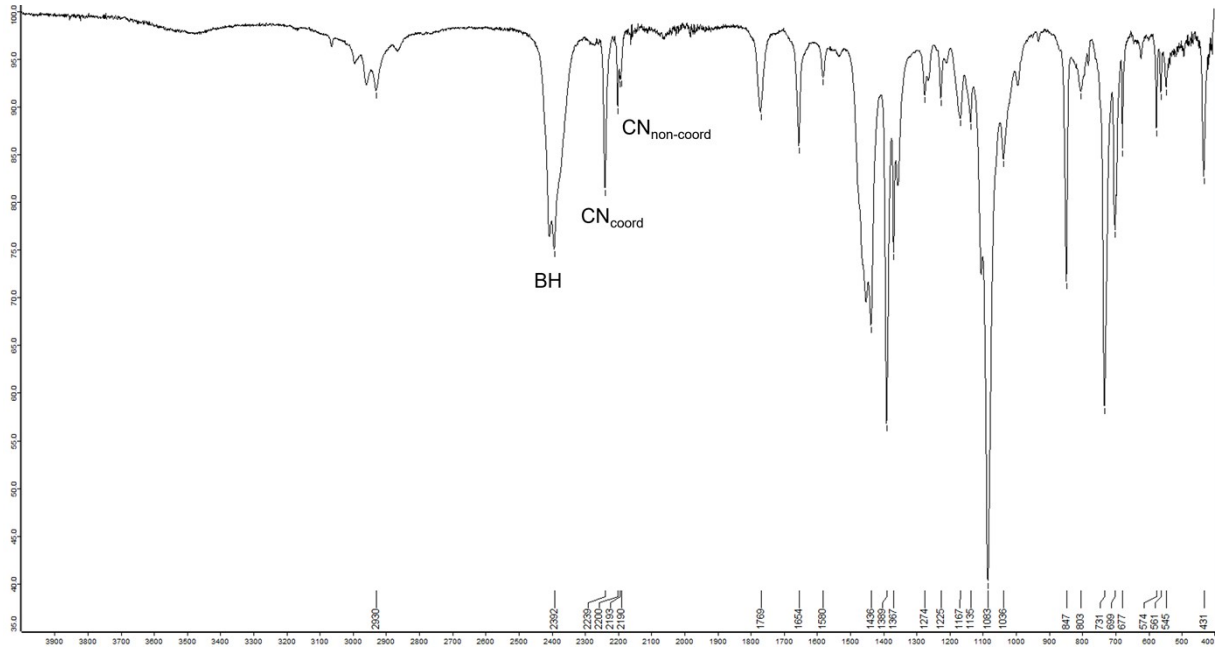

Figure S91. FT-IR spectrum (ATR) of *cis*-[Ni(Me_2Im^{Me})$_2$(NC-$BH_2CN)_2$] (*cis*-**13b**).

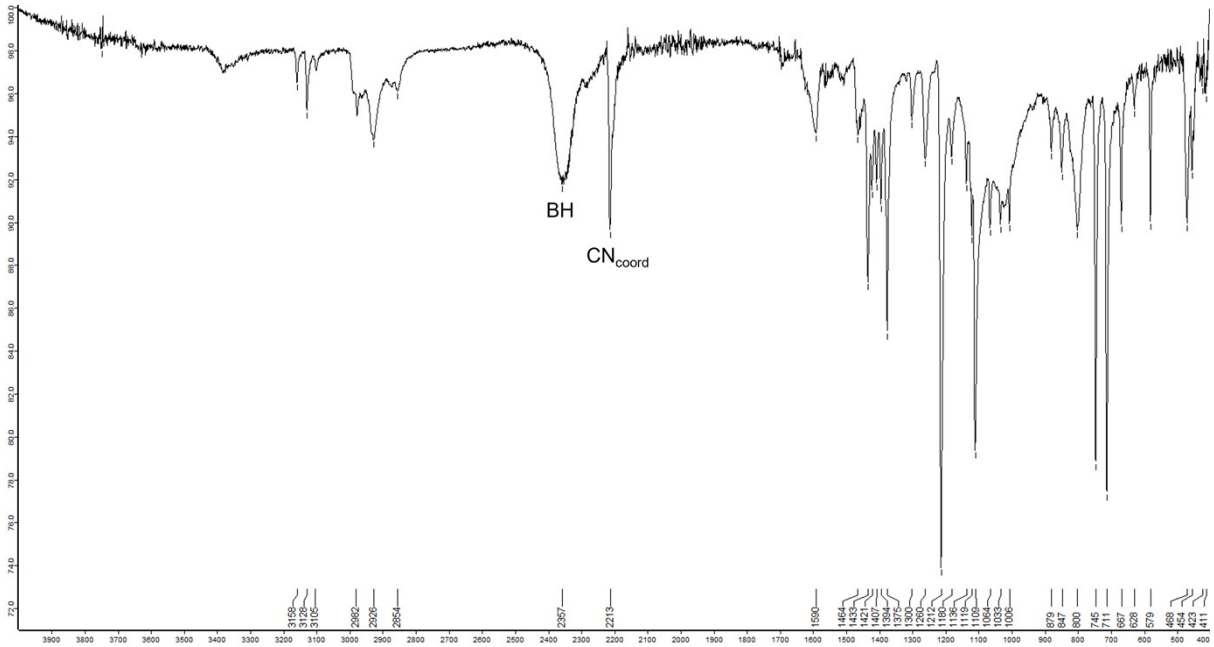

Figure S92. FT-IR spectrum (ATR) of *trans*-[Ni(*i*Pr$_2$Im)$_2$(NC-BH$_3$)$_2$] (*trans*-**14a**).

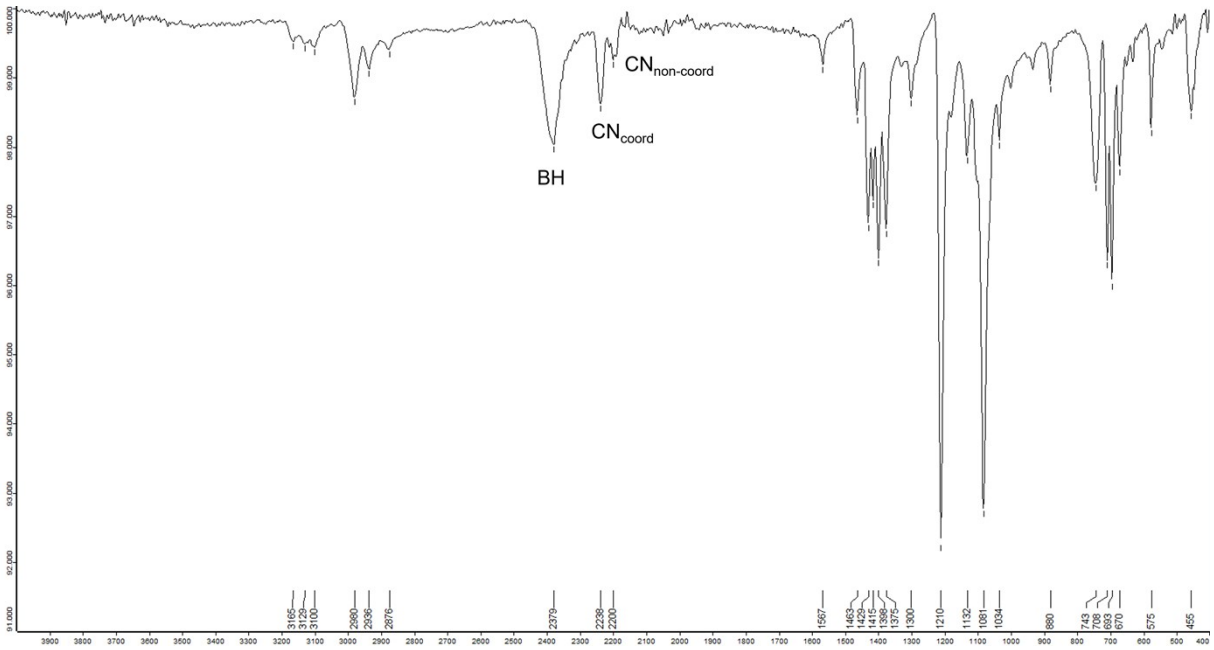

Figure S93. FT-IR spectrum (ATR) of *cis*-/*trans*-[Ni(*i*Pr$_2$Im)$_2$(NC-BH$_2$CN)$_2$] (*cis*-/*trans*-**14b**).

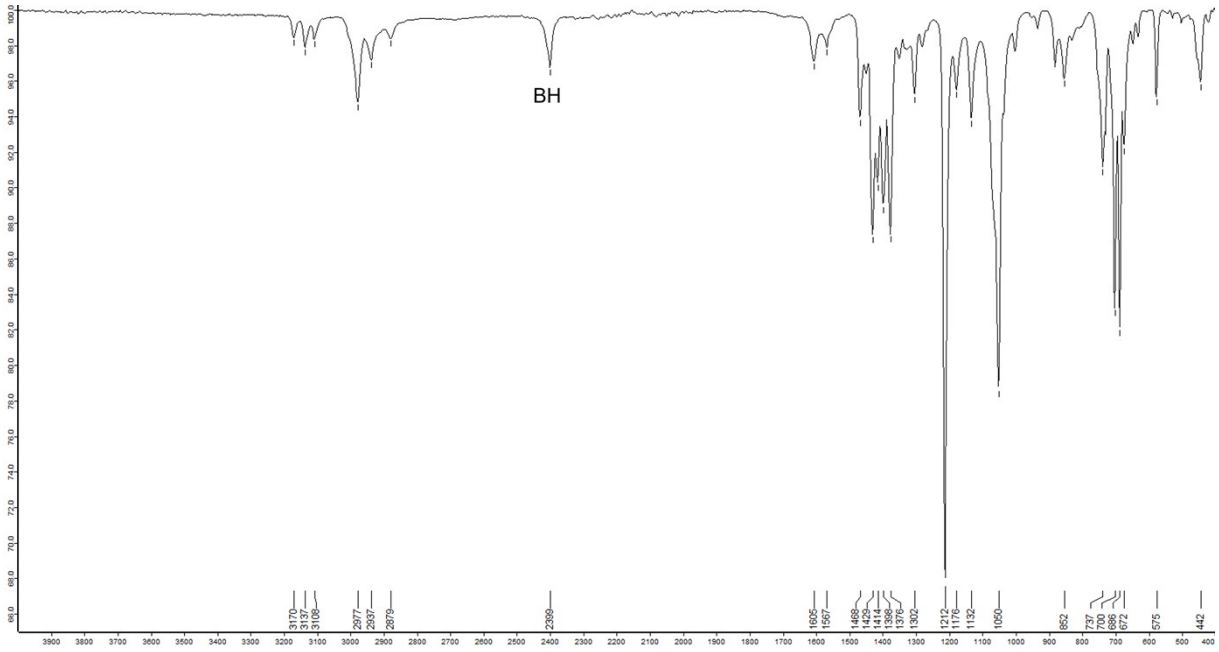

Figure S94. FT-IR spectrum (ATR) of crude *cis*-[Ni(*i*Pr$_2$Im)$_2${NC-BH(CN)$_2$}$_2$] (*cis*-**14c**). CN-bands were not detected.

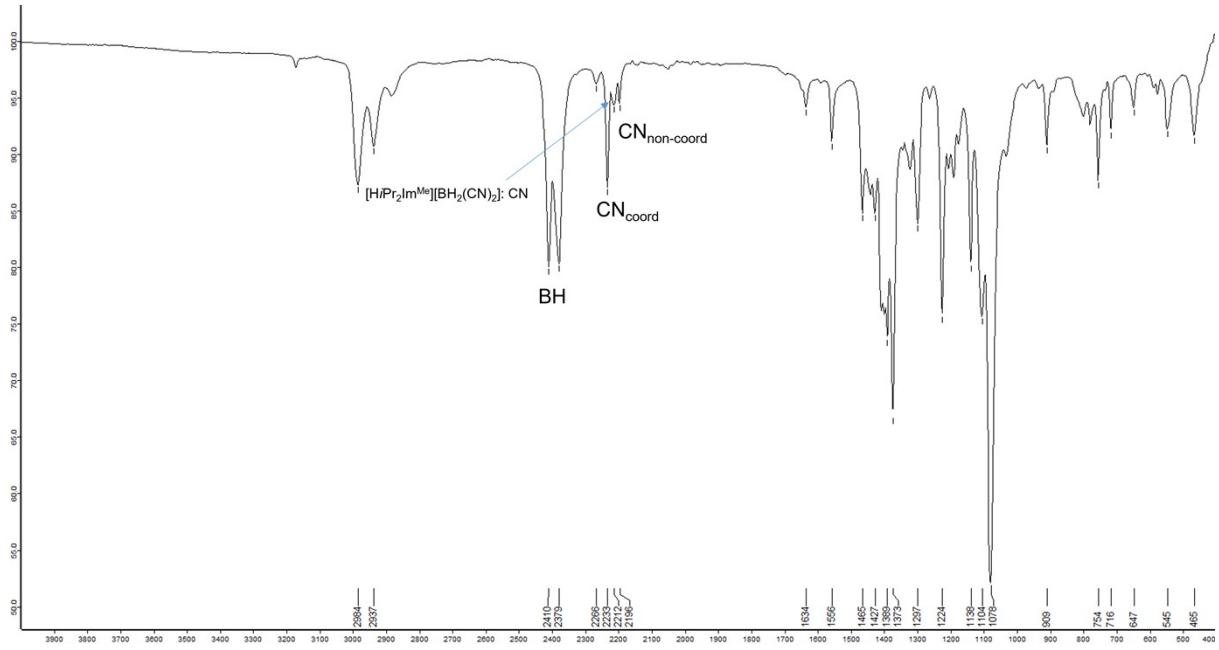

Figure S95. FT-IR spectrum (ATR) of a mixture of [H*i*Pr$_2$Im^{Me}][BH$_2$(CN)$_2$] and *trans*-[Ni(*i*Pr$_2$Im^{Me})$_2${NC-BH(CN)$_2$}$_2$] (*trans*-**15b**).

5 Crystallographic Section

5.1 General Information

Crystal data were either collected on a Rigaku XtaLAB Synergy-DW diffractometer with an Hy-Pix-6000HE detector and monochromated CuK_α or MoK_α radiation equipped with an Oxford Cryo 800 cooling unit or on a XtaLAB Synergy Dualflex HyPix diffractometer with a Hybrid Pixel array detector and multi-layer mirror monochromated CuK_α radiation or either on a Bruker X8-Apex II with a CCD Apex II detector and MoK_α radiation from a graphite source. The crystals were immersed in a film of perfluoropolyether oil on a glass fiber MicroMount™ (MiTeGen) and data were collected at 100 K. The images were processed with the Bruker or Crysalis software packages and equivalent reflections were merged. Corrections for Lorentz-polarization effects and absorption were performed if necessary and the structures were solved by direct methods. Subsequent difference Fourier syntheses revealed the positions of all other non-hydrogen atoms. The structures were solved by using the ShelXTL software package.[16] All non-hydrogen atoms were refined anisotropically. Hydrogen atoms were assigned to idealized positions and were included in structure factor calculations. Figures are created using Diamond Crystal and Molecular Structure Visualisation software.[17]

Crystallographic data (excluding structure factors) for the structures in this paper have been deposited with the Cambridge Crystallographic Data Centre, CCDC, 12 Union Road, Cambridge CB21EZ, UK. Copies of the data can be obtained free of charge on quoting the depository numbers 2328052 (**trans_14a**), 2328053 (**trans_12b**), 2328054 (**cis_11c**), 2328055 (**2c**), 2328056 (**1d**), 2328057 (**trans_15b**), 2328058 (**trans_5c**), 2328059 (**2d**), 2328060 (**16c**), 2328061 (**trans_4b**), 2328062 (**trans_5b_Ag**), 2328063 (**cis_10c**), 2328064 (**cis_14b**), 2328065 (**8d**), 2328066 (**cis_13b**), 2328067 (**7d**), 2328068 (**9b**), 2328069 (**3b**), 2328070 (**trans_6c**) (Fax: +44-1223-336-033; E-Mail: deposit@ccdc.cam.ac.uk, http://www.ccdc.cam.ac.uk).

5.2 Crystal Data

Crystal data for [Ni(Me$_2$Im^{Me})$_4$][B(CN)$_4$]$_2$·3THF (1d): $C_{156}H_{216}B_8N_{64}Ni_4O_3$, M_r = 3357.24 g/mol, T = 100.00(10) K, λ = 1.54184 Å, yellow block, 0.280 × 0.110 × 0.060 mm^3, tetragonal, space group *I*422, a = 18.15920(10) Å, b = 18.15920(10) Å, c = 28.63700(10) Å, α = 90 °, β = 90 °, γ = 90 °, V = 9443.24(11) Å^3, Z = 2, ρ_{calcd} = 1.181 Mg/m^3, μ = 0.964 mm^{-1}, F(000) = 3552, 64912 reflections, –23 ≤ h ≤ 21, –23 ≤ k ≤ 23, –36 ≤ l ≤ 36, 2.8780 ° < θ < 79.3920 °, completeness 99.9%, 5174 independent reflections, 5083 reflections observed with [I > 2σ(I)], 285 parameters, 369 restraints, R indices (all data) R_1 = 0.0702, wR_2 = 0.2008, final R indices [I > 2σ(I)] R_1 = 0.0695, wR_2 = 0.1999, largest difference peak and hole 1.557 and –0.755 e Å^{-3}, Goof = 1.071.

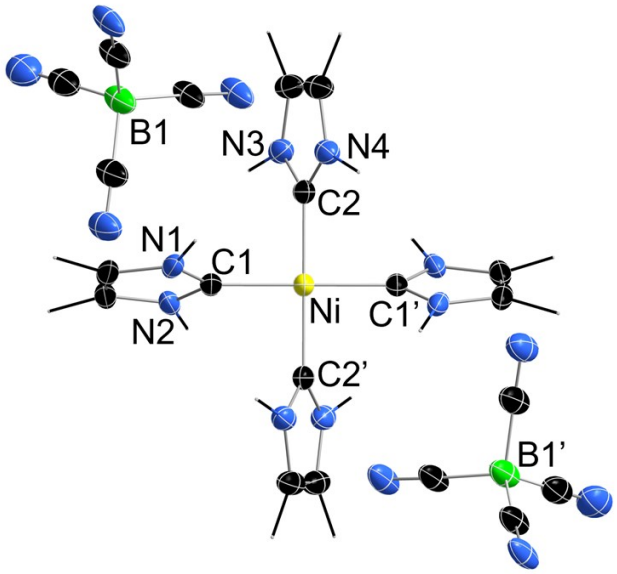

Figure S96. Molecular structure of [Ni(Me$_2$Im^{Me})$_4$][B(CN)$_4$]$_2$ (**1d**) in the solid-state (ellipsoids set at 50% probability level). The hydrogen atoms are omitted for clarity. Selected bond lengths [Å] and angles [°]: Ni–C1 1.930(2), Ni–C2 1.929(2), plane (N1C1N2) – plane (N1'C1'N2') 49.2(9), plane (N3C2N4) – plane (N3'C2'N4') 42.4(9).

Crystal data for [Ni(*i*Pr$_2$Im)$_4$][BH(CN)$_3$]$_2$·0.5(C$_6$H$_{14}$)·MeCN (2c): $C_{47}H_{76}B_2N_{15}Ni$, M_r = 931.55 g/mol, T = 100.00(10) K, λ = 1.54184 Å, colorless block, 0.120 × 0.160 × 0.220 mm^3, monoclinic, space group $P2_1/c$, a = 18.5687(6) Å, b = 12.8671(4) Å, c = 21.6604(7) Å, α = 90 °, β = 100.151(3) °, γ = 90 °, V = 5094.2(3) Å^3, Z = 4, ρ_{calcd} = 1.215 Mg/m^3, μ = 0.429 mm^{-1}, F(000) = 2004, 60393 reflections, –23 ≤ h ≤ 26, –16 ≤ k ≤ 17, –29 ≤ l ≤ 31, 1.849 ° < θ < 31.040 °, completeness 100%, 13459 independent reflections, 9890 reflections observed with [I > 2σ(I)], 666 parameters, 381 restraints, R indices (all data) R_1 = 0.1096, wR_2 = 0.2348, final R indices [I > 2σ(I)] R_1 = 0.0824, wR_2 = 0.2194, largest difference peak and hole 1.770 and –1.421 e Å^{-3}, Goof = 1.058.

Figure S97. Molecular structure of [Ni(*i*Pr$_2$Im)$_4$][BH(CN)$_3$]$_2$ (**2c**) in the solid-state (ellipsoids set at 50% probability level). The hydrogen atoms except for those bound to boron are omitted for clarity. Selected bond lengths [Å] and angles [°]: Ni–C1 1.945(4), Ni–C2 1.958(2), Ni–C3 1.936(4), Ni–C4 1.957(2), plane (N1C1N2) – plane (N5C3N6) 58.7(2), plane (N3C2N4) – plane(N7C4N8) 62.8(3).

Crystal data for [Ni(*i*Pr$_2$Im)$_4$][B(CN)$_4$)]$_2$ · 2 (C$_6$H$_6$) (2d): $C_{56}H_{76}B_2N_{16}Ni$, M_r = 1053.65 g/mol, T = 100.00(10) K, λ = 1.54184 Å, yellow block, 0.240 × 0.140 × 0.120 mm^3, orthorhombic, space group *P*bcn, a = 18.2256(2) Å, b = 15.88110(10) Å, c = 20.8977(2) Å, α = 90 °, β = 90 °, γ = 90 °, V = 6048.68(10) Å^3, Z = 4, ρ_{calcd} = 1.157 Mg/m^3, μ = 0.840 mm^{-1}, F(000) = 2248, 47155 reflections, –22 ≤ h ≤ 22, –19 ≤ k ≤ 19, –25 ≤ l ≤ 26, 3.692 ° < θ < 74.481 °, completeness 99.9%, 6179 independent reflections, 5665 reflections observed with [I > 2σ(I)], 402 parameters, 290 restraints, R indices (all data) R_1 = 0.0747, wR_2 = 0.1291, final R indices [I > 2σ(I)] R_1 = 0.0707, wR_2 = 0.1886, largest difference peak and hole 1.061 and –0.365 e Å^{-3}, Goof = 1.047.

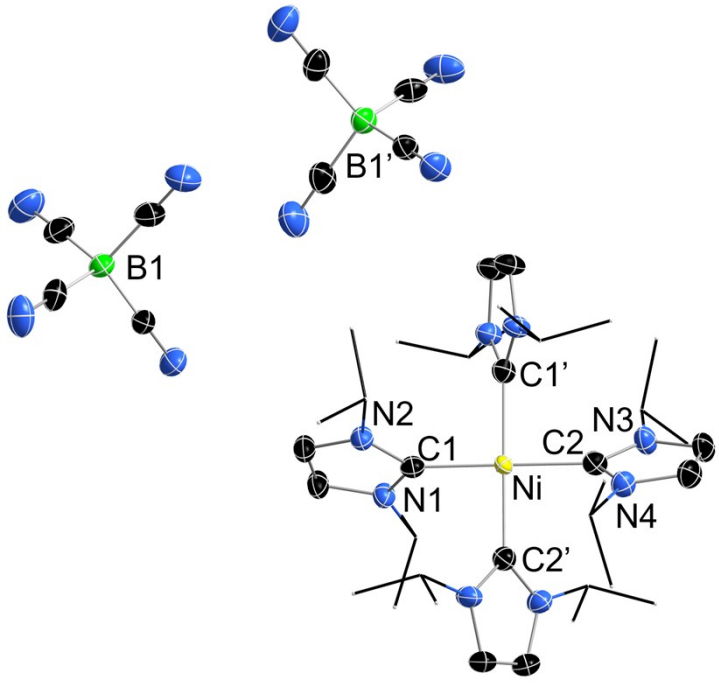

Figure S98. Molecular structure of [Ni(*i*Pr$_2$Im)$_4$][B(CN)$_4$]$_2$ (**2d**) in the solid-state (ellipsoids set at 50% probability level). The hydrogen atoms are omitted for clarity. Selected bond lengths [Å] and angles [°]: Ni–C1 1.948(3), Ni–C2 1.946(3), Ni–C3 1.946(3), Ni–C4 1.948(3), plane (N1C1N2) – plane (N3'C2'N4') 61.9(1).

Crystal data for [Ni(*i*Pr$_2$Im^{Me})$_3$(NC-BH$_2$CN)][BH$_2$(CN)$_2$] (3b): $C_{43}H_{70}B_2N_{10}Ni$, M_r = 806.95 g/mol, T = 100.00(10) K, λ = 1.54184 Å, yellow block, 0.420 × 0.160 × 0.150 mm^3, triclinic, space group $P\bar{1}$, a = 9.5546(10) Å, b = 12.4025(2) Å, c = 20.5915(2) Å, α = 105.8210(10) °, β = 95.0690(10) °, γ = 98.6360(10) °, V = 2299.52(5) Å^3, Z = 2, ρ_{calcd} = 1.166 Mg/m^3, μ = 0.912 mm^{-1}, F(000) = 872, 51385 reflections, –12 ≤ h ≤ 10, –15≤ k ≤ 15, –25 ≤ l ≤ 26, 2.251 ° < θ < 77.663 °, completeness 99.9%, 9706 independent reflections, 8692 reflections observed with [I > 2σ(I)], 574 parameters, 234 restraints, R indices (all data) R_1 = 0.0505, wR_2 = 0.1239, final R indices [I > 2σ(I)] R_1 = 0.0460, wR_2 = 0.1202, largest difference peak and hole 0.494 and –0.437 e Å^{-3}, Goof = 1.085.

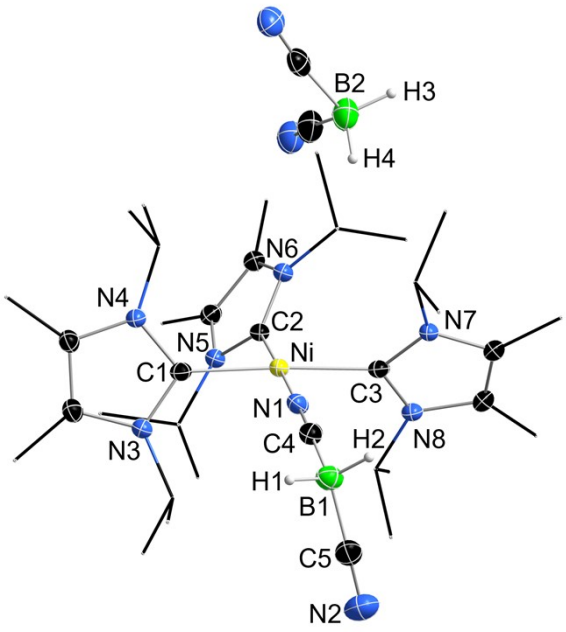

Figure S99. Molecular structure of [Ni(*i*Pr$_2$Im^{Me})$_3$(NC-BH$_2$CN)][BH$_2$(CN)$_2$] (**3b**) in the solid-state (ellipsoids set at 50% probability level). The hydrogen atoms not bound at boron are omitted for clarity. Selected bond lengths [Å] and angles [°]: Ni–C1 1.952(2), Ni–C2 1.948(2), Ni–C3 1.954(2), Ni–N1 1.897(2), N1–C4 1.141(2), C4–B1 1.601(3), B1–C5 1.586(2), C5–N2 1.150(2), <NiN1C4 171.0(1), <N1C4B1 177.6(2), plane (N3C1N4) – plane (N7C3N8) 49.5(1).

Crystal data for *trans*-[Ni(Dipp$_2$Im)$_2$(NC-BH$_2$CN)$_2$] · (C$_6$H$_6$) (*trans*-4b): $C_{64}H_{82}B_2N_8Ni$, M_r = 1043.70 g/mol, T = 100.00(10) K, λ = 1.54184 Å, yellow block, 0.250 × 0.210 × 0.140 mm^3, monoclinic, space group $P2_1/n$, a = 12.05340(10) Å, b = 16.85110(10) Å, c = 15.24350(10) Å, α = 90 °, β = 95.4100(10) °, γ = 90 °, V = 3082.36(4) Å^3, Z = 2, ρ_{calcd} = 1.125 Mg/m^3, μ = 0.781 mm^{-1}, F(000) = 1120, 62601 reflections, –15 ≤ h ≤ 15, –20 ≤ k ≤ 21, –18 ≤ l ≤ 19, 3.920 ° < θ < 77.654 °, completeness 100%, 6511 independent reflections, 5988 reflections observed with [I > 2σ(I)], 356 parameters, 0 restraints, R indices (all data) R_1 = 0.0370, wR_2 = 0.0927, final R indices [I > 2σ(I)] R_1 = 0.0344, wR_2 = 0.0909, largest difference peak and hole 0.516 and –0.378 e Å^{-3}, Goof = 1.063.

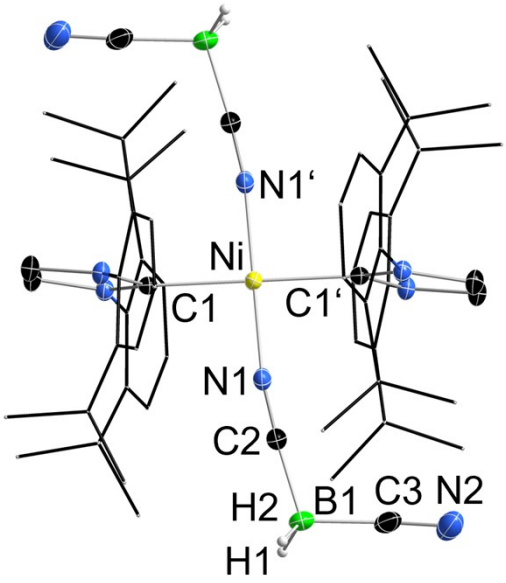

Figure S100. Molecular structure of *trans*-[Ni(Dipp$_2$Im)$_2$(NC-BH$_2$CN)$_2$] (*trans*-**4b**) in the solid-state (ellipsoids set at 50% probability level). The hydrogen atoms except for those bound at boron are omitted for clarity. Selected bond lengths [Å] and angles [°]: Ni–C1 1.957(1), Ni–N1 1.848(9), N1–C2 1.148(1), C2–B1 1.597(2), B1–C3 1.590(2), C3–N2 1.149(2), <NiN1C2 171.6(1), <N1C2B1 176.4(1).

Crystal data for $^{1}_{\infty}${[Ni(Mes$_2$Im)$_2${κ^2*N*(NC-BH$_2$CN)}$_2$]·2Ag(μ^2-[BH$_2$(CN)$_2$])}·THF (*trans*-5b·Ag): $C_{58}H_{72}Ag_2B_4N_{12}NiO_2$, M_r = 1286.95 g/mol, T = 100.00(10) K, λ = 1.54184 Å, yellow block, 0.210 × 0.150 × 0.100 mm^3, monoclinic, space group *C*2/c, a = 29.8698(3) Å, b = 13.0489(2) Å, c = 15.7689(2) Å, α = 90 °, β = 94.1530(10) °, γ = 90 °, V = 6130.07(14) Å^3, Z = 4, ρ_{calcd} = 1.394 Mg/m^3, μ = 5.825 mm^{-1}, F(000) = 4097, 24200 reflections, –35 ≤ h ≤ 37, –16 ≤ k ≤ 13, –19 ≤ l ≤ 19, 2.967° < θ < 73.782 °, completeness 99.2%, 6082 independent reflections, 5240 reflections observed with [I > 2σ(I)], 416 parameters, 162 restraints, R indices (all data) R_1 = 0.0449, wR_2 = 0.1421, final R indices [I > 2σ(I)] R_1 = 0.0390, wR_2 = 0.1364, largest difference peak and hole 0.527 and –1.047 e Å^{-3}, Goof = 1.126.

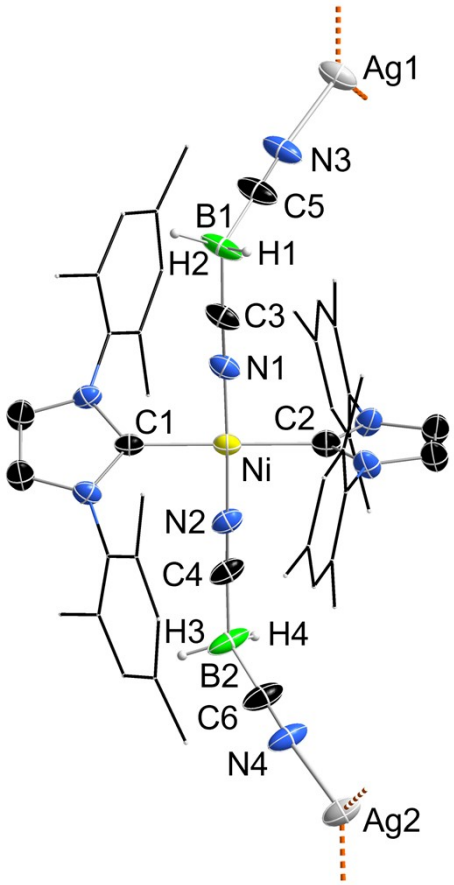

Figure S101. Molecular structure of $^{1}_{\infty}${*trans*-[Ni(Mes$_2$Im)$_2$(μ^2-[NC-BH$_2$-CN])$_2$]·2Ag(μ^2-[BH$_2$(CN)$_2$])} (*trans*-**5b**·Ag) in the solid-state (ellipsoids set at 50% probability level). The hydrogen atoms except for those bound at boron are omitted for clarity. Selected bond lengths [Å] and angles [°]: Ni–C1 1.938(4), Ni–C2 1.964(4), Ni–N1 1.846(3), N1–C3 1.151(4), C3–B1 1.600(5), B1–C4 1.587(5), C4–N2 1.137(4), Ag1–N2 2.181(3), Ag1–N3 2.206(3), N3–C5 1.141(4), C5–B2 1.587(5), B2–C6 1.583(5), C6–N4 1.133(4), Ag1–N4 2.256(3), <NiN1C3 175.8(3), <N1C3B1 178.7(5), <Ag1N2C4 175.8(4), <N2C4B1 178.1(4), <Ag1N3C5 161.4(3), <N3C5B2 178.8(4), <Ag1N4C6 167.0(2), <N4C6B2 176.7(3), plane (N5C1N6) – plane (N7C2N8) 39.6(2).

Crystal data for *trans*-[Ni(Mes$_2$Im)$_2${NC-BH(CN)$_2$}$_2$]·0.5MeCN (*trans*-5c): $C_{98}H_{103}B_4N_{21}Ni_2$, M_r = 1735.67 g/mol, T = 100.00(10) K, λ = 1.54184 Å, colorless plate, 0.150 × 0.100 × 0.090 mm^3, monoclinic, space group *C*2 , a = 34.8025(3) Å, b = 11.91890(10) Å, c = 23.7047(2) Å, α = 90 °, β = 104.6480(10) °, γ = 90 °, V = 9513.29(15) Å^3, Z = 4, ρ_{calcd} = 1.212 Mg/m^3, μ = 0.933 mm^{-1}, F(000) = 3656, 33948 reflections, –44 ≤ h ≤ 41, –15 ≤ k ≤ 10, –30 ≤ l ≤ 30, 2.625 ° < θ < 80.327 °, completeness 99.6%, 15582 independent reflections, 13900 reflections observed with [I > 2σ(I)], 1178 parameters, 791 restraints, R indices (all data) R_1 = 0.0524, wR_2 = 0.1439, final R indices [I > 2σ(I)] R_1 = 0.0488, wR_2 = 0.1395, largest difference peak and hole 0.611 and –0.426 e Å^{-3}, Goof = 1.081.

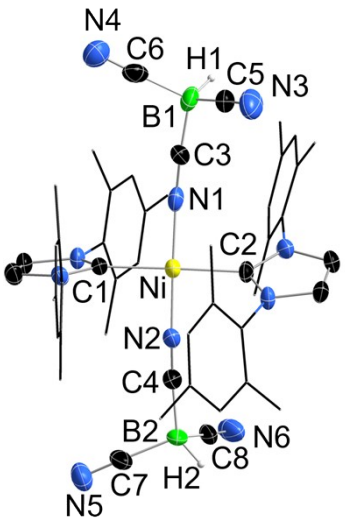

Figure S102. Molecular structure of *trans*-[Ni(Mes$_2$Im)$_2${NC-BH(CN)$_2$}$_2$] (*trans*-**5c**) in the solid-state (ellipsoids set at 50% probability level). The hydrogen atoms except for those bound at boron are omitted for clarity. Selected bond lengths [Å] and angles [°]: Ni–C1 1.949(4), Ni–C2 1.951(3), Ni–N1 1.848(5), N1–C3 1.117(7), C3–B1 1.614(8), B1–C5 1.600(7), C5–N3 1.130(7), B1–C6 1.566(9), C6–N4 1.139(7), Ni–N2 1.827(5), N2–C4 1.187(7), C4–B2 1.540(8), B2–C7 1.589(7), C7–N5 1.129(7), B2–C8 1.610(7), C8–N6 1.157(7), <NiN1C3 172.3(4), <N1C3B1 175.4(5), <NiN2C4 175.0(4), <N2C4B2 174.9(5), plane (N7C1N8) – plane (N9C2N10) 24.8(3).

Crystal data for *trans*-[Ni(Mes$_2$Im)$_2${NC-BH(CN)$_2$}Cl]·1.5MeCN (*trans*-6c): $C_{96}H_{107}B_2Cl_2N_{17}Ni_2$, M_r = 1708.92 g/mol, T = 100.00(10) K, λ = 1.54184 Å, yellow block, 0.170 × 0.130 × 0.110 mm^3, triclinic, space group $P\bar{1}$, a = 10.6146(2) Å, b = 13.8399(3) Å, c = 17.0596(4) Å, α = 88.042(2) °, β = 89.663(2) °, γ = 68.476(2) °, V = 2329.95(9) Å^3, Z = 1, ρ_{calcd} = 1.218 Mg/m^3, μ = 1.447 mm^{-1}, F(000) = 902, 29320 reflections, –13 ≤ h ≤ 13, –14 ≤ k ≤ 17, –21 ≤ l ≤ 21, 2.592 ° < θ < 80.150 °, completeness 99.7%, 9905 independent reflections, 8916 reflections observed with [I > 2σ(I)], 598 parameters, 93 restraints, R indices (all data) R_1 = 0.0458, wR_2 = 0.1162, final R indices [I > 2σ(I)] R_1 = 0.0419, wR_2 = 0.1132, largest difference peak and hole 0.568 and –0.621 e Å^{-3}, Goof = 1.072.

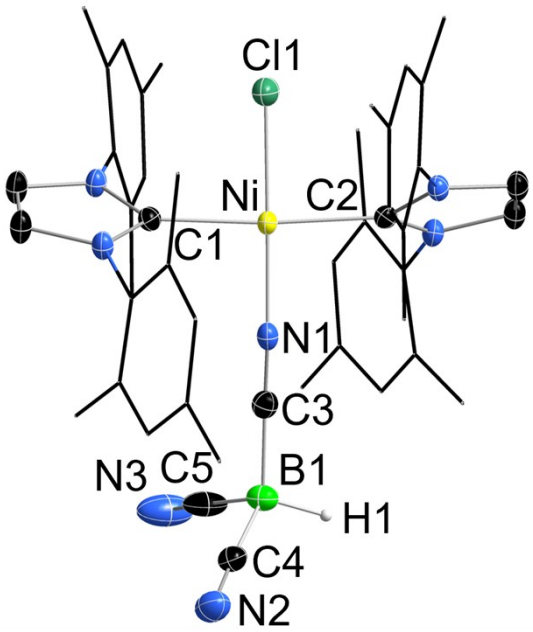

Figure S103. Molecular structure of *trans*-[Ni(Mes$_2$Im)$_2${NC-BH(CN)$_2$}Cl] (*trans*-**6c**) in the solid-state (ellipsoids set at 50% probability level). The hydrogen atoms except for those bound to boron are omitted for clarity. Selected bond lengths [Å] and angles [°]: Ni–Cl1 2.150(5), Ni–C1 1.929(2), Ni–C2 1.933(2), Ni–N1 1.863(1), N1–C3 1.143(2), C3–B1 1.598(2), B1–C4 1.590(3), C4–N2 1.145(2), B1–C5 1.585(3), C5–N3 1.141(3), <NiN1C3 173.6(1), <N1C3B1 174.1(2).

Crystal data for [Ni(*i*Pr$_2$Im)$_3$(OH)][B(CN)$_4$] (7d): $C_{31}H_{49}BN_{10}NiO$, M_r = 647.32 g/mol, T = 100.00(10) K, λ = 1.54184 Å, yellow block, 0.130 × 0.220 × 0.320 mm^3, monoclinic, space group $P2_1$, a = 9.3855 Å, b = 24.4893 Å, c = 16.2200 Å, α = 90 °, β = 101.316 °, γ = 90 °, V = 3655.60(8) Å^3, Z = 4, ρ_{calcd} = 1.176 Mg/m^3, μ = 1.056 mm^{-1}, F(000) = 1384, 50202 reflections, –11 ≤ h ≤ 11, –30 ≤ k ≤ 29, –20 ≤ l ≤ 20, 2.778 ° < θ < 77.684 °, completeness 100%, 13078 independent reflections, 11959 reflections observed with [I > 2σ(I)], 819 parameters, 1 restraint, R indices (all data) R_1 = 0.0508, wR_2 = 0.1198, final R indices [I > 2σ(I)] R_1 = 0.0456, wR_2 = 0.1164, largest difference peak and hole 0.434 and –0.425 e Å^{-3}, Goof = 1.029.

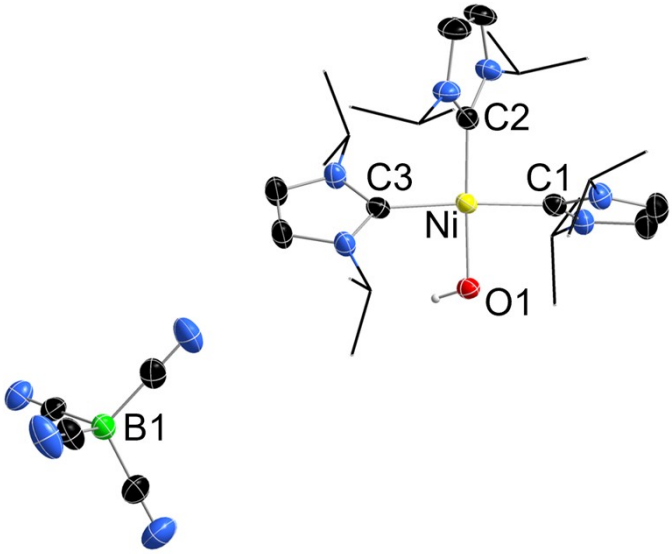

Figure S104. Molecular structure of [Ni(*i*Pr$_2$Im)$_3$(OH)][B(CN)$_4$] (**7d**) in the solid-state (ellipsoids set at 50% probability level). The hydrogen atoms not bound at oxygen are omitted for clarity. Selected bond lengths [Å] and angles [°]: Ni–O1 1.891(3), Ni–C1 1.938(3), Ni–C2 1.904(4), Ni–C3 1.933(3), plane (N1C1N2) – plane (N5C3N6) 61.1(2).

Crystal data for [{Ni(*i*Pr$_2$Im)$_2$(μ^2-OH)}$_2$][B(CN)$_4$]$_2$ (8d): $C_{44}H_{66}B_2N_{16}Ni_2O_2$, M_r = 990.16 g/mol, T = 100.00(10) K, λ = 1.54184 Å, yellow block, 0.350 × 0.280 × 0.210 mm^3, monoclinic, space group $P2_1/c$, a = 23.60270(10) Å, b = 13.97570(10) Å, c = 17.11730(10) Å, α = 90 °, β = 99.3610(10) °, γ = 90 °, V = 5571.19(6) Å^3, Z = 4, ρ_{calcd} = 1.181 Mg/m^3, μ = 1.219 mm^{-1}, F(000) = 2096, 57956 reflections, –29 ≤ h ≤ 30, –16 ≤ k ≤ 17, –21 ≤ l ≤ 21, 3.688 ° < θ < 80.337 °, completeness 99.7%, 11812 independent reflections, 10693 reflections observed with [I > 2σ(I)], 617 parameters, 0 restraints, R indices (all data) R_1 = 0.0396, wR_2 = 0.0990, final R indices [I > 2σ(I)] R_1 = 0.0362, wR_2 = 0.0965, largest difference peak and hole 0.458 and –0.274 e Å^{-3}, Goof = 1.036.

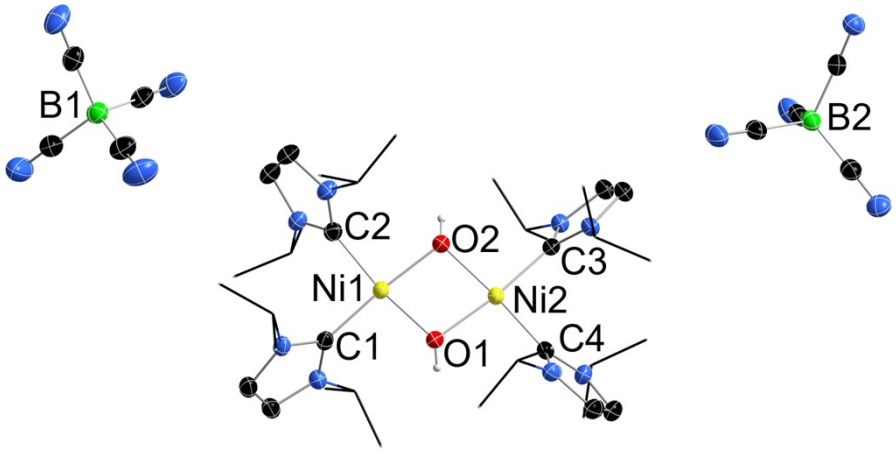

Figure S105. Molecular structure of [{Ni(*i*Pr$_2$Im)$_2$(μ^2-OH)}$_2$][B(CN)$_4$]$_2$ (**8d**) in the solid-state (ellipsoids set at 50% probability level). The hydrogen atoms except for those bound to oxygen are omitted for clarity. Selected bond lengths [Å] and angles [°]: Ni1–O1 1.888(1), Ni1–O2 1.884(1), Ni2–O1 1.887(1), Ni2–O2 1.880(1), Ni1–C1 1.879(1), Ni1–C2 1.886(1), Ni2–C3 1.883(1), Ni2–C4 1.880(1).

Crystal data for [{Ni(Dipp$_2$Im)(NC-BH$_2$CN)(μ^2-OH)}$_2$]·2THF (9b): $C_{66}H_{98}B_2N_8Ni_2O_6$, M_r = 1238.56 g/mol, T = 100.00(10) K, λ = 1.54184 Å, yellow block, 0.250 × 0.150 × 0.110 mm^3, monoclinic, space group $P2_1/c$, a = 11.59850(10) Å, b = 14.49150(10) Å, c = 20.77000(10) Å, α = 90 °, β = 91.5110(10) °, γ = 90 °, V = 3489.80(4) Å^3, Z = 2, ρ_{calcd} = 1.179 Mg/m^3, μ = 1.078 mm^{-1}, F(000) = 1328, 88385 reflections, –14 ≤ h ≤ 11, –18 ≤ k ≤ 18, –26 ≤ l ≤ 26, 3.720 ° < θ < 77.644 °, completeness 100%, 7414 independent reflections, 6865 reflections observed with [I > 2σ(I)], 448 parameters, 141 restraints, R indices (all data) R_1 = 0.0370, wR_2 = 0.0950, final R indices [I > 2σ(I)] R_1 = 0.0347, wR_2 = 0.0934, largest difference peak and hole 0.321 and –0.360 e Å^{-3}, Goof = 1.059.

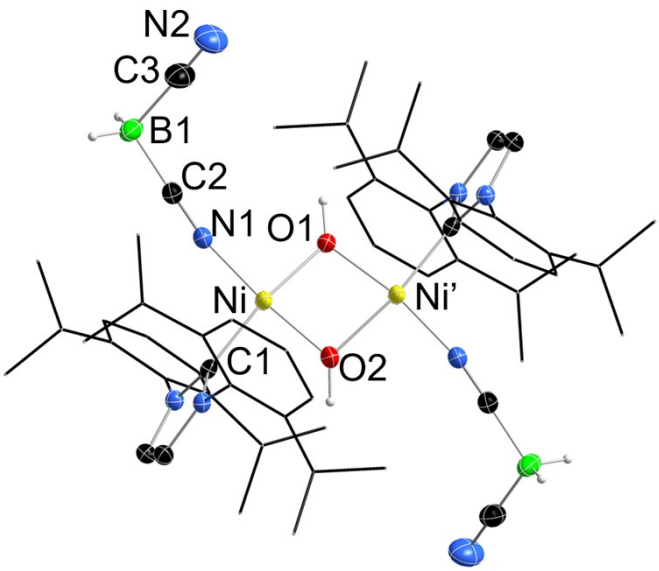

Figure S106. Molecular structure of [{Ni(Dipp$_2$Im)(NC-BH$_2$CN)(μ^2-OH)}$_2$] (**9b**) in the solid-state (ellipsoids set at 50% probability level). The hydrogen atoms except for those bound to boron and oxygen are omitted for clarity. Selected bond lengths [Å] and angles [°]: Ni1–O1 1.880(3), Ni1–O2 1.863(4), Ni–C1 1.868(1), Ni–N1 1.849(1), N1–C3 1.147(2), C3–B1 1.590(2), B1–C4 1.70(3), C4–N2 1.09(2), <NiN1C3 170.1(1), <N1C3B1 178.8(1).

Crystal data for *cis*-[Ni(Me$_2$Im^{Me})$_2${NC-BH(CN)$_2$}Br] (*cis*-10c): $C_{29}H_{37}BBrN_7Ni$, M_r = 633.06 g/mol, T = 100.00(10) K, λ = 1.54184 Å, yellow block, 0.180 × 0.080× 0.050 mm^3, monoclinic, space group $P2_1/c$, a = 16.8608(3) Å, b = 9.8305(2) Å, c = 19.1245(4) Å, α = 90 °, β = 101.488(2) °, γ = 90 °, V = 3106.38(11) Å^3, Z = 4, ρ_{calcd} = 1.354 Mg/m^3, μ = 2.632 mm^{-1}, F(000) = 1312, 14078 reflections, –20 ≤ h ≤ 21, –12 ≤ k ≤ 12, –24 ≤ l ≤ 21, 2.674 ° < θ < 77.335 °, completeness 99.6%, 6418 independent reflections, 5473 reflections observed with [I > 2σ(I)], 418 parameters, 252 restraints, R indices (all data) R_1 = 0.0628, wR_2 = 0.1402, final R indices [I > 2σ(I)] R_1 = 0.0536, wR_2 = 0.1346, largest difference peak and hole 1.808 and –1.056 e Å^{-3}, Goof = 1.060.

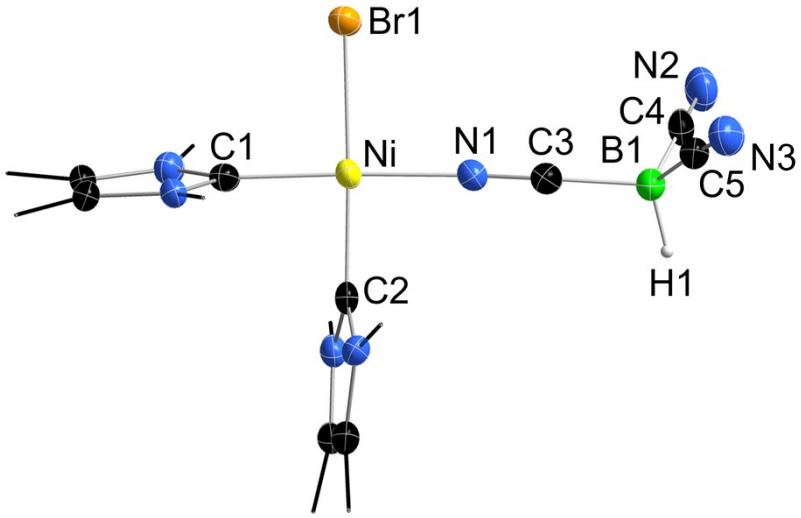

Figure S107. Molecular structure of *cis*-[Ni(Me$_2$Im^{Me})$_2${NC-BH(CN)$_2$}Br] (*cis*-**10c**) in the solid-state (ellipsoids set at 50% probability level). The hydrogen atoms except for those bound to boron are omitted for clarity. Selected bond lengths [Å] and angles [°]: Ni–Br1 2.344(7), Ni–C1 1.896(3), Ni–C2 1.901(3), Ni–N1 1.896(3), N1–C3 1.139(4), C3–B1 1.600(5), B1–C4 1.592(6), C4–N2 1.142(5), B1–C5 1.589(6), C5–N3 1.144(5), <NiN1C3 177.4(3), <N1C3B1 177.0(4).

Crystal data for *cis*-[Ni(*i*Pr$_2$Im)$_2${NC-BH(CN)$_2$}Br] (*cis*-11c): $C_{21}H_{33}BBrN_7Ni$, M_r = 532.94 g/mol, T = 100.00(10) K, λ = 1.54184 Å, yellow block, 0.044 × 0.158 × 0.370 mm^3, monoclinic, space group *C*2/c, a = 25.4701 Å, b = 8.9526 Å, c = 23.2828 Å, α = 90 °, β = 96.051 °, γ = 90 °, V = 5279.4(3) Å^3, Z = 8, ρ_{calcd} = 1.341 Mg/m^3, μ = 2.988 mm^{-1}, F(000) = 2208, 17417 reflections, –30 ≤ h ≤ 30, –10≤ k ≤ 10, –27 ≤ l ≤ 14, 3.490 ° < θ < 67.067 °, completeness 98.9%, 4654 independent reflections, 4246 reflections observed with [I > 2σ(I)], 292 parameters, 0 restraints, R indices (all data) R_1 = 0.0589, *w*R_2 = 0.1527, final R indices [I > 2σ(I)] R_1 = 0.0548, *w*R_2 = 0.1496, largest difference peak and hole 1.087 and –0.556 e Å^{-3}, Goof = 1.089.

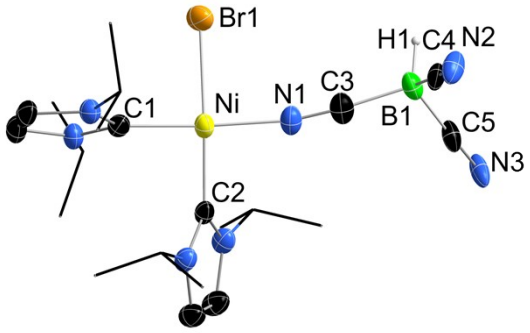

Figure S108. Molecular structure of *cis*-[Ni(*i*Pr$_2$Im)$_2${NC-BH(CN)$_2$}Br] (*cis*-**11c**) in the solid-state (ellipsoids set at 50% probability level). The hydrogen atoms except for those bound to boron are omitted for clarity. Selected bond lengths [Å] and angles [°]: Ni–Br1 2.345(1), Ni–C1 1.878(3), Ni–C2 1.903(4), Ni–N1 1.891(3), N1–C3 1.137(5), C3–B1 1.606(7), B1–C4 1.571(7), C4–N2 1.129(6), B1–C5 1.578(8), C5–N3 1.122(7), <NiN1C3 169.8(4), <N1C3B1 174.8(4).

Crystal data for *trans*-[Ni(Mes$_2$Im)$_2$(NC-BH$_2$CN)Br]·THF (*trans*-12b): $C_{48}H_{58}BBrN_6NiO$, M_r = 884.40 g/mol, T = 100(2) K, λ = 1.54184 Å, yellow block, 0.280 × 0.110 × 0.060 mm^3, orthorhombic, space group *P*2ac, a = 10.7733(2) Å, b = 12.1983(2) Å, c = 34.4222(6) Å, α = 90 °, β = 90 °, γ = 90 °, V = 4523.63(14) Å^3, Z = 4, ρ_{calcd} = 1.299 Mg/m^3, μ = 1.972 mm^{-1}, F(000) = 1856, 23816 reflections, –13 ≤ h ≤ 12, –8 ≤ k ≤ 14, –43 ≤ l ≤ 41, 2.567 ° < θ < 77.144 °, completeness 98.9%, 8673 independent reflections, 8096 reflections observed with [I > 2σ(I)], 542 parameters, 0 restraints, R indices (all data) R_1 = 0.0424, wR_2 = 0.1011, final R indices [I > 2σ(I)] R_1 = 0.0391, wR_2 = 0.0993, largest difference peak and hole 0.691 and –0.560 e Å^{-3}, Goof = 1.041.

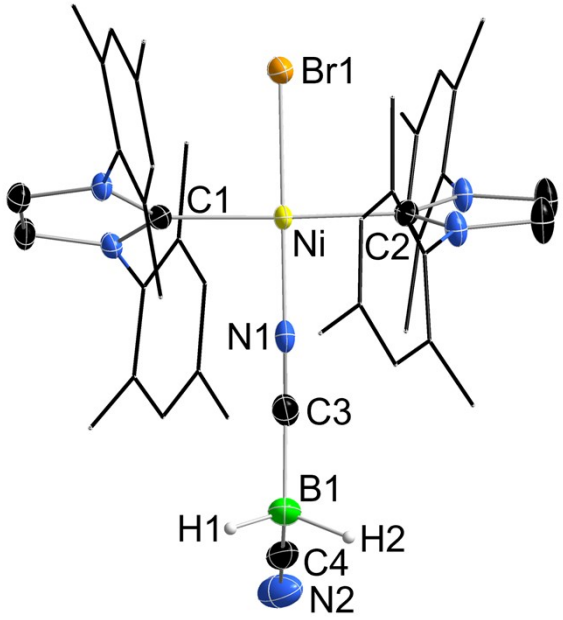

Figure S109. Molecular structure of *trans*-[Ni(Mes$_2$Im)$_2$(NC-BH$_2$CN)Br] (*trans*-**12b**) in the solid-state (ellipsoids set at 50% probability level). The hydrogen atoms except for those bound to boron are omitted for clarity. Selected bond lengths [Å] and angles [°]: Ni–Br1 2.307(7), Ni–C1 1.930(4), Ni–C2 1.931(4), Ni–N1 1.865(3), N1–C3 1.149(5), C3–B1 1.593(6), B1–C4 1.582(8), C4–N2 1.145(7), <NiN1C3 178.2(3), <N1C3B1 177.5(5), plane (N3C1N4) – plane (N5C2N6) 39.7(3).

Crystal data for *cis*-[Ni(Me$_2$Im^{Me})$_2$(NC-BH$_2$CN)$_2$]·(CH$_2$Cl$_2$) (*cis*-13b): $C_{19}H_{30}B_2Cl_2N_8Ni$, M_r = 521.74 g/mol, T = 100.00(10) K, λ = 1.54184 Å, yellow block, 0.280 × 0.250 × 0.200 mm^3, monoclinic, space group *C*2/c, a = 10.4717(2) Å, b = 14.7360(2) Å, c = 17.6069(3) Å, α = 90 °, β = 106.022(2) °, γ = 90 °, V = 2611.40(8) Å^3, Z = 4, ρ_{calcd} = 1.327 Mg/m^3, μ = 3.130 mm^{-1}, F(000) = 1088, 24108 reflections, –13 ≤ h ≤ 12, –18 ≤ k ≤ 17, –21 ≤ l ≤ 22, 5.227 ° < θ < 76.763 °, completeness 99.5%, 2727 independent reflections, 2618 reflections observed with [I > 2σ(I)], 166 parameters, 12 restraints, R indices (all data) R_1 = 0.0493, wR_2 = 0.1497, final R indices [I > 2σ(I)] R_1 = 0.0482, wR_2 = 0.1490, largest difference peak and hole 0.962 and –0.366 e Å^{-3}, Goof = 1.109.

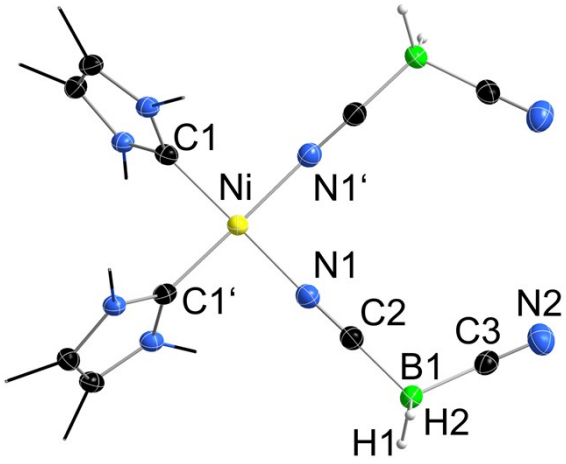

Figure S110. Molecular structure of *cis*-[Ni(Me$_2$Im^{Me})$_2$(NC-BH$_2$CN)$_2$] (*cis*-**13b**) in the solid-state (ellipsoids set at 50% probability level). The hydrogen atoms except for those bound to boron are omitted for clarity. Selected bond lengths [Å] and angles [°]: Ni–C1 1.894(2), Ni–N1 1.888(2), N1–C2 1.146(3), C2–B1 1.588(4), B1–C3 1.584(4), C3–N2 1.138(4), <NiN1C2 177.8(2), <N1C2B1 178.9(3).

Crystal data for *trans*-[Ni(*i*Pr$_2$Im)$_2$(NC-BH$_3$)$_2$] (*trans*-14a): $C_{20}H_{38}B_2N_6Ni$, M_r = 442.88 g/mol, T = 100.00(10) K, λ = 1.54184 Å, yellow block, 0.116 × 0.147 × 0.246 mm^3, monoclinic, space group $P2_1/c$, a= 9.9831 Å, b = 12.2036 Å, c = 10.5823 Å, α = 90 °, β = 97.0070(10) °, γ = 90 °, V = 1279.61(3) Å^3, Z = 2, ρ_{calcd} = 1.149 Mg/m^3, μ = 1.204 mm^{-1}, F(000) = 476, 12539 reflections, –11 ≤ h ≤ 12, –13 ≤ k ≤ 14, –12 ≤ l ≤ 12, 4.462 ° < θ < 70.071 °, completeness 100%, 2430 independent reflections, 2314 reflections observed with [I > 2σ(I)], 149 parameters, 0 restraints, R indices (all data) R_1 = 0.0298, wR_2 = 0.0827, final R indices [I > 2σ(I)] R_1 = 0.0287, wR_2 = 0.0819, largest difference peak and hole 0.215 and –0.243 e Å^{-3}, Goof = 1.094.

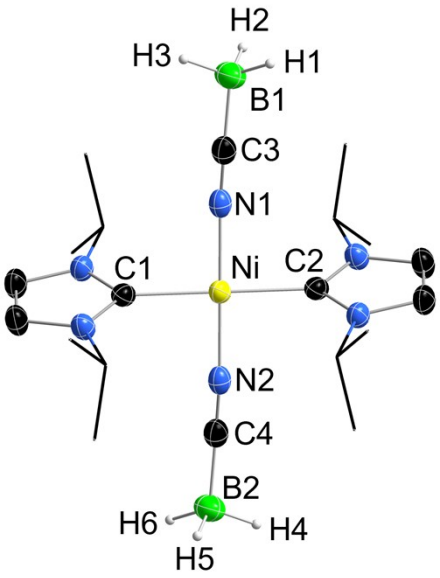

Figure S111. Molecular structure of *trans*-[Ni(*i*Pr$_2$Im)$_2$(NC-BH$_3$)$_2$] (*trans*-**14a**) in the solid-state (ellipsoids set at 50% probability level). The hydrogen atoms not bound at boron are omitted for clarity. Selected bond lengths [Å] and angles [°]: Ni–C1 1.932(1), Ni–C2 1.932(1), Ni–N1 (1.856(1), N1–C3 1.121(2), C3–B1 1.599(2), Ni–N2 1.856(1), N2–C4 1.121(2), C4–B2 1.590(2), <NiN1C3 176.4(1), <N1C3B1 179.1(2), <NiN2C4 176.4(1), <N2C4B2 179.1(2).

Crystal data for *cis*-[Ni(*i*Pr$_2$Im)$_2$(NC-BH$_2$CN)$_2$] (*cis*-14b): $C_{22}H_{36}B_2N_8Ni$, M_r = 492.90 g/mol, T = 100.00(10) K, λ = 1.54184 Å, yellow block, 0.145 × 0.154 × 0.185 mm^3, orthorhombic, space group *I*2/a, a = 12.7837 Å, b = 12.1439 Å, c = 17.1982 Å, α = 90 °, β = 95.899 °, γ = 90 °, V = 2655.78(3) Å^3, Z = 4, ρ_{calcd} = 1.233 Mg/m^3, μ = 1.239 mm^{-1}, F(000) = 1048, 26921 reflections, –15 ≤ h ≤ 15, –15 ≤ k ≤ 15, –21 ≤ l ≤ 17, 4.465 ° < θ < 74.450 °, completeness 100%, 2710 independent reflections, 2682 reflections observed with [I > 2σ(I)], 162 parameters, 0 restraints, R indices (all data) R_1 = 0.0276, wR_2 = 0.0708, final R indices [I > 2σ(I)] R_1 = 0.0275, wR_2 = 0.0708, largest difference peak and hole 0.346 and –0.292 e Å^{-3}, Goof = 1.045.

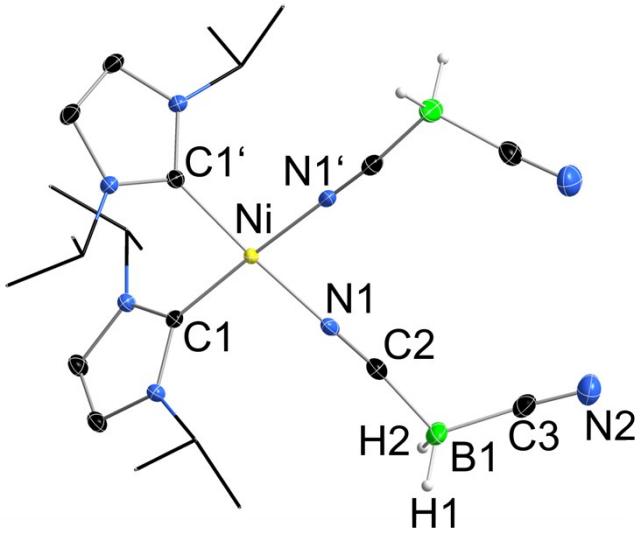

Figure S112. Molecular structure of *cis*-[Ni(*i*Pr$_2$Im)$_2$(NC-BH$_2$CN)$_2$] (*cis*-**14b**) in the solid-state (ellipsoids set at 50% probability level). The hydrogen atoms not bound at boron are omitted for clarity. Selected bond lengths [Å] and angles [°]: Ni–C1 1.898(1), Ni–N1 1.901(1), N1–C2 1.132(2), C2–B1 1.594(2), B1–C3 1.581(2), C3–N2 1.144(2), <NiN1C2 179.4(1), <N1C2B1 174.7(1).

Crystal data for *trans*-[Ni(*i*Pr$_2$Im^{Me})$_2$(NC-BH$_2$CN)$_2$] (*trans*-15b): $C_{26}H_{44}B_2N_8Ni$, M_r = 459.02 g/mol, T = 100.00(10) K, λ = 1.54184 Å, yellow block, 0.380 × 0.320 × 0.290 mm^3, triclinic, space group $P\bar{1}$, a = 8.9341(5) Å, b = 9.5418(6) Å, c = 10.1375(6) Å, α = 69.393(6) °, β = 85.022(5) °, γ = 74.058(5) °, V = 777.74(9) Å^3, Z = 1, ρ_{calcd} = 1.172 Mg/m^3, μ = 0.651 mm^{-1}, F(000) = 294, 10775 reflections, –12 ≤ h ≤ 12, –13 ≤ k ≤ 12, –14 ≤ l ≤ 13, 2.146 ° < θ < 31.079 °, completeness 99.1%, 4040 independent reflections, 3206 reflections observed with [I > 2σ(I)], 206 parameters, 69 restraints, R indices (all data) R_1 = 0.0880, wR_2 = 0.2283, final R indices [I > 2σ(I)] R_1 = 0.0759, wR_2 = 0.2095, largest difference peak and hole 0.656 and –1.357 e Å^{-3}, Goof = 1.036.

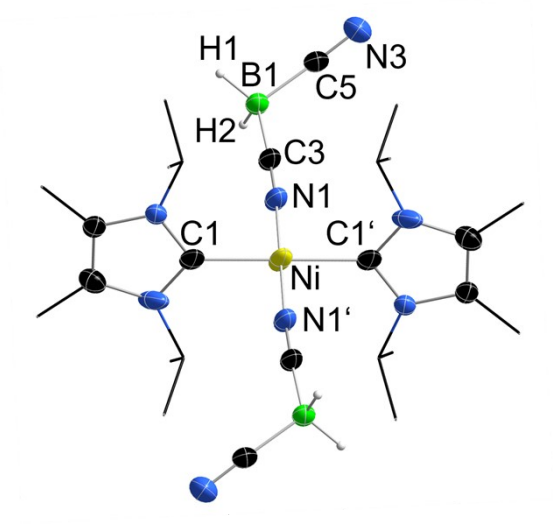

Figure S113. Molecular structure of *trans*-[Ni(*i*Pr$_2$Im^{Me})$_2$(NC-BH$_2$CN)$_2$] (*trans*-**15b**) in the solid-state (ellipsoids set at 50% probability level). The hydrogen atoms except for those bound to boron are omitted for clarity. Selected bond lengths [Å] and angles [°]: Ni–C1 1.931(2), Ni–N1 1.855(2), Ni–N2, N1–C2 1.145(5), C2–B1 1.595(5), B1–C3 1.586(4), C3–N2 1.142(4), <NiN1C2 174.3(2), <N1C2B1 177.0(2).

Crystal data for [Ni(*i*Pr$_2$Im)$_3${NC-BH(CN)$_2$}][BH(CN)$_3$] (16c): $C_{33}H_{50}B_2N_{12}Ni$, M_r = 695.16 g/mol, T = 100(2) K, λ = 1.54184 Å, yellow block, 0.276 × 0.162 × 0.131 mm^3, monoclinic, space group $P2_1/c$, a = 10.64010(10) Å, b = 20.81840(10)Å, c = 17.61290(10)Å, α = 90 °, β = 100.6940(10) °, γ = 90 °, V = 3833.67(5) Å^3, Z = 4, ρ_{calcd} = 1.204 Mg/m^3, μ = 1.035 mm^{-1}, F(000) = 1480, 80215 reflections, –13 ≤ h ≤ 13, –26 ≤ k ≤ 26, –18 ≤ l ≤ 22, 3.321 ° < θ < 77.527 °, completeness 99.9%, 8100 independent reflections, 7521 reflections observed with [I > 2σ(I)], 445 parameters, 0 restraints, R indices (all data) R_1 = 0.0384, wR_2 = 0.0944, final R indices [I > 2σ(I)] R_1 = 0.0360, wR_2 = 0.0929, largest difference peak and hole 0.789 and –0.312 e Å^{-3}, Goof = 1.081.

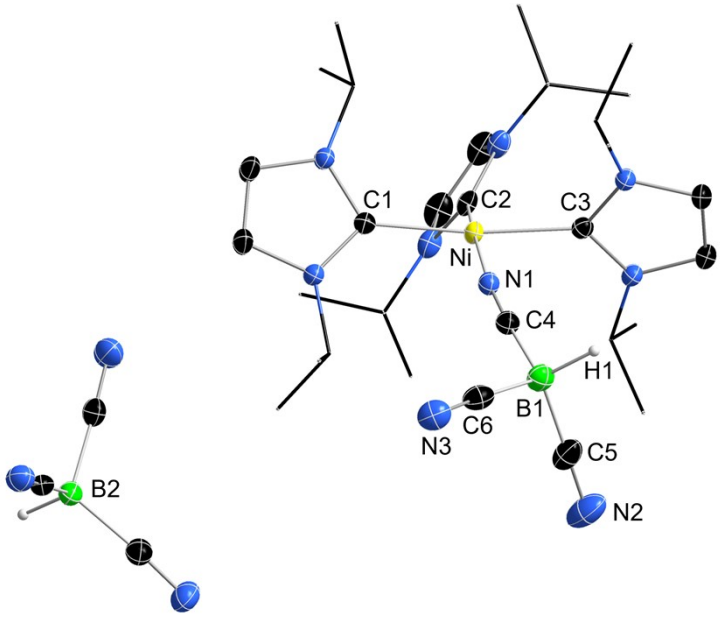

Figure S114. Molecular structure of [Ni(*i*Pr$_2$Im)$_3${NC-BH(CN)$_2$}][BH(CN)$_3$] (**16c**) in the solid-state (ellipsoids set at 50% probability level). The hydrogen atoms not bound at boron are omitted for clarity. Selected bond lengths [Å] and angles [°]: Ni–C1 1.948(1), Ni–C2 1.901(1), Ni–C3 1.92381), Ni–N1 1.898(1), N1–C4 1.144(2), C4–B1 1.603(2), B1–C5 1.593(2), C5–N2 1.147(2), B1–C6 1.589(2), C6–N3 1.151(2), <NiN1C4 166.4(1), <N1C4B1 175.4(1), plane (N1C1N2) – plane (N5C3N6) 55.8(9).

6 References

1 J. Attner, U. Radius, *Chem. Eur. J.* 2001, ***7***, 783–790.

2 X. Bantreil, S. P. Nolan, *Nat. Protoc.* 2011, ***6***, 69–77.

3 T. T. Schaub, *1,3-dialkyl-imidazole-2-ylidenes, Vol.* ***35***, 2010.

4 A. J. Arduengo, H. V. R. Dias, R. L. Harlow, M. Kline, *J. Am. Chem. Soc.* 1992, ***114***, 5530–5534.

5 M. S. Luff, C. Kerpen, J. A. P. Sprenger, M. Finze, U. Radius, *unpublished work* 2023.

6 C. Kerpen, *Cyanoborate - Salze reaktiver Kationen sowie Übergangs-metallverbindungen*, *Dissertation*, Julius-Maximilian-Universität (Würzburg), 2018.

7 E. Bernhardt, G. Henkel, H. Willner, *Z. Anorg. Allg. Chem.* 2000, ***626***, 560–568.

8 L. A. Bischoff, M. Drisch, C. Kerpen, P. T. Hennig, J. Landmann, J. A. P. Sprenger, R. Bertermann, M. Grune, Q. Yuan, J. Warneke, X. B. Wang, N. V. Ignat'ev, M. Finze, *Chem. Eur. J.* 2019, ***25***, 3560–3574.

9 E. Bernhardt, M. Finze, H. Willner, *Z. Anorg. Allg. Chem.* 2003, ***629***, 1229–1234.

10 J. H. J. Berthel, L. Tendera, M. W. Kuntze-Fechner, L. Kühn, U. Radius, *Eur. J. Inorg. Chem.* 2019, 3061–3072.

11 P. Fischer, T. Linder, U. Radius, *Z. Anorg. Allg. Chem.* 2012, ***638***, 1491–1496.

12 L. Falivene, Z. Cao, A. Petta, L. Serra, A. Poater, R. Oliva, V. Scarano, L. Cavallo, *Nat. Chem.* 2019, ***11***, 1759–1766.

13 A. Poater, F. Ragone, S. Giudice, C. Costabile, R. Dorta, S. P. Nolan, L. Cavallo, *Organometallics* 2008, ***27***, 2679–2681.

14 A. Poater, F. Ragone, R: Mariz, R. Dorta, L. Cavallo, *Chem. Eur. J.* 2010, ***16***, 14348–14353.

15 L. Zapf, M. Riethmann, S. A: Föhrenbacher, M. Finze, U. Radius, *Chem. Sci.* 2023, ***14***, 2275–2288.

16 G. M. Sheldrick, *Acta Crystallogr. Sect. C: Cryst. Struct. Commun.* 2015, ***71***, 3–8.

17 K. Brandenburg, Crystal Impact GbR, Bonn, Germany, 1997–2022.